DESIGN OF MEDIUM ACCESS CONTROL PROTOCOL FOR AGGREGATED VLC-IR AND VLC-RF WIRELESS NETWORKS

A THESIS SUBMITTED TO THE
GRADUATE SCHOOL OF NATURAL AND APPLIED SCIENCES
OF
KOCAELI UNIVERSITY

BY

DAWSON LADISLAUS MSONGALELI

IN PARTIAL FULFILLMENT OF THE REQUIREMENTS
FOR
THE DEGREE OF DOCTOR OF PHILOSOPHY
IN
COMPUTER ENGINEERING

KOCAELI 2019

DESIGN OF MEDIUM ACCESS CONTROL PROTOCOL FOR AGGREGATED VLC-IR AND VLC-RF WIRELESS NETWORKS

A THESIS SUBMITTED TO
GRADUATE SCHOOL OF NATURAL AND APPLIED SCIENCES
OF
KOCAELI UNIVERSITY

BY

DAWSON LADISLAUS MSONGALELI

IN PARTIAL FULFILLMENT OF THE REQUIREMENTS
FOR
THE DEGREE OF DOCTOR OF PHILOSOPHY
IN
COMPUTER ENGINEERING

Assoc. Prof. Dr. Kerem KÜÇÜK		
Supervisor,	**Kocaeli University**	....
Assist. Prof. Dr. Orhan AKBULUT		
Jury member,	**Kocaeli University**	....
Assoc. Prof. Dr. Cüneyt BAYILMIŞ		
Jury member,	**Sakarya University**	....
Prof. Dr. Adnan KAVAK		
Jury member,	**Kocaeli University**	....
Assoc. Prof. Dr. Ali ÇALHAN		
Jury member,	**Düzce University**	....

Thesis Defense Date: 26.07.2019

ACKNOWLEDGMENT

First of all I would like to thank the Lord for the blessings that he has given me in my life. My warmest thanks to my supervisor, Assoc. Prof. Dr. Kerem KÜÇÜK, for accepting and supervising me during my Doctorate degree study.

I'm indebted to my thesis committee members: Assoc. Prof. Dr. Cüneyt BAYILMIŞ and Assist. Prof. Dr. Orhan AKBULUT for their guidance that helped me very much to improve the quality of this work. Their benevolent support is significant to the accomplishment of this thesis. My thanks to Prof. Dr. Adnan KAVAK for his great support, encouragement, and valuable advice.

I owe my colleagues from the Computer Networks and Communication Research Laboratory big thanks for creating a friendly and supportive working environment. I will remember each and every one of them in good memories. They have certainly become good companions for me (and for my family as well) during my journey from the beginning to the end of my PhD. career.

I am thankful to the Turks Abroad and Related Communities Presidency for giving me the opportunity to study in Turkey and for supporting my PhD. study.

I extend my appreciation to my sister Happyness LADISLAUS MSONGALELI, my causin Deonatus FORTUNATUS and other relatives who supported me in various aspects in my PhD. career.

I am grateful to my beautiful wife Jacqueline ROGATH MASSAWE, and my angel Ivanna DAWSON LADISLAUS for their love, moral support, and for creating a warm environment that I needed during my study.

Finally, and most importantly, I am thankful to my parents Ladislaus MSONGALELI and Anna WILLIAM who raised me as a free spirit and encouraged me for higher education.

July – 2019 Dawson LADISLAUS MSONGALELI

CONTENTS

ACKNOWLEDGMENT i
CONTENTS ii
LIST OF FIGURES iv
LIST OF TABLES vi
SYMBOLS AND ABBREVIATIONS vii
ÖZET xi
ABSTRACT xiii
INTRODUCTION 1
1. OPTIC WIRELESS COMMUNICATION 4
1.1. Classification of Applications of OWC Wireless Networks 4
1.2. Classification of OWC Wireless Networks 6
1.2.1. Ultraviolet communication (UVC) 6
1.2.2. Infared communication (IRC) 7
1.2.3. Visible light communication (VLC) 8
1.3. OWC Standardization and Working Groups 10
1.3.1. IRC working groups 10
1.3.2. VLC working groups 10
1.3.3. UVC working groups 11
1.4. Coexistence of VLC and Other Wireless Networks 12
1.5. MAC Protocols for Coexisting VLC and Other Networks 15
1.6. The Contribution of this Thesis 18
1.7. Thesis Outline 20
2. VISIBLE LIGHT COMMUNICATION 22
2.1. VLC Building Components 22
2.2. VLC Transmitter 23
2.3. VLC Receiver 24
2.4. VLC Link Configuration 25
2.5. VLC Channel Model 25
2.6. VLC Modulation Techniques 30
2.6.1. Single-carrier modulation (SCM) 30
2.6.2. Multi-carrier modulation (MCM) 30
2.6.3. VLC specific modulation techniques 31
2.7. VLC MAC Protocols 32
2.8. Challenges of VLC Wireless Networks 35
2.8.1. Uplink augmentation 35
2.8.2. Network addressing challenge 36
2.8.3. Mobility and coverage 37
2.8.4. Inter-cell interference 37
2.8.5. Energy efficiency 37
2.8.6. FOV alignment and shadowing 38

3. DESIGN OF MAC PROTOCOL FOR AGGREGATED VLC-IR WIRELESS NETWORKS 39
3.1. Aggregated VLC-IR Wireless Networks 39
3.2. APMAC Protocol for Aggregated Wireless Networks 41
3.2.1. APMAC frames structure 41
3.2.1.1. Superframe structure 41
3.2.1.2. Frame structure 42
3.2.2. Network association, channel allocation, and dissociation 42
3.2.2.1. Association phase 42
3.2.2.2. Data transmission phase 45
3.2.2.3. Dissociation phase 45
3.3. Experimental Setup and Numerical Results 46
3.3.1. Network delay versus network size and load 47
3.3.2. Collision versus network size and network load 48
3.3.3. System utilization versus network size and throughput 48
3.3.4. Fairness versus network throughput and load 49
3.4. Conclusion 50
4. DESIGN OF MAC PROTOCOL FOR AGGREGATED VLC-RF WIRELESS NETWORKS 51
4.1. Introduction 51
4.1.1. Related studies 53
4.2. Aggregated VLC-RF Wireless Networks and Problem Statement 55
4.3. Self-Adaptive Medium Access Control Protocol 56
4.3.1. SA-MAC superframe structure 57
4.3.2. Access point flow 59
4.3.3. Nodes flow 61
4.4. Performance Analysis 63
4.4.1. Defining transition probabilities 64
4.4.2. Throughput analysis 66
4.4.3. Network delay 70
4.4.4. Power consumption 70
4.4.5. Collision 71
4.5. Experimental Setup and Numerical results 72
4.5.1. Throughput 73
4.5.2. Non transmission time 73
4.5.3. Collision 75
4.5.4. Energy consumption 76
4.5.5. Transmission time 77
4.6. A comparison of APMAC and SA-MAC Protocols 78
4.7. Conclusion 79
5. CONCLUSION 81
REFERENCES 83
PUBLICATIONS AND WORKS 95
CURRICULUM VITAE 96

LIST OF FIGURES

Figure 1.1.	The electromagnetic spectrum.	4
Figure 1.2.	Categories of OWC application based on the distance of communication.	5
Figure 1.3.	The Ultra-violent spectrum.	6
Figure 1.4.	NLOS configuration in UVC.	7
Figure 1.5.	Hybrid VLC-RF wireless network.	12
Figure 1.6.	Aggregated VLC-RF wireless network.	13
Figure 1.7.	OSI network reference model.	15
Figure 1.8.	Classification of MAC protocols.	16
Figure 2.1.	A sample VLC system.	23
Figure 2.2.	The basic VLC system channel model.	23
Figure 2.3.	Single LED in 2.3a and Multi-colour LEDs in 2.3b.	24
Figure 2.4.	The basic architecture of a VLC receiver.	25
Figure 2.5.	Link configuration in OWC.	26
Figure 2.6.	VLC channel model as baseband linear and time-variant.	26
Figure 2.7.	The geometry of a VLC downlink channel for both LOS and NLOS link.	28
Figure 2.8.	Distance versus channel DC gain.	29
Figure 3.1.	Aggregated VLC-IR for indoor wireless networks.	40
Figure 3.2.	The APMAC protocol superframe structure.	41
Figure 3.3.	The frame structure used in the APMAC protocol.	42
Figure 3.4.	The APMAC protocol for aggregated VLC-IR wireless networks.	42
Figure 3.5.	The VLAP deterministic finite state machine in the APMAC protocol.	45
Figure 3.6.	The node deterministic finite state machine in the APMAC protocol.	46
Figure 3.7.	Delay versus network size in (a) and delay versus network load in (b).	47
Figure 3.8.	Collision versus network size in (a) and collision versus throughput in (b).	48
Figure 3.9.	Utilization vs. network size in (a) and utilization vs. network load in (b).	49
Figure 3.10.	Fairness index vs. throughput in (a) and fairness vs. network load in (b).	49
Figure 4.1.	Aggregated RF-VLC indoor wireless network.	56
Figure 4.2.	The SA-MAC superframe structure.	57
Figure 4.3.	SA-MAC protocol access point flowchart.	59
Figure 4.4.	SA-MAC protocol node flowchart.	62

Figure 4.5. SA-MAC protocol sequence diagram. 63
Figure 4.6. The Markov chain model for SA-MAC protocol. 64
Figure 4.7. A screen-shot of the SA-MAC simulation in NS3. 72
Figure 4.8. Network size versus throughput. 74
Figure 4.9. Network size versus NTT in (a) and Network size
versus link NTT in (b). 75
Figure 4.10. Network size versus collision. 75
Figure 4.11. Network size versus energy consumption. 76
Figure 4.12. Network size versus transmission time. 77
Figure 4.13. Network size versus throughput. 78
Figure 4.14. Network size versus transmission time. 79

LIST OF TABLES

Table 1.1. A summary of classification of OWC technologies based on wavelength 9
Table 1.2. A summary of research publications on MAC protocols for VLC-based wireless networks. 19
Table 2.1. A summary of VLC modulation techniques 34
Table 4.1. 2D Markov chain model states definition. 65
Table 4.2. Simulation parameters 73

SYMBOLS AND ABBREVIATIONS

2D	: Two-Dimensional
α_t	: Average round trip time (RTT) between nodes and AP in a network
δ_k	: The delay of node k
η	: Average maximum number of users per AP
$\otimes$	: Convolution
τ	: Stationary probability that a node transmits a packet at a random time
ε_k	: The the normalized energy consumed by node k for each transmission
π_0	: The probability of being in state $(S,0)$ in steady state condition
π_1	: The probability of being in state $(S,1)$ in steady state condition
π_2	: The probability of being in state $(2S,0)$ in steady state condition
π_3	: The probability of being in state $(2S,1)$ in steady state condition
π_4	: The probability of being in state $(3S,0)$ in steady state condition
π_5	: The probability of being in state $(3S,M)$ in steady state condition
π_6	: The probability of being in state $(3S,M+1)$ in steady state condition
π_7	: The probability of being in state $(3S,M+2)$ in steady state condition
π_8	: The probability of being in state $(MS,M+2)$ in steady state condition
π_9	: The probability of being in state $(4S,0)$ in steady state condition
π_{10}	: The probability of being in state $(4S,(n-r)L)$ in steady state condition
π_{11}	: The probability of being in state $(4S,nL)$ in steady state condition
C_γ	: The normalized collision of node γ
$E(\gamma)$	: The normalized power consumed by node γ in state e
nm	: Nanometer
mm	: Millimeter
n(t)	: Additive White Gaussian Noise (AWGN)
N_D	: The network delay
N_E	: The normalized network energy consumption
h(t)	: Impulse response
H(O)	: The channel DC gain
$p(\gamma_i)$	: The probability of node γ to generate packets in idle state
$p(\gamma_b)$	: The probability of node γ receiving the beacon frame
$p(\gamma_{rts})$	: The probability of node γ sending RTS
$p(\gamma_{cts})$	: The probability of node γ sending CTS
$p(\gamma_c)$	: The probability of node γ sending RTS and receiving CTS
$p(\gamma_s)$	: The probability of node γ successful transmission
p_{co}	: The probability of collision
P_t	: Average transmitted optical power
P_r	: Average received optical power
x(t)	: Instantaneous optical power (channel input intensity)
y(t)	: Channel output intensity
X_{new}	: New normalized value
X_{min}	: Minimum value
X_{max}	: Maximum value

Abbreviations

ACK	: Acknowledgment
ACO-OFDM	: Asymmetrically Clipped Optical Orthogonal Frequency Division Multiplexing
ADF	: Availability Declaration Frame
ADFT	: Availability Declaration Frame Transmission
ARF	: Access Request Frame
ARFR	: Access Request Frame Reception
AGF	: Access Grant Frame
AGFT	: Access Grant Frame Transmission
AIr	: Advanced Infrared
AP	: Access Point
APMAC	: Adaptive Polling Medium Access Control
AT	: Assignment Table
BC	: Beacon Command
BE	: Beacon Exponents
BER	: Bit Error Rate
CAP	: Contention Access Period
CCA	: Clear Channel Assessment
CCM	: Code Cycle Modulation
CDMA	: Code Division Multiple Access
CFCA	: Control Frame Collision Avoidance Algorithm
CFP	: Contention Free Period
CIM	: Colour Intensity Modulation
CO-OFDM	: Coherent Optical Orthogonal Frequency Division Multiplexing
CRC	: Cyclic Redundancy Check
CSK	: Colour Shift Keying
CSMA/CD-HA	: Carrier Sense Multiple Access with Collision Detection Hidden node Avoidance
CSMA/CA	: Carrier Sense Multiple Access/Collision Avoidance
CTS	: Clear-To-Send
CTA	: Connection Termination Acknowledgement
CTAT	: Connection Termination Acknowledgement Transmission
CTRR	: Connection Termination Request Reception
CTR	: Connection Termination Request
DAF	: Data Acknowledgement Frame
DAFT	: Data Acknowledgement Frame Transmission
DC	: Direct Current
DCSK	: Digital Colour Shift Keying
DCO-OFDM	: DC biased Optical Optical Orthogonal Frequency Division Multiplexing
DCW-ST	: Dynamic Contention Window-based Successive Transmission
DF	: Data Frame
DFK-MTU	: Dynamic Future Knowledge Maximum Transmission Unit
DM	: Demodulation
DTF	: Data Transmission Frame

DTFR	: Data Transmission Frame Reception
FOV	: Field Of View
F-OFDM	: Fast-Orthogonal Frequency Division Multiplexing
FWHT	: Fast Walsh-Hadamard Transform
GLIM	: Generalized LED Index Modulation
HCM	: Hadamard Coded Modulation
IrDA	: Infrared Data Association
IR	: Infrared
IRC	: Infrared Communication
IM	: Index Modulation
IM	: Intensity Modulation
IM/DD	: Intensity Modulation with Direct Detection
IP	: Internet Protocol
KHz	: Kilohertz
LED	: Light Emitting Diode
LiFi	: Light Fidelity
LOS	: Line of Sight
MCM	: Multi-Carrier Modulation
MD	: Modulation
MFR	: Medium-access-control footer
MHR	: Medium Access Control Header
MIMO	: Multiple Input Multiple Output
MM	: Metameric Modulation
MSDU	: Medium-access-control service-data unit
MTU	: Maximum Transmission Unit
NACK	: Negative Acknowledgment
NIC	: Network Interface Card
NLOS	: Non Line of Sight
NOMA	: Non-Orthogonal Multiple Access
OCDMA	: Optical Orthogonal Code Division Multiple Access
OOC	: Optical Orthogonal Codes
OF	: Optical Filter
OFDMA	: Orthogonal Frequency Division Multiple Access
OSI	: Open Systems Interconnection
OOK	: On-Off Keying
O-OFDMA	: Optical Orthogonal Frequency Division Multiple Access
O-OFDM-IDMA	: Optical Orthogonal Frequency Division Multiplexing Interleave Division Multiple Access
PAM	: Pulse Amplitude Modulation
PPM	: Pulse Position Modulation
PD	: Photo Diode
PT	: Polling Table
PRO-OFDM	: Polarity Reversed Optical Orthogonal Frequency Division Multiplexing
QoS	: Quality of Services
RGB	: Red Blue Green
RF	: Radio Frequency

R-OFDM	: Reshaped Orthogonal Frequency Division Multiplexing
RTS	: Request-To-Send
RTT	: Round Trip Time
SA-MAC	: Self-Adaptive Medium Access Control
SCM	: Single-Carrier Modulation
SIFS	: Short Inter Frame Spacing
SIR	: Serial Infrared
SNR	: Signal-Noise-Ratio
SYN	: Synchronize
TCP	: Transmission Control Protocol
TDMA	: Time Division Multiple Access
UE	: User Equipment
UV	: Ultraviolent
UVC	: Ultraviolent Communication
VL	: Visible light
VLC	: Visible Light Communication
VLCA	: Visible Light Communications Associations
VLCC	: Visible Light Communication Consortium
VPPM	: Variable Pulse Position Modulation
WBAN	: Wireless Body Area Network
WiFi	: Wireless Fidelity
WLANs	: Wireless Local Area Networks
WMANs	: Wireless Metropolitan Area Networks
WPAN	: Wireless Personal Area Network

BİRLEŞTİRİLMİŞ VLC-IR VE VLC-RF KABLOSUZ AĞLARI İÇİN ORTAM ERİŞİM KONTROL PROTOKOLÜ TASARIMI

ÖZET

Günümüzde dünya üzerindeki İnternet erişimi talebinde kayda değer bir artış yaşanmaktadır. İnternet erişimi talebindeki bu artış, İnterneti kullanan yeni cihaz ve uygulamaların, sosyal medya ortamlarının, ortaya cıkarılmasındakı yeniliklerden kaynaklanmaktadır. Yüksek miktardaki İnternet trafiği ihtiyacının giderilmesinde genellikle kablosuz iletişim kullanılmaktadır. Özellikle radyo frekansı (Radio Frequency, RF), kablosuz ağ bağlantısı için en çok kullanılan spektrumdur. İnternet abone sayısı hızla artarken, radyo spektrumunun limitlerine ulaştığı görülmektedir. Sürekli olarak artan İnternet erişim talebi için yeterli spektrum bulunmamaktadır. Optik spektrumun iletişim amaçlı kullanılması, İnternet endüstrisindeki bant genişliği sorununu iyileştirebileceği varsayılmaktadır. Literatürdeki güncel çalışmalar, kızılötesi (Infrared, IR), görünür ışık (Visible Light, VL) ve ultraviyole (Ultraviolet, UV) spektrumlarının sinyal iletimi için kullanılabileceğini göstermektedir. Optik spektrumun iletişim amaçlı kullanılmasında, yüksek bant genişliği ve güvenlik başta olmak üzere farklı yararları vardır. Buna göre, görünür ışık iletişimi (Visible Light Communication, VLC), kızılötesi iletişim (Infrared Communication, IRC) ve ultraviyole iletişim (Ultraviolet Communication, UVC) gibi optik spektrum tabanlı kablosuz ağların kullanımı artmaktadır.

Son yapılan çalışmalar, VLC'nin iç mekan kablosuz ağları için daha uygun olduğunu göstermektedir. Dayanıklı, uygun maliyetli ve enerji verimliliği sağlayan ışık yayan diyotun (Light Emitted Diode, LED) iyileştirilmesi, VLC teknolojisinin gelişmesine neden olmuştur. Bu nedenle, iç mekan kablosuz ağlarında VLC teknolojisi kullanılarak İnternet bant genişliği sorunu ele alınabilmektedir. Bununla birlikte, VLC'yi sadece fiziksel katman perspektifinden ilerletmek için önemli çabalar bulunmaktadır. Mevcut VLC teknolojisi çalışmaları, noktadan noktaya bağlantılar ve yarı çift yönlü iletişim gibi basit varsayımları göz önünde bulundurmaktadır. VLC teknolojisini ölçeklenebilir ve çift yönlü ağa (mesh network) dönüştürmek gerekmektedir. VLC kablosuz ağların temel zorluklarından biri, yukarı bağlantı kanalının oluşturulmasıdır. Enerji tüketimi ve ışık kaynaklarından kaynaklanan görsel bozukluklar, VLC kablosuz ağlarda yukarı bağlantı kanalının gerçekleşmesini engelleyen ana faktörlerdir. Bu nedenle, VLC kablosuz ağlarda çift yönlü iletişim elde etmek için kızılötesi veya radyo spektrumu gibi diğer spektrumların kullanılması zorunludur.

Bu tezde, VLC ve diğer kablosuz ağların bir arada bulunması durumunda ortam erişim kontrolü problemi üzerinde durulmaktadır. VLC ve diğer kablosuz ağların bir arada bulunmasında, iki olası senaryo bulunmaktadır; (i) her bir ağın bağımsız bir sistem olarak çalıştığı hibrit bir sistem ve (ii) iki sistemin birlikte çalıştığı, bir ağın yukarı bağlantı kanalı için diğer ağın aşağı bağlantı kanalı için kullanıldığı birleştirilmiş bir ağ. Literatürde, birleştirilmiş sistemin hibrit sistemden daha iyi performans sergilediği

gösterilmiştir. Bu nedenle tezde ortam erişim kontrol protokolü tasarımında birleştirilmiş sistem göz önüne alınmaktadır. Ek olarak, VLC kablosuz ağlarda yukarı bağlantı kanalını gerçekleştirmenin iki uygulanabilir çözümünü göz önünde bulundurulmaktadır; (i) yukarı bağlantı kanalı için kızılötesi spektrumun kullanımı ve (ii) yukarı bağlantı kanalı için radyo spektrumunun kullanımı. Sonrasında, ölçeklenebilir, çift yönlü ve çok noktalı kablosuz ağ faktörleri dikkate alınmaktadır. İlk durumda, Uyarlamalı Sorgulama Ortam Erişim Kontrolü (Adaptive Polling Medium Access Control, APMAC) protokolü adı verilen birleştirilmiş VLC-IR kablosuz ağlar için ortam erişim kontrol protokolü tasarlanmıştır. APMAC protokolünde, aşağı bağlantı kanalı VLC, yukarı bağlantı kanalı ise IR kullanmaktadır. İkinci olarak, birleştirilmiş VLC-RF kablosuz ağları için Kendinden Uyarlamalı Ortam Erişim Kontrolü (Self-Adaptive Medium Access Control, SA-MAC) protokolü tasarlanmıştır. Bu durumda, aşağı bağlantı kanalı VLC'yi kullanırken yukarı bağlantı kanalı RF'nı kullanmaktadır. Simülasyonlardan elde edilen sayısal sonuçlar bu tezin avantajlarını ortaya koymaktadır. Özetle, bu tezin teknik katkısı, birleştirilmiş VLC-IR ve VLC-RF kablosuz ağları için ortam erişim kontrol protokollerinin tasarımını içermektedir.

Anahtar Kelimer: Görünür Işık Haberleşmesi, Kablosuz Ağlar, Optik Kablosuz Haberleşme, Ortam Erişim Kontrolü.

DESIGN OF MEDIUM ACCESS CONTROL PROTOCOL FOR AGGREGATED VLC-IR AND VLC-RF WIRELESS NETWORKS

ABSTRACT

Over the past decades the world has experienced a monumental increase in internet demand. The rise in internet demand is prompted by innovations of new devices and applications that use the internet, viz., the invention of social media, mobile devices, and smartphones. The huge internet traffic relies on wireless communication to provide access networks, in particular, the radio frequency (RF) is the most used spectrum for wireless network connectivity. While internet subscription is on the rise, the radio spectrum has reached its limit. There is no sufficient spectrum for the ever-increasing internet demand. Exploiting the optical spectrum for communication purpose can ameliorate the problem of bandwidth scarcity in the internet industry. Several research publications have demonstrated that the infrared (IR), visible light (VL), and ultraviolet (UV) spectra can be used for signal transmission. There are several potential benefits of using the optical spectrum for communication purpose such as the huge bandwidth, and security. Accordingly, optical spectrum based wireless networks such as visible light communication (VLC), infrared communication (IRC), and ultraviolet communication (UVC) are on the rise.

Recent studies have demonstrated that VLC is more suitable for indoor wireless networks. The development of durable, cost effective, and energy efficiency light emitting diode (LED) has prompted the rise of the VLC technology. Therefore, the problem of internet bandwidth can be addressed by utilizing the VLC technology in indoor wireless networks. Nonetheless, there is significant effort in advancing VLC from the physical layer perspective only. Current studies of VLC technology consider simple assumptions such as point-to-point links and half duplex communication. There is the need of transforming VLC technology into scalable, full-duplex, and fully mesh networks. One of the challenges of VLC wireless networks is the provision of the uplink channel. Energy consumption and visual disturbances from light sources are major factors that hinder the realization of the uplink channel in VLC wireless networks. Therefore, it is imperative to use other spectrum such as infrared or radio spectrum in order to achieve full duplex in VLC wireless networks.

In this thesis, we investigate the problem of medium access control for the coexistence of VLC and other wireless networks. In the coexistence of VLC and other wireless networks there are two possible scenarios, i.e., (i) a hybrid system where each network works as a standalone system and (ii) an aggregated network where the two system work together, one for the uplink channel and the other for the downlink channel. Several research publications have demonstrated that aggregated system outperforms hybrid system, therefore, in this thesis we consider aggregated system in our design. In addition, we consider two viable solutions of realizing the uplink channel in VLC wireless networks, viz., (i) the use of the infrared spectrum for the uplink channel, and

(ii) the use of the radio spectrum for the uplink channel. Moreover, we take into account a scalable, full-duplex, and multi-point wireless network factors. In the first case, we design the medium access control protocol for aggregated VLC-IR wireless networks named the Adaptive Polling Medium Access control (APMAC) protocol. In APMAC protocol, the downlink channel uses VLC while the uplink channel uses IR. Secondly, we design the Self-Adaptive Medium Access Control (SA-MAC) protocol for aggregated VLC-RF wireless networks. In this context, the downlink channel uses VLC whereas the uplink channel uses RF. Numerical results from simulations demonstrate advantages of this thesis. In a nutshell, the technical contributions of this thesis include the design of the medium access control protocol for aggregated VLC-IR and VLC-RF wireless networks.

Keywords: Visible Light Communication, Wireless Networks, Optical Wireless Communication, Medium Access Control.

INTRODUCTION

The high reliance on the internet is the major cause of sudden increase in new internet subscribers. In fact, the number of internet subscribers increases every year at unpredictable rate. For example, Cisco forecasts that the global mobile data traffic will grow from an annual rate of 87 Exabytes of the year 2016 to 587 Exabytes in 2021 [1]. Statistics show that between 2016 and 2021, mobile traffic is expected to increase two times faster than fixed network traffic [1]. Furthermore, the high reliance on social networks and other web-based applications available on the internet are the major cause of high traffic from mobile devices such as smartphones, tablets, and other hand-held devices [2].

Over the past decades, the radio waves of the electromagnetic spectrum have been exploited for wireless networks. However, excessive internet subscribers have stretched the radio spectrum to its limit. There is no more spectrum for new subscribers while the number of new users is increasing every year. Several solutions have been proposed to address the problem of new bandwidth demand such as the use of unlicensed radio spectrum. However, the proposed new solutions cause other problems such as high energy consumption, signal interference, high capital, and operating expenditure [3]. Moreover, the design of VLC-based uplink channel is challenging considering limitations such as transmitter and receiver alignment [4]. Therefore, in order to improve the performance of wireless networks, exploiting other spectra such as the visible light spectrum or the infrared spectrum is more ideal rather than relying on the already congested radio spectrum.

The recent development in solid state lighting has resulted in the availability of durable, energy efficiency, and cost effective light emitting diodes (LEDs). Accordingly, LEDs are ubiquitously used in indoor and outdoors environments for lighting. Exploiting the visible light spectrum for signal transmission is the promising solution to the ever increasing bandwidth demand. There are many reasons that support this argument such as the huge bandwidth available in the visible light spectrum i.e., from 430 nm to 790 nm, inherent physical security, no impact on human health, low capital expenditure, and energy efficiency. Different groups such as [5–9] have demonstrated that visible light spectrum can be used for transmission of signals. The visible light communication (VLC) is on the rise, and it is currently standardized by the IEEE 802.15.7 [10]. Light Fidelity (LiFi) demonstrated in [11] extends the concept of VLC to achieve visible light-based wireless access networks [11]. Applications of VLC include vehicular networks, indoor mobile network, indoor localization, visible light sensing, gesture recognition, under water communication systems, security systems, smart home, and smart cities [12].

Despite recent development in VLC technology, several challenges need to be addressed in order to realize its potential benefits. These challenges are inter-cell interference, back-bone network design, uplink design, multi-user access control and network addressing. In VLC wireless networks, access points have small radii whilst with high capacity. This prompts the deployment of large number of access points to increase network coverage. In indoor environment, deploying large number of access points causes inter-cell interference. Thus, user equipment would experience low signal to noise ratio (SNR). Therefore, the design of optimal small cell deployment in VLC is significant for improving the VLC networks performance. In addition, the deployment of large number of access points increases the cost of back-bone network. Accordingly, optimal back-bone design in VLC wireless networks should be considered.

Most of the existing research publications in VLC focus on the downlink channel. There is little attention on the uplink channel in VLC wireless networks. LEDs can cause visual disturbances and consume a lot of energy than available energy in mobile devices. This is a limiting factor of using LEDs to transmit information from mobile devices. Therefore, achieving full-duplex communication in VLC standalone system is not realistic unless it is complemented by infrared or radio frequency for the uplink channel. Hybrid VLC-RF and infrared-VLC systems have been proposed in the literature as the best way to achieve full-duplex communication in VLC wireless networks. Nevertheless, such systems introduce new challenges such as network addressing and medium access control. This thesis investigates the problem of multiple user access control in coexisting VLC-Infrared and VLC-RF wireless networks.

1. OPTIC WIRELESS COMMUNICATION

Optical wireless communication (OWC) uses unlicensed ultraviolet (UV), visible light (VL), and infrared (IR) spectra to provide wireless network connectivity. There are several benefits of using OWC such as low cost, and high bandwidth. Currently, OWC technology is at its infancy stage, however, it is a promising solution that will provide reliable and high data rate wireless network connectivity at low cost. The optical spectrum is categorized into UV that ranges from 200 nm to 280 nm, VL between 390 nm and 750 nm, and IR between 750 nm and 1600 nm. Figure 1.1 shows the optical spectrum in the electromagnetic spectrum. Each spectrum has its own benefits and drawbacks. For instance, IR is invisible, therefore, it is more ideal to be used where illumination is not required. The applications of OWC include airport network systems, smart city, smart home, smart health-care etc.

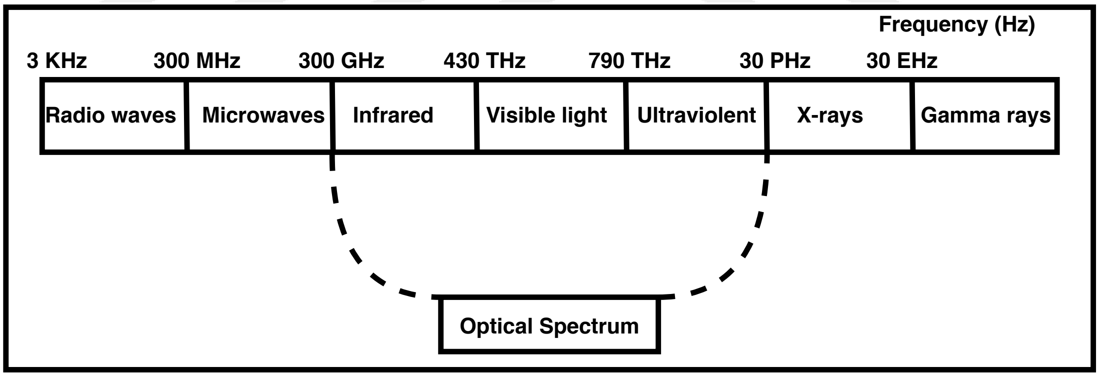

Figure 1.1. The electromagnetic spectrum.

1.1. Classification of Applications of OWC Wireless Networks

OWC can be used in many applications, viz., airport and aviation systems, transportation, indoor wireless networks, smart home and smart cities, underwater communication systems, smart health-care etc. Existing research publications classify the applications of OWC based on the communication distance. The classification of OWC applications based on communication distance has been presented in [13] and [14] where the authors classify OWC applications into six categories such as:

(a) Ultra-short range OWC. This category involves very short communication distance, i.e., communication within a couple of nm or mm. The ever increasing demand in chip-to-chip communication presented in [15] and [16], is appealing the development of ultra-short range OWC [13].

(b) Short-range OWC. In this category, communication distance is within tens of centimeters. Wireless personal area network (WPAN) is one example of this category where an individual's devices are connected together. Moreover, the wireless body area network (WBAN) is another potential application of OWC that falls within short-range OWC [13].

(c) Medium range. In the medium range category of OWC applications, communication distance is within a couple of meters. This category includes indoor wireless local area networks (WLANs) and outdoor communications such as vehicle to vehicle (V2V) and vehicle to infrastructure (V2I) [17].

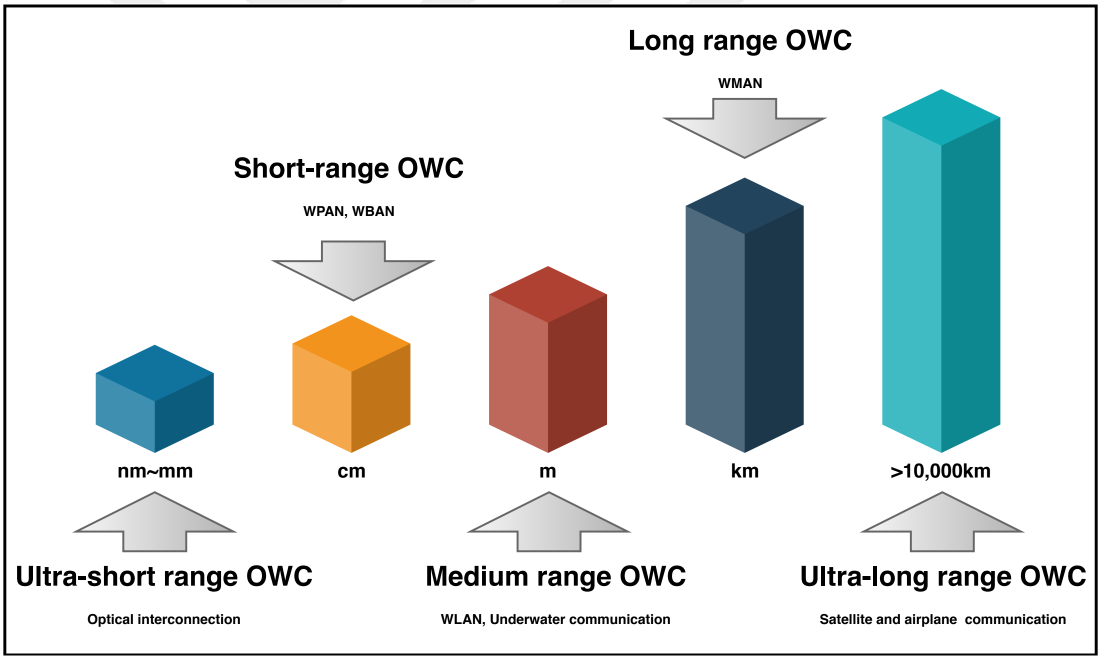

Figure 1.2. Categories of OWC application based on the distance of communication.

(d) Long range. In long range communication, the communication distance is a range of kilometers i.e., wireless metropolitan area networks (WMANs), which can be used to connect WLANs [18].

(e) Ultra-long range. The ultra-long range communication occurs in thousands of kilometers. Examples of application areas of this category are satellite to satellite communication, satellite to earth communication, satellite to airplane communication, airplane to earth communication, and airplane to airplane communication [14, 19]. Figure 1.2, shows categories of applications of OWC based on the distance of communication.

1.2. Classification of OWC Wireless Networks

In the literature, OWC wireless networks are classified according to the spectrum used in communication, i.e., infrared, visible light, and ultra-violent. Below we provide a brief description of each of category.

1.2.1. Ultraviolet communication (UVC)

Generally, the UV spectrum can be divided into three groups as shown in Figure 1.3. The UV-C that is from 10 nm to 280 nm, the UV-B that is from 280 nm to 320 nm, and the UV-A that starts from 320 nm to 400 nm. Although UV spectrum ranges from 10 to 400 nm, only a fraction of its spectrum can be used for signal propagation, i.e., 200-280 nm (the UV-C band). This is because the deep UV-C band (200-280 nm) is solar blind at the ground level due to ozone absorption in the atmosphere [20]. Accordingly, this band is immune to solar radiation.

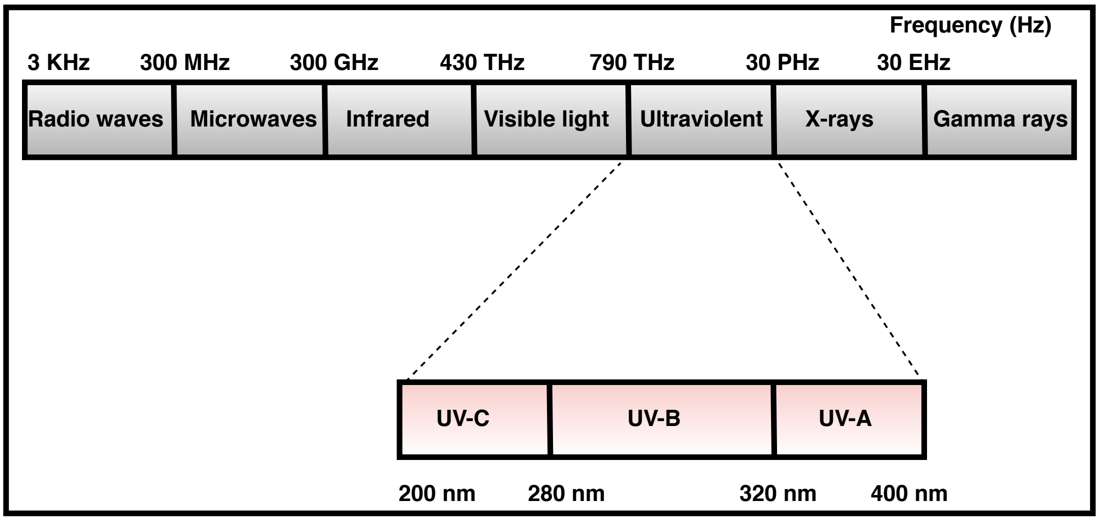

Figure 1.3. The Ultra-violent spectrum.

OWC systems that operate in the 200-280 nm band are referred to as Ultraviolet communication (UVC). UVC is suitable for scientific, industrial, long range, and medical environment applications. In addition, UV spectrum is immune from interference caused by radio frequency (RF) systems, therefore, UVC can co-exist with

RF-based systems. Moreover, while IR and VLC are affected by noise from solar energy, UV systems operating in the 200-280 nm (UV-C band) are immune to noise prompted by solar energy, therefore, UV can be used in outdoor communication without significant performance deterioration [21, 22].

In UVC both line of sight (LOS) and non-line of sight (NLOS) communication can be achieved without affecting the performance of the system [23–28]. Unlike IRC and VLC, UVC can achieve NLOS without light reflection requirement. The NLOS in UVC is considered as the combination of two LOS paths, i.e. one from the transmitter and another form the receiver. Figure 1.4 shows the UVC NLOS configuration where TX is the transmitter and RX is the receiver. In Figure 1.4, the combination TX and RX paths in region A forms the NLOS.

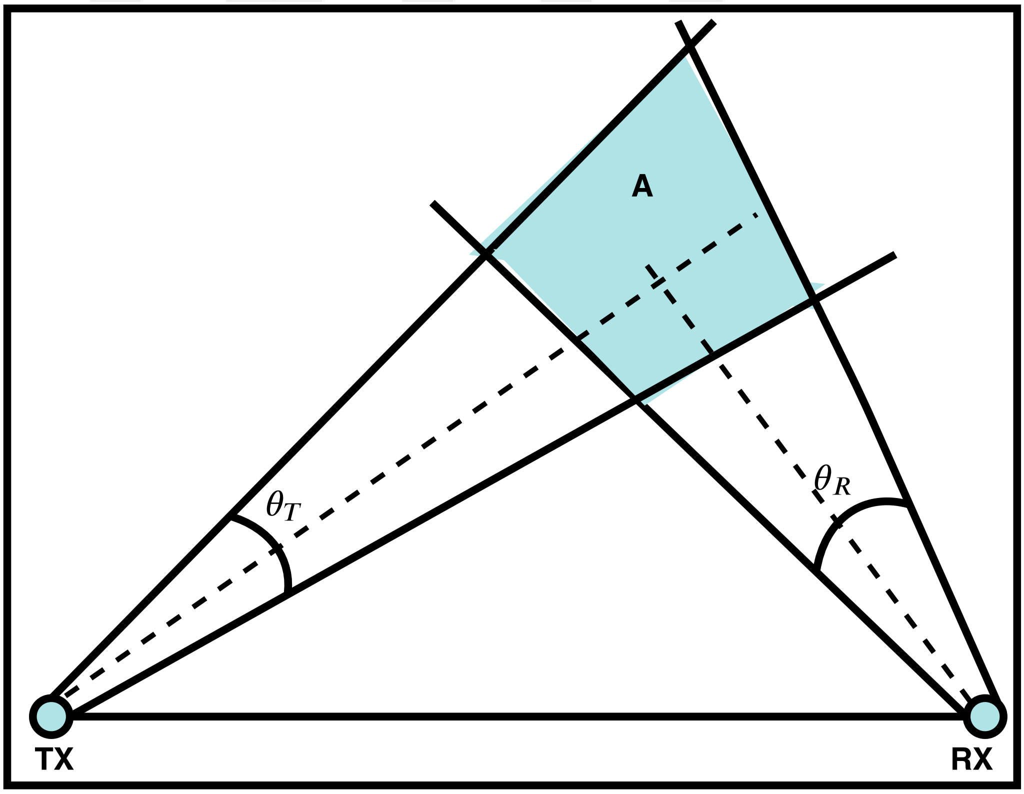

Figure 1.4. NLOS configuration in UVC.

1.2.2. Infared communication (IRC)

Infrared communications (IRC) refers to the OWC that uses 750-1600 nm band as the medium of signal propagation. Over the past decades, IRC has attracted many researchers considering it potential benefits for short range wireless connectivity. The infrared data association (IrDA) plays key role in developing and promoting infrared wireless networks standards [29]. Serial infrared (SIR) and advanced infrared (AIr) are two main protocols developed by the IrDA to provide cost effective, and energy efficiency IRC. The AIr protocol supports between 250kbps to 4Mbps. IRC systems can be categorized into two types based on link configuration, i.e. LOS and NLOS also known as diffuse systems. Existing research publications such as [30]-[31] have demonstrated that infrared can be used for data transfer. IRC has been used in many indoor wireless network applications like infrared remote control and other home appliances [32]. Therefore, it can be used to augment the uplink channel in VLC systems without causing visual disturbance and energy consumption problems.

1.2.3. Visible light communication (VLC)

VLC is the type of OWC that exploits the visible light spectrum (from 380 nm to 750 nm) for signals propagation. The emergence of low powered and energy efficiency white light LEDs has attracted the rise of VLC technology [33]. The huge bandwidth available in the visible light spectrum can significantly address the ever increasing bandwidth demand. The following are advantages of using visible light in communication; immunity to electromagnetic interference, it is unlicensed, signal propagation can be controlled thereby alleviating the problem of eavesdroppers. In addition, VLC does not have any health risk to human being. Ubiquitous availability of LEDs in lighting infrastructure reduces the cost of installing VLC systems. VLC has many applications such as indoor wireless networks, transport communication system, health care communication systems, underwater communication systems, and other domains where communication via radio spectrum cannot be realized because of challenges like electromagnetic interference. Uplink realization, field of view (FOV) alignment, receiver design, mobility, coverage, and interference are the main challenges facing the realization of VLC wireless networks. In terms of link configuration, VLC supports LOS and NLOS link configuration. However, in NLOS link configuration, the performance of VLC systems deteriorates [14]. A summary of these categories is presented in Table 1.1.

Table 1.1. A summary of classification of OWC technologies based on wavelength

	Ultraviolet	**Visible light**	**Infrared**
Spectrum	10-400nm	380-700nm	760nm-1mm
Standardization	No standard	IEEE 802.15.7	IrDA
Link orientation	NLOS and LOS	LOS	NLOS and LOS
Propagation distance	Long (>10,000 km)	Medium range (Up to 100 m)	Short range
Mode of communication	Full-duplex	Half-duplex	Half-duplex
Energy consumption	Higher than IR and VLC	Low	Low
Illumination	Not required	Required	Not required
Application domain	Outdoor communication	Indoor communication	Indoor and outdoor communication
Advantage	High data rate NLOS communication is possible	Safe for human	Not visible for human eye considering the cases when illumination is not required
Shortcomings	Affects skin and and eyes	• Low data rate in NLOS link configuration. • Difficult implementation of uplink channel. • Affected by solar radiation, not ideal for outdoor wireless networks. • Small network coverage.	• High energy consumption due to high transmission power requirement. • Limited coverage • Eye safety

1.3. OWC Standardization and Working Groups

Below we chronicle different groups that have contributed to the growth of OWC technology. Here, we discuss these groups according to the spectrum used in communication.

1.3.1. IRC working groups

The development of IRC dates back to 1993 when the Infrared Data Association (IrDA) was founded by different companies aiming at developing, reviewing, and promoting standards for IRC [9]. Initially, the IrDA proposed the serial infrared (SIR) protocol. The focus of the SIR protocol is ensuring point-to-point IRC under low cost and energy constraints [34]. Short-range communication, point-to-point, and half-duplex IR links are some of the limitations of the SIR protocol. In order to address these challenges, the IrDA proposed the Advanced Infrared (AIr) protocol in 1999 [29]. Similar to its predecessor, the AIr protocol defines the physical layer and the MAC of IRC. Increased data rate and SNR are some of the benefits of the AIr protocol. Currently, the IEEE 802.15.7 standard is responsible for designing and promoting IRC standards, in particular, the link and physical layer standards [10].

1.3.2. VLC working groups

The first efforts of using LEDs for both illumination and communication can be found in [35] where the authors suggested a novel access network which uses LEDs as access point and light sources. This study attracted attention of many researchers, especially in Japan. Eventually, in 2003 the visible light communication consortium (VLCC) was formed in order to develop standards for VLC-based wireless networks [6]. In 2007, the VLCC proposed two standards, i.e., (i) the visible light communications system standards (CP-1221) and (ii) the visible light ID system standards (CP-1222) [6]. The CP-1221 standards considers two fundamental issues; (i) it prevents fragmentation and proprietary protocols and (ii) it prevents interference among communicating entities. This is achieved by restricting the spectrum used in communication to be between 380 nm and 750 nm and emitted light to be within a specified range with an accuracy of 1 nm. CP-1222 provides several parameters such as 28.8 KHz sub-carrier frequency, 4.8

Kbps transmission rate, and cyclic redundancy check (CRC) for error detection and correction. Later on, the Japan Electronics and Information Technology Association (JEITA) accepted these standards and assigned the following names; JEITA CP-1221 for the VLC system standards and CP-1222 for the visible light ID system standards.

Following these two standards, in 2013 JEITA and VLCC released the visible light beacon system (CP-1223) [8]. The visible light communications associations (VLCA) was founded in 2014 as the successor of the VLCC in standardizing VLC [8]. Furthermore, the Home Gigabit Access (OMEGA) project that is funded by European union has provided remarkable contribution to the development of VLC [36]. One of the objectives of the OMEGA project is developing global standards for VLC-based indoor wireless networks [37]. Following efforts from different groups, the IEEE 802.15.7 Task group is designing and revising different standards for short range optical wireless communication since 2009 [10]. The initial draft of VLC standards from IEEE 802.15.7 was released in 2011.

1.3.3. UVC working groups

The development of outdoor UVC dates back to the 1960s when the UVC-based applications were introduced by different research groups such as [38]. The lack of UVC building blocks (devices such as transmitter and receiver) prevented the development of the UVC technology in the 1980s [20]. This is due to the fact that, available devices by then were not suitable for UVC considering their cost, size, and energy consumption. Recently, researchers such as [39] and [40] have demonstrated that it is possible to exploit avalanche PD for VLC. The development of deep UV LEDs by the Sensor Electronic Technology (SET) Corporation in 2002 revamped the development of UVC technology significantly. Sponsored by the Defense Advanced Research Projects Agency (DARPA), SET developed UV LEDs which could be used in UVC. Moreover, the inception of the DARPA Deep Ultraviolet Avalanche Photodetector (DUVAP) program also stimulated further progress of the UVC technology. While there is significant progress in designing UVC devices, the standardization of UVC technologies is at infancy. Moreover, existing research publications on UVC considers point-to-point and half-duplex communication. Extending UVC into a full-duplex and mesh network is an open research issue.

1.4. Coexistence of VLC and Other Wireless Networks

Over the past decade, researchers have demonstrated significant efforts in VLC industry. Research in solid state lighting, downlink VLC, infrared communication, and hybrid VLC-RF wireless networks are areas that have attracted attention of many researchers. As noted earlier, the realization of VLC depends on exploiting radio frequency or infrared for the uplink channel. Therefore, the co-existence of RF and VLC should be investigated thoroughly. There are several terms in the literature which describe the coexistence of VLC and other technology like IR and RF.

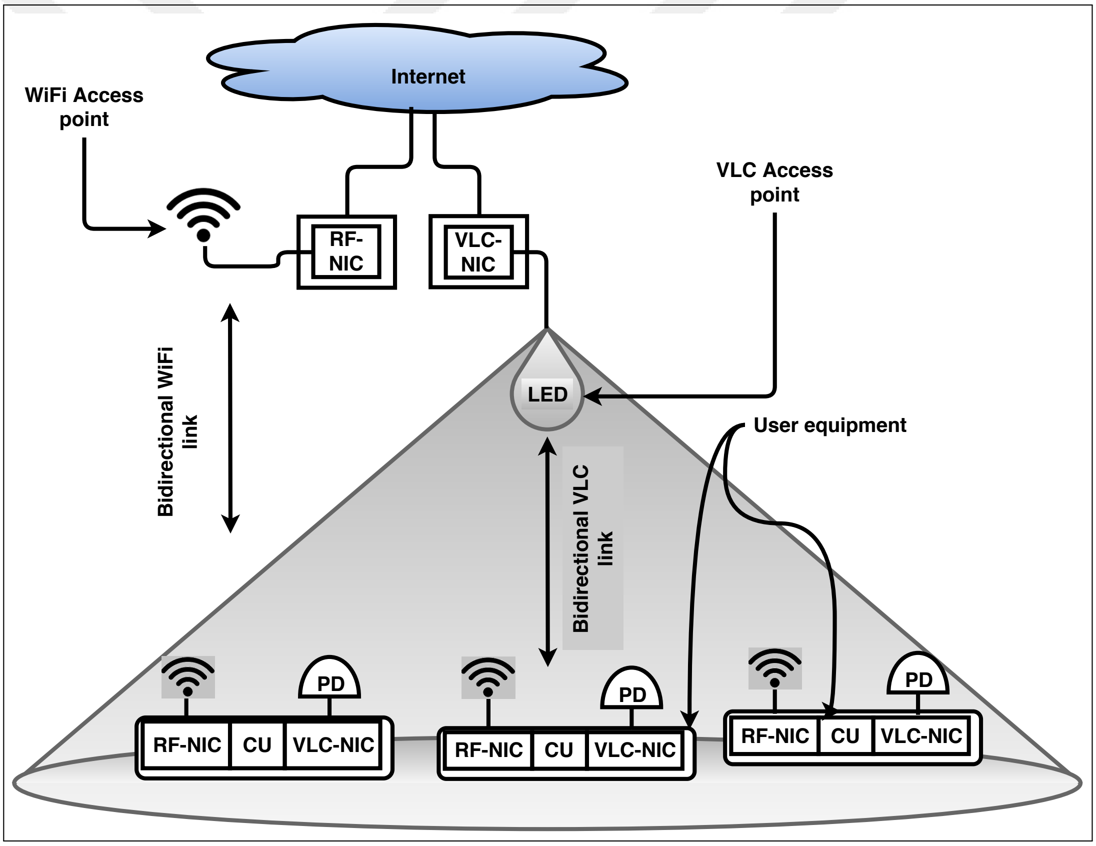

Figure 1.5. Hybrid VLC-RF wireless network.

Hybrid VLC-RF, heterogeneous VLC-RF, and aggregated VLC-RF are the common terms that describe the coexistence of VLC and other wireless networks. The integration of these technology is prompted by the challenge of designing VLC-based uplink channel. In hybrid and heterogeneous VLC-RF wireless networks, VLC and RF wireless networks are implemented as standalone systems that complement each other. In one way, the VLC can be used when there is more internet traffic in RF especially for the downlink channel. Thus, VLC is used to complement RF-based wireless networks in the downlink channel. The realization of hybrid, heterogeneous, and aggregate VLC-RF systems requires proper coordination between the uplink and downlink channel. However, in the aggregate VLC-RF system, RF and VLC are implemented as part of one system each performing a specific role. In general, the RF is used for the uplink channel while the VLC is used in the downlink channel. Figure 1.5 shows the hybrid VLC-RF wireless network and Figure 1.6 shows aggregate VLC-RF wireless network.

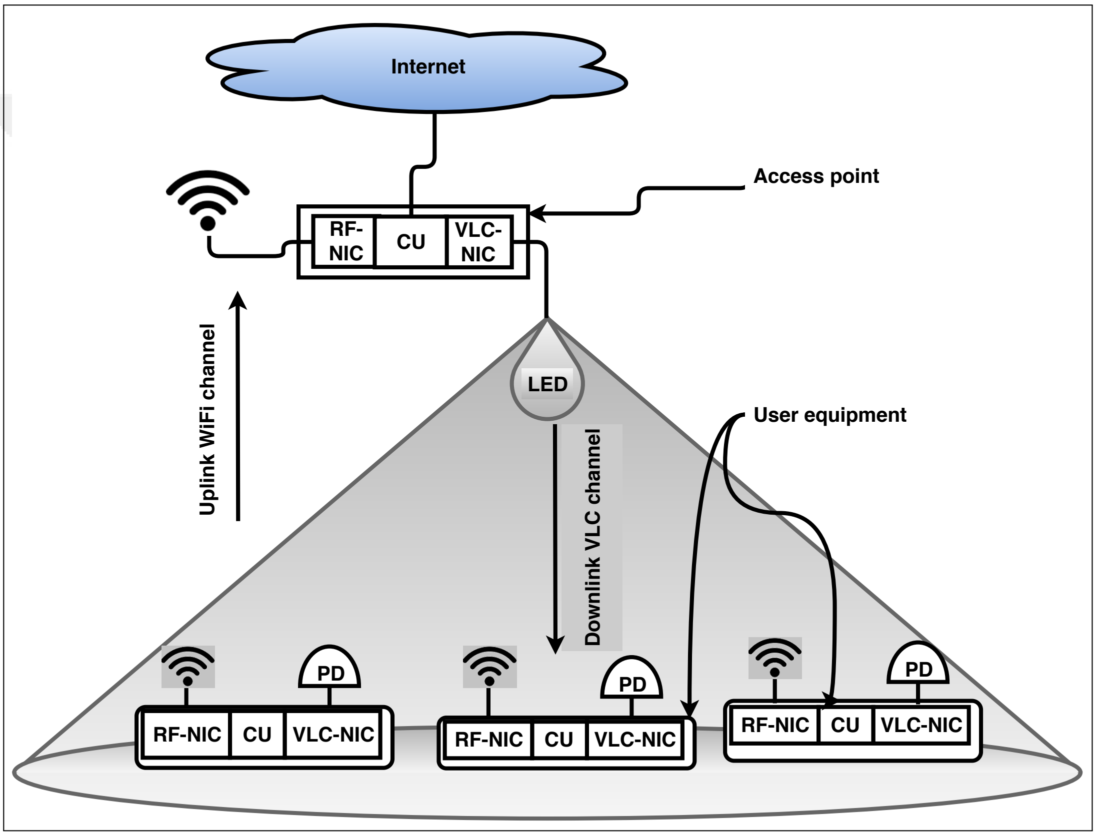

Figure 1.6. Aggregated VLC-RF wireless network.

The review of concepts, opportunities, and challenges of the coexistence of RF and VLC is presented in [41]. The authors explore characteristics of RF and VLC and discuss the possibility of both technologies to coexist. Moreover, the authors in [41] articulate future challenges for the coexistence of VLC-RF wireless networks as follows: (i) the coexistence of CSMA/CA and OFDMA is a future challenge that should be investigated, (ii) channel aggregation should also be studied considering the coexistence of different channels, and (iii) the effects of the two technologies on the upper layer protocols is another interesting area that should be studied extensively, i.e., networking addressing.

In order to improve the capacity of RF-based wireless networks, in [42] an indoor hybrid VLC-RF system is proposed. Numerical results from this study demonstrate improvements in terms of throughput and delay compared to RF standalone system. A practical hybrid VLC-RF wireless network that uses the same link for the uplink and downlink channel is implemented in [43]. In order to achieve full-duplex communication, an indoor hybrid WiFi-VLC wireless network is suggested and implemented in [44]. Experimental results from this study suggest that the hybrid system performs better than the WiFi standalone system in terms of throughput especially in user congested environments.

Energy efficiency hybrid VLC-RF system is demonstrated in [45] wherein the authors formulate the optimization model that minimize energy consumption in VLC-RF system subject to satisfying users' requirement and the acceptable minimum level of illumination. A hybrid VLC-RF based system for video transmission is suggested in [46]. This scheme enhances the quality of transmitted video depending on the quality of the VLC channel. One of the limitations of VLC wireless networks is limited coverage. Thus, in order to increase network coverage, VLC needs to be augmented by RF-based wireless networks. Therefore, the authors in [47] designed and analyzed the hybrid VLC-RF networks. Results from their study show significant improvement in terms of per user data rate network coverage.

The performance of an indoor broadcasting hybrid VLC-RF wireless network is studied in [48]. A novel expression of signal to noise ratio (SNR) is derived in order to evaluate outage performance and bit error rate (BER). Quality of services (QoS) based hybrid VLC-RF wireless networks is investigated in [49, 50]. The authors define the effective capacity of RF and VLC channels based on user distribution and channel gains. Eventually they present a closed-form approximation of the effective capacity of VLC channel. Moreover, in [51] symmetric and asymmetric network topologies for heterogeneous VLC-RF are presented. In this context, VLC small cells are implemented within the RF cells to enhance reliability and continuity of wireless network coverage. In [52], the authors designed and implemented room division multiplexing for hybrid VLC networks. The uplink channel uses WiFi while the downlink channel uses VLC technology. Experimental results from their study demonstrates benefits of the hybrid VLC-RF architecture.

1.5. MAC Protocols for Coexisting VLC and Other Networks

The MAC protocol belongs to the medium access control sub-layer of the data link layer of the open systems interconnection (OSI) network reference model as shown in Figure 1.7. The main function of the MAC sub-layer is data packets transfer between network-interface cards. Accordingly, provision of addressing mechanism and channel access mechanism are core functions of the MAC sub-layer. Considering channel access mechanism, existing MAC protocol can be categorized into three categories as follows [53]:

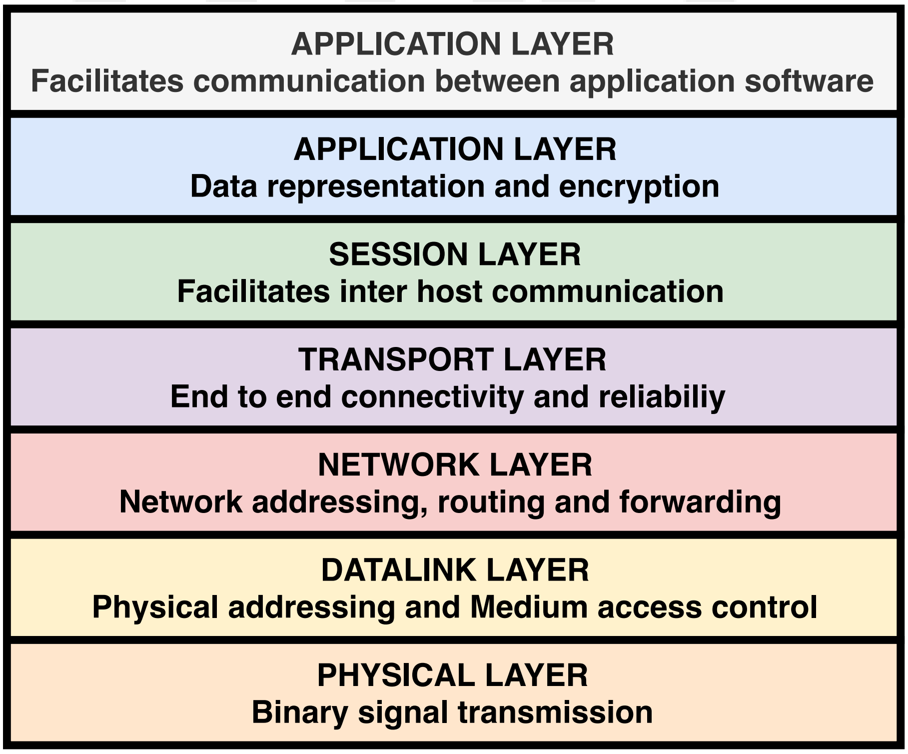

Figure 1.7. OSI network reference model.

(a) Contention based or random access protocols, wherein network devices contend for the use of the channel, thereby prompting collisions. ALOHA, Slotted ALOHA, Carrier Sense Multiple Access (CSMA), and CSMA/CA protocols are good example of this category.

(b) Contention free protocols, in which scheduling occur in a fixed manner and each device is assigned a part of the channel resource. Token passing, random address polling, and polling based protocols fall into this category [54].

(c) Channelization protocols is the third category of MAC protocols. In channelization protocols, a fixed potion of channel resource is assigned to each user based on time or frequency domain. Code division multiple access (CDMA), time division multiple access (TDMA), and frequency division multiple access (FDMA) protocols fall into this category. A combination of these three categories yields the hybrid MAC protocols such as HAMAC, RAH-MAC and WISPER. Figure 1.8 presents the classification of these protocols.

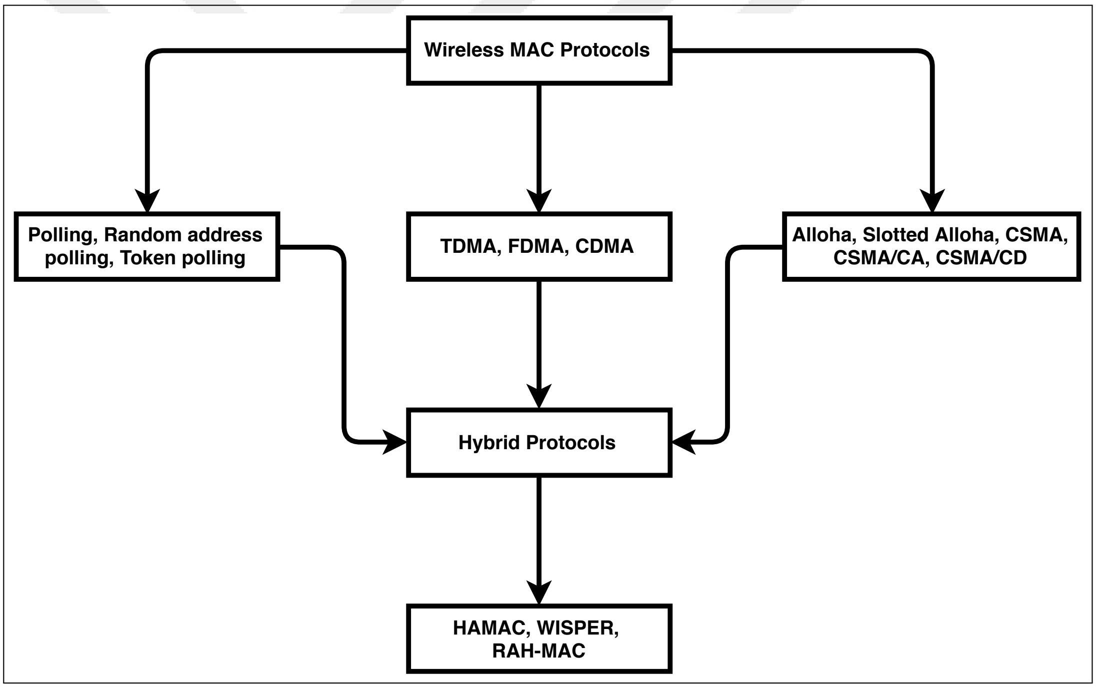

Figure 1.8. Classification of MAC protocols.

Currently, RF-based wireless networks use the CSMA/CA MAC protocol while OFDMA and NOMA are proposed MAC protocols for VLC-based wireless networks [54]. In aggregated and hybrid VLC-RF wireless networks there is the need for designing a new MAC protocol that takes into consideration the coexistence of different devices at the physical layer. Below we chronicle existing MAC protocols for VLC wireless networks. The multi-channel MAC protocol for hybrid VLC-RF wireless networks is presented in [55]. The authors suggest the use of IEEE 802.11 WiFi

CSMA/CA and IEEE 802.15.7 VLC CSMA/CA protocols in hybrid VLC-RF wireless networks and add a new sub-layer MAC protocol, that dynamically selects channels based on channel and traffic aware. Ref. [56] suggests a novel protocol that combines WiFi and VLC for access wireless networks. The designed protocol takes into consideration medium access control and handover aspects. In [57], a VLC-based MAC protocol that combines TDMA and CDMA for vehicle-to-vehicle (V2V) communication is presented. The performance of the system is evaluated based on network throughput, and delay.

The broadcasting MAC protocol for VLC networks is investigated in [58] wherein the authors use the frame synchronization based TDMA to support quality of service (QoS) in VLC based wireless networks. In order to enhance VLC based wireless network coverage and reliability, a cooperative MAC protocol for VLC is presented in [59]. Moreover, in [60] the authors suggest a novel medium access scheme that uses dynamic contention window aiming at improving channel access, and efficiency in VLC systems. Ref. [61] presents the contention-based MAC protocol for VLC wireless networks that minimizes dual transmission over multiple access points. In order to improve the performance of VLC wireless networks under unsaturated conditions, the novel energy efficient medium access scheme is proposed in [62]. Wang *et al.,* in [63] investigate the problem of MAC for VLC wireless networks by taking into consideration full-duplex communication. They propose the use of self-adaptive contention window that increases the probability of uplink and downlink channel transmission.

In [64], the polling-based MAC protocol for wireless networks is presented; wherein the focus is reducing polling overhead, dropping probability, and delay. A novel MAC protocol that combines RF and VLC to provide collisionless medium access is suggested [65]. The proposed protocol in [65] increases throughput by 40% comparing to CSMA/CA. In order to mitigate the problem of signal interference caused by intersecting angle of irradiance, the authors in [63] propose the hidden avoidance enabled CSMA/CA protocol for VLC. The dynamic contention window-based MAC protocol that increases channel utilization for VLC is presented in [60]. Moreover, in [55] a multi-channel MAC protocol for the integration of VLC and radio waves networks is presented. In a nutshell, the problem of MAC in VLC is not well investigated especially when the coexistence of VLC and other wireless networks is taken into consideration. In addition, most of existing research works on MAC protocols for VLC wireless networks assume that VLC standalone systems can provide full-duplex communication, this assumption is not realistic considering the limitations of using VLC in the uplink channel. A summary of existing MAC protocols for VLC is presented in Table 1.2.

1.6. The Contribution of this Thesis

In this thesis, we investigate the problem of MAC for aggregated VLC and other wireless networks. We explore: (i) the physical properties of VLC technology, then we consider, (ii) the coexistence of VLC and RF, (iii) implementation of full-duplex communication in aggregated VLC and other wireless networks and (iv) existing MAC protocols for both VLC and RF. It can be seen that, currently, there is no MAC protocol that takes into account the coexistence of VLC and other wireless networks as a single system. In Chapter 1, we chronicle the type, properties, and challenges of optical wireless networks (OWC). We also highlight MAC protocols for VLC currently available in the literature. By leveraging available information, we address the problem of MAC for aggregated VLC and other wireless networks as a two folds:

First is the design of MAC protocol for aggregated VLC-IR wireless networks. IR can be used for the uplink channel in VLC wireless network. We propose the MAC protocol named Adaptive Polling MAC protocol (APMAC) for aggregated VLC-IR wireless networks. In this context, the VLC-IR wireless network system is a full-duplex system. VLC works for the downlink channel and IR is responsible for the uplink channel. Such kind of a system improves the performance of system significantly. The APMAC protocol improves the performance of VLC-IR systems in terms of delay, throughput, utilization, and fairness significantly. Chapter 3 provides sufficient description about the APMAC protocol.

Second is the design of MAC protocol for aggregated VLC-RF wireless networks.

Table 1.2. A summary of research publications on MAC protocols for VLC-based wireless networks.

Reference	**Type of MAC**	**Medium**	**Collision**	**Delay**	**Utilization**	**Fairness**	**Throughput**	**Energy efficiency**
[54]	Non-contention	VLC and IR	χ	✓	✓	✓	✓	χ
[55]	Contention	RF and VLC	χ	✓	✓	χ	✓	χ
[57]	Channelization (TDMA and CDMA)	VLC	χ	✓	χ	χ	✓	χ
[60]	Contention	VLC	χ	✓	✓	✓	✓	χ
[61]	Contention	VLC	χ	χ	χ	χ	✓	χ
[62]	Contention	VLC	χ	χ	χ	χ	✓	✓
[63]	Contention	VLC	χ	χ	χ	χ	✓	χ
[64]	Non-contention	RF	✓	✓	χ	χ	χ	χ
[65]	Contention	RF and VLC	χ	χ	χ	χ	✓	χ
[66]	Channelization (TDMA)	VLC	χ	χ	χ	χ	✓	χ
[67]	Channelization (TDM)	VLC	χ	χ	χ	χ	✓	χ
[68]	Contention	VLC	✓	✓	χ	χ	✓	✓
[69]	Contention	RF and VLC	✓	✓	✓	✓	✓	✓
SA-MAC (Chapter 4)	Contention	RF and VLC	✓	✓	✓	✓	✓	✓

Here, the uplink channel uses RF while the downlink channel uses VLC. The VLC and RF work together as a single system to provide bidirectional communication. We propose the Self-Adaptive MAC (SA-MAC) protocol for aggregated VLC-RF wireless networks. The objective is minimizing delay, collision, and energy consumption while maximizing throughput. Moreover, we provide the Markov chain model that analyzes the performance of our protocol under varying conditions. Sufficient details about the SA-MAC protocol can be found in Chapter 4.

Besides designing these protocols, we conduct simulations of these protocols by using the NS3 discrete event network simulator and we present numerical results that show potential benefits of this thesis. In a nutshell, this thesis introduces a new problem for network users, and we explored the problem in details. We believe that, this thesis has significant contribution to the internet industry and the general public.

1.7. Thesis Outline

In Chapter 1 we discuss motivating factors for the development and applications of OWC technologies. Classifications of OWC technologies, working groups, and applications are also presented. In addition, we briefly discuss the coexistence of VLC and other wireless networks such IR and RF.

A brief discussion of the VLC technology is presented in Chapter 2 where we present the basic architecture of VLC system and its main building blocks, i.e., transmitter, receiver, and channel. In addition, VLC link configuration, modulation techniques, and VLC based MAC protocols are discussed. We conclude Chapter 2 by highlighting challenges of VLC wireless networks.

The realization of the uplink channel in VLC wireless networks is very challenging because of several limitations such as energy efficiency and visual disturbances. In order to achieve full-duplex network, the use of IR and RF for the uplink channel in VLC wireless networks has been demonstrated as the potential solution. Therefore, we study the problem of MAC protocol for aggregated VLC and other wireless networks as the two folds, i.e., (i) aggregated VLC-IR wireless networks in Chapter 3, and (ii) aggregated VLC-RF wireless networks in Chapter 4.

The MAC protocol for aggregated VLC-IR wireless networks is presented in Chapter 3. In this context, we suppose that the VLC wireless networks provides the downlink while the IR provides the uplink channel. We design the MAC protocol that defines the mechanism of channel access for aggregated VLC-IR wireless networks. We evaluate the performance of our protocol by running the simulation on the NS3 network simulator. In evaluating our results, we consider network fairness, throughput, collision, utilization, and delay.

We extend our study by considering the hybrid VLC-RF wireless network in Chapter 4. Here, we assume that VLC provides the downlink channel whereas the uplink channel is achieved by using the RF channel. We present the Markov chain model that analyzes the performance of our protocol in steady state. In addition, we simulate our protocol in NS3 network simulator and obtain the results by taking into consideration the following performance metrics; throughput, collision, delay, and energy consumption. Eventually, we present our results by comparing them with conventional MAC protocols.

2. VISIBLE LIGHT COMMUNICATION

VLC is the type of OWC that exploits the visible light spectrum (from 380 nm to 750 nm) for propagation of signals. The emergence of low powered and energy efficiency white light LEDs has attracted the rise of VLC technology [70]. The huge bandwidth available in the visible light spectrum can significantly address the ever increasing bandwidth demand. There are several advantages of using VLC such as immunity to electromagnetic interference, it is unlicensed, and signal propagation can be controlled thereby alleviating the problem of eavesdroppers. In addition, VLC does not have any health risk to human being. Moreover, ubiquitous availability of LEDs in lighting infrastructure reduces the cost of installing VLC systems. VLC has many applications such as indoor wireless networks, transport communication system, health care communication systems, underwater communication systems, and other domains where communication via radio spectrum cannot be realized because of challenges like electromagnetic interference. Uplink realization, field of view (FOV) alignment, receiver design, mobility, coverage, and interference are the main challenges facing the realization of OWC technologies such as VLC. In terms of link configuration, VLC supports both the LOS and the NLOS link configurations. However, in NLOS link configuration, the performance of VLC systems deteriorates [14].

2.1. VLC Building Components

VLC belongs to the OWC family, therefore, the physical properties of OWC cannot be ignored in VLC systems. A simple VLC system consists of three parts: a transmitter, a channel, and a receiver. Figure 2.1 demonstrates the relationship between these parts. Generally, a VLC transmitter consists of devices for coding, modulation, conversion of electrical to optical (E/O) signals and an LED for transmitting optical signals. On the other hand, a VLC receiver includes a PD for detecting optical signals, optical to electrical (O/E) signals conversion device, demodulator, and channel decoding devices. Moreover, optical channel depends on the orientation of the transmitter and receiver,

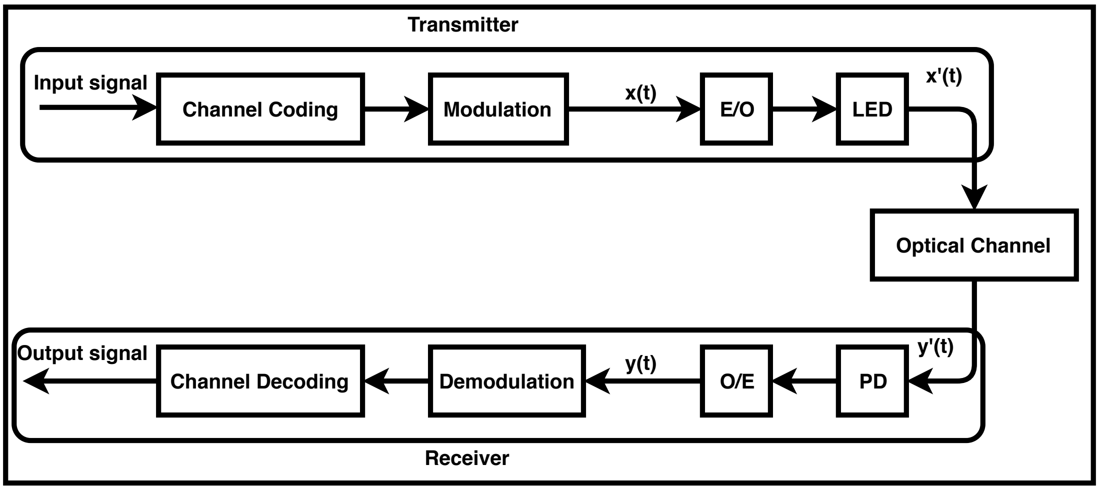

Figure 2.1. A sample VLC system.

i.e. LOS or NLOS link configuration. Nonetheless, VLC systems perform better in LOS link configuration, the NLOS configuration deteriorates the performance of VLC systems significantly. At the VLC transmitter, signals from the source are modulated and added to a DC voltage that powers the LED. Consequently, the LED produces light and simultaneously transmit signals through optical channel. At the receiver, the PD detects the light and converts it to electrical signals. Note that, light detected by the PD is composed of noise from the channel. Figure 2.2 shows the VLC system model in electrical and optical domains.

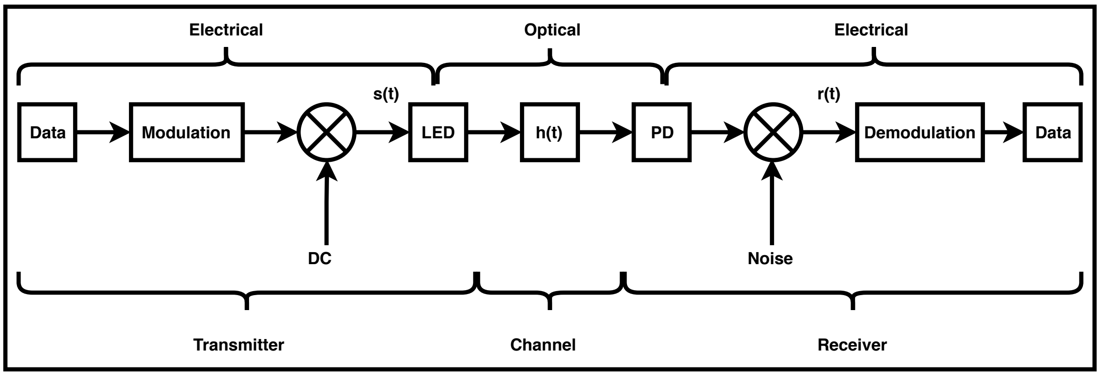

Figure 2.2. The basic VLC system channel model.

2.2. VLC Transmitter

LEDs are main parts of a VLC system because they are responsible for conveying electrical signals to optical signals. In principle, both Laser diodes (LDs) and LEDs can be used in VLC transmitter. However, LEDs are durable, cost effective, and can be modulated at high speed. Accordingly, they are preferred for lighting and networking purpose. In addition, LDs produce high output optical power compared to LEDs, that is harmful to human eyes. Therefore, they are not suitable for indoor application. Moreover, LEDs consume less energy compared to LDs, this is another factor that makes LEDs suitable for indoor and other applications where energy efficiency is important. Thus, white light LEDs are potential candidates for data transmission in VLC. White light LEDs can be produced in two ways, (i) single coloured LED such as blue LED with phosphor, and (ii) multi-colour LEDs such as RGB LED [70].

In Figure 2.3, we show the orientation of single colour and multi-colour LEDs in VLC systems. Blue colour LED with Phosphor are cheap and easy to implement. Nevertheless, they are not preferred in communication because the phosphor coating limits the operating speed of the LED [70]. Multi-colour LEDs are preferred because they provide an opportunity of using colour shift keying (CSK) modulation and enhancing multi-users access. There are three common methods of producing multi-colour LEDs namely dichromatic, trichromatic, and tetrachromatic. However, trichromatic (red, green, and blue) method is the most preferred way considering its high bandwidth and data rate [2].

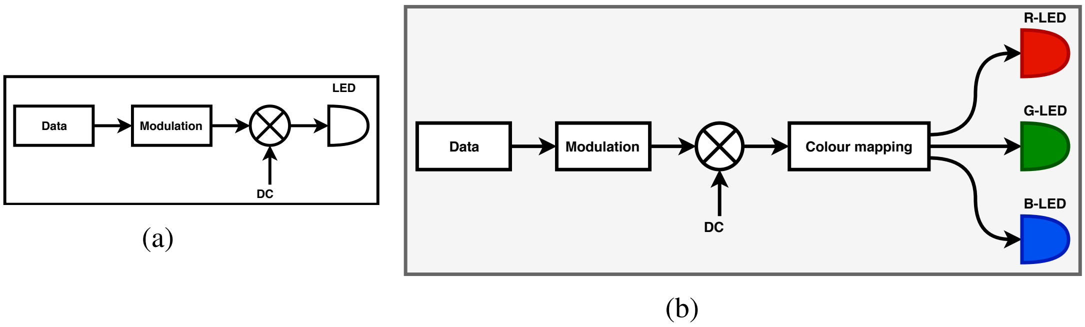

Figure 2.3. Single LED in 2.3a and Multi-colour LEDs in 2.3b.

2.3. VLC Receiver

In VLC systems, PD also referred as photodetector, and camera sensor also known as imaging sensor can be used to detect signals from LEDs [71]. Photodetectors are semiconductor devices that can receive and convert light into electric current. Existing commercial photodetectors can convert received light at high rates [72]. Camera sensors can also be used to receive visible light signals. They consist of many photodetectors organized in a matrix on a circuit. The ubiquitous availability of camera sensors in mobile devices such as smartphones makes them potential candidate for VLC receivers. Nevertheless, image sensor requires a high number of photodetectors in order to achieve high resolution image. Accordingly, the use of camera sensor for signal detection contributes to low data rate. Unlike image sensors, existing standalone PDs have proved to provide high data rates, therefore, they are the preferred for signal detection in VLC systems and other OWC systems like IRC systems. The basic building blocks of the VLC receiver are optical filter (OF), PD, optical to electrical converter, demodulating unit, and signal decoding unit. Light rays pass through OF before reaching PD. Figure 2.4 shows the basic architecture of a VLC receiver.

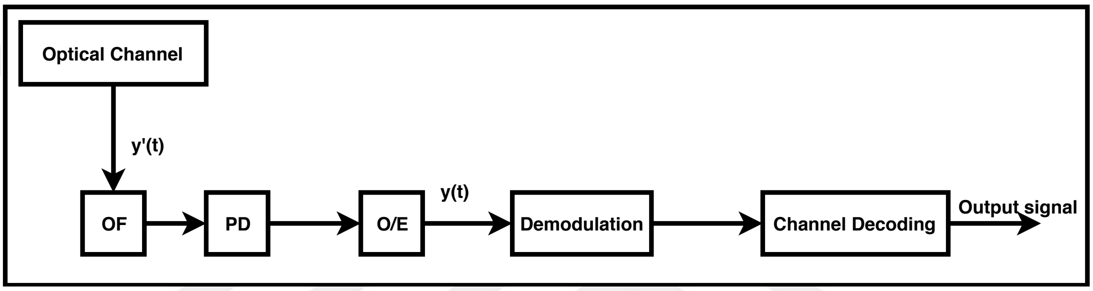

Figure 2.4. The basic architecture of a VLC receiver.

2.4. VLC Link Configuration

Generally, in OWC there are main two types of link configurations, viz., LOS and NLOS link configurations. LOS and NLOS link configurations can be combined with directed, non-directed, and hybrid configuration, thereby forming six configurations [4]. Figure 2.5 shows the combination of LOS, NLOS, and directionality of transmitter and receiver. VLC systems can operate in both LOS and NLOS link configurations, however, in NLOS link configuration, the performance of VLC systems deteriorates significantly [73]. NLOS link configuration is suitable for IRC and UVC [74].

2.5. VLC Channel Model

Generally, in communication, the channel refers to the space that separate a transmitter and a receiver. Similarly, in VLC systems the channel is the space that separates the transmitter (LED) and the receiver (PD). The main characteristics of a channel are: the ability to transmit carrier signals, noise, interference, and attenuation. VLC channels, like other OWC channels are affected by channel distortion. In the literature, OWC

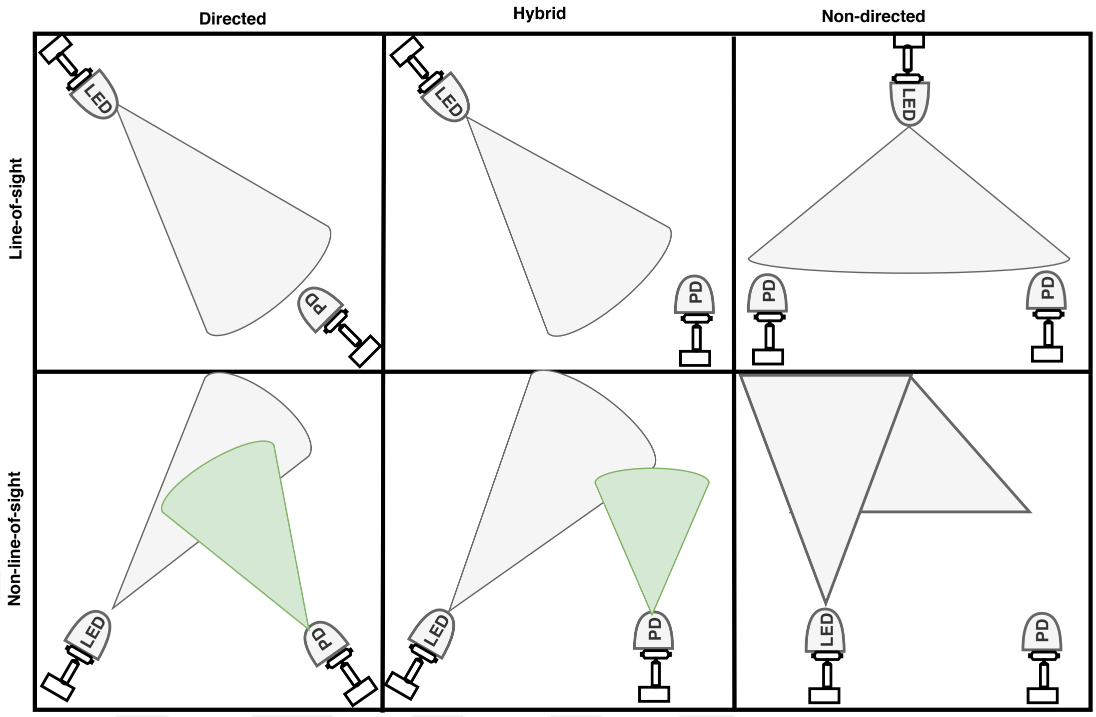

Figure 2.5. Link configuration in OWC.

channels can be modeled as a linear time-variant (LTI) that consists of the following parameters: (i) input intensity x(t), (ii) output intensity y(t), and (iii) impulse response h(t). Figure 2.6 shows the relationship between these parameters.

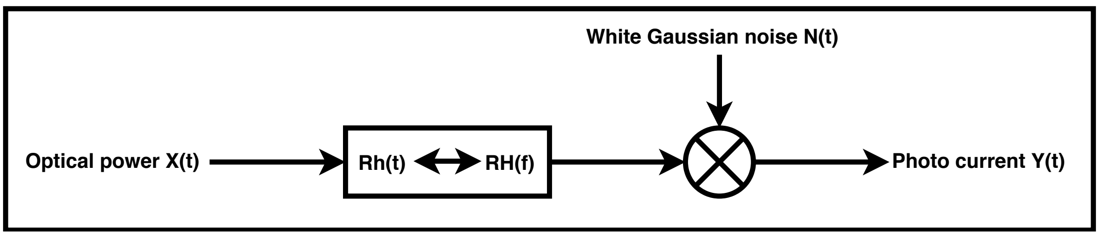

Figure 2.6. VLC channel model as baseband linear and time-variant.

For a given physical design of transmitter and receiver, the impulse response is fixed [74, 75]. Moreover, for an infinity short optical pulse transmitted, the channel impulse response (CIR) is the time evolution of the received signal by the receiver. CIR can be used to determine the output of the VLC system in the time domain. Given the CIR of the system, it is possible to predict the system output and waveform distortion that is caused by multipath propagation. The relationship between input intensity, output intensity, and impulse response can be used to represent the baseband model of the

VLC channel as follows [72, 74–76]:

$$y(t) = Rx(t) \otimes h(t) + n(t) \tag{2.1}$$

where R refers to the detector responsivity, n(t) is the additive white Gaussian noise (AWGN), and the symbol $\otimes$ denotes the convolution. VLC systems and other OWC differ from other transmission systems such as radio and electrical systems because the channel input in Equation 2.1 represents the non-negative instantaneous optical power, i.e., $x(t) > 0$. Average optical power transmitted is governed by the relation,

$$P_t = \lim_{T\to\infty} \frac{1}{2T} \int_{-T}^{T} x(t)dt, \tag{2.2}$$

and the average received optical power is mathematically written as [76]

$$P_r = H(0)P_t. \tag{2.3}$$

Moreover, the signal-to-noise ratio (SNR) of a unipolar system with intensity modulation is proportional to the square of the channel DC gain [76].

$$SNR = \frac{R^2 P_r^2}{R_b N_0} = \frac{H^2(0) P_t^2}{R_b N_0} \tag{2.4}$$

Furthermore, the channel gain of VLC systems, which is a fraction of power detected by the receiver has been investigated in [74] and [76]. The channel DC gain H(0) of a VLC system is expressed in terms of frequency response as follows [74, 77, 78]:

$$H(0) = \int_{-\infty}^{\infty} h(t)dt. \tag{2.5}$$

Note that, Equation 2.5 is commonly known as channel DC gain and alternatively, can be expressed in frequency domain as follows [76]:

$$H(f) = \int_{-\infty}^{\infty} h(t)e^{-j2\pi ft}d(t). \tag{2.6}$$

Furthermore, the channel DC gain of a VLC channel can be determined based on the geometry of the LED, reflector, and PD. We demonstrate the basic geometry of the VLC downlink channel in Figure 2.7. Here, the LOS is the straight line between the access point i and the user device u. The distance between i and u is denoted by $d_{i,u}$. Moreover, the angles of incidence and irradiance for the LOS link configuration are $\psi_{i,u}$ and $\phi_{i,u}$ respectively. Based on these parameters, the LOS channel DC gain between the access point i and node u can be written as [76, 79].

$$H_{i,u}^{LOS} = \frac{(m+1)A_{pd}}{2\pi d_{i,u}^2}\cos^m(\phi_{i,u})g_f g_c(\psi_{i,u})\cos(\psi_{i,u}). \tag{2.7}$$

Note that, m refers to the Lambertian emission order and it is determined by the following relation

$$m = -\ln 2/\ln\cos(\Phi_{1/2}), \tag{2.8}$$

where, $\Phi_{1/2}$ refers to the angle of radiation at which the intensity is half of the intensity at the main-beam direction. Apd is physical area of the PD, g_f and $g_c(\psi_{i,u})$ denote the gain of the optical filter and the gain of the optical concentrator respectively.

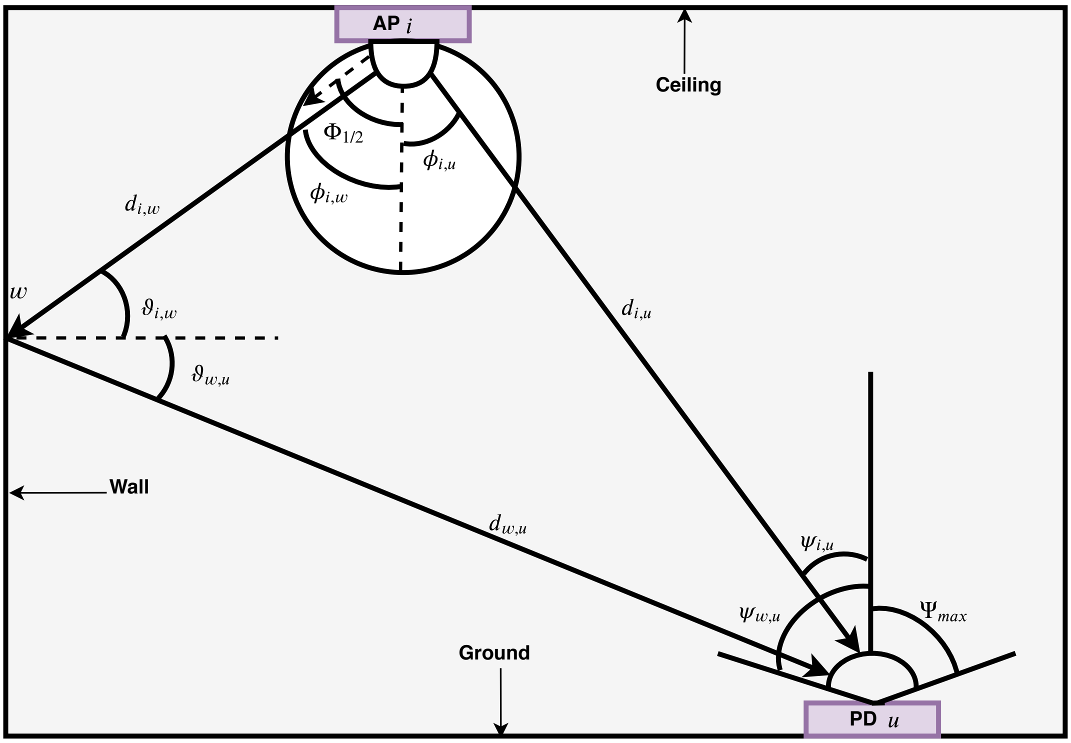

Figure 2.7. The geometry of a VLC downlink channel for both LOS and NLOS link.

For simplicity and without loss of generality, in LOS configuration, first-order reflection is considered only. In VLC, first-order reflection includes two segments, viz., from the access point to the wall and from the wall to the user. In Figure 2.7, the distance of these portions are represented by $d_{i,w}$ and $d_{w,u}$ respectively. Moreover, for the first segment the angle of radiance and incidence are given as $\phi_{i,w}$ and $\vartheta_{i,w}$; while for the second segment, the angle of radiance and incidence are defined as $\vartheta_{w,u}$ and $\psi_{w,u}$. The delay due to propagation in indoor environment is very short, therefore, it is often neglected. Thus, it is assumed that signals from different sources arrive at the same time. Accordingly, the NLOS channel of a VLC channel can be represented mathematically as follows [79].

$$H_{i,u}^{NLOS} = \int_{A_w} \frac{(m+1)A_{pd}}{2(\pi d_{i,w} d_{w,u})^2} \rho_w \cos^m(\phi_{i,w}) g_f g_c(\psi_{w,u}) \cos(\psi_{w,u}) \cos(\vartheta_{i,w}) \cos(\vartheta_{w,u}) dA_w \tag{2.9}$$

Here, Aw refers to the reflective area on the wall, and ρ_w is the reflectivity of the wall. By combining Equations 2.7 and 2.9, we get the total DC channel gain from the access point to the receivers:

$$H_{i,u} = H_{i,u}^{LOS} + H_{i,u}^{NLOS} \tag{2.10}$$

While the channel model described in this section can be applied for all types of OWCs, the performance of each type of OWC differs significantly. Figure 2.8, shows the channel DC gain versus distance for VLC and IRC adopted from [77].

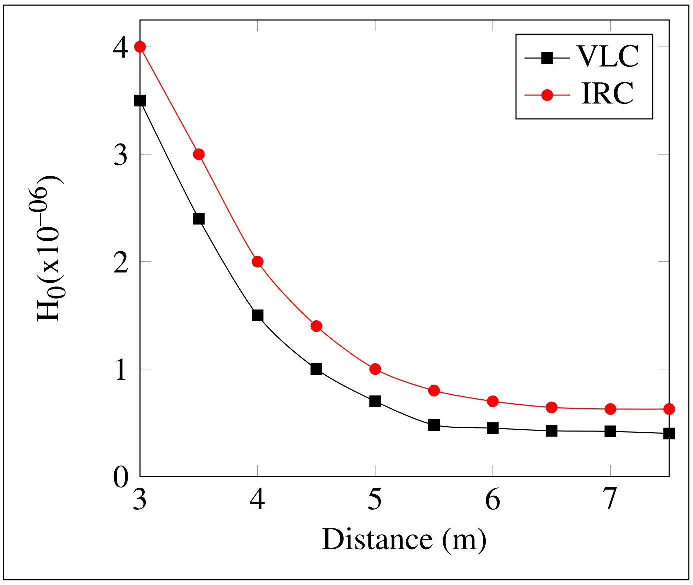

Figure 2.8. Distance versus channel DC gain.

2.6. VLC Modulation Techniques

This section highlights digital modulation techniques applicable in VLC. In principle VLC uses electromagnetic radiation for transmission of signals. Existing RF wireless networks based modulation techniques can be exploited in VLC if they are slightly modified to meet VLC specific requirements. In general, VLC modulation techniques can be categorized into single-carrier modulation (SCM), multi-carrier modulation (MCM) techniques, and VLC specific modulation techniques [80].

2.6.1. Single-carrier modulation (SCM)

Existing RF wireless networks modulation techniques that can be considered as SCM are (i) on-off keying (OOK), (ii) pulse position modulation (PPM), and (iii) pulse amplitude modulation (PAM) [11, 76]. In OOK modulation technique data can be transmitted sequentially by turning on and off the LED. Accordingly, it can ensure dimming support by adjusting the ON/OFF levels of LED or by using symbol compensation [10]. It is possible to maintain the same data rate when dimming by adjusting the ON/OFF levels of the LED, however, low dimming levels decreases the reliable communication range. The main advantage of OOK modulation technique is that its circuits are simple and inexpensive. However, OOK is severely affected by atmospheric noise. Another variation of SCM is PPM, this is more efficient in terms of power but with low spectral efficiency compared to OOK. Variable pulse position modulation (VPPM) is one form of PPM that is more suitable for VLC because it supports dimming by adjusting the size of signal pulses based on a specific level of brightness [81].

2.6.2. Multi-carrier modulation (MCM)

At high data rates, SCM techniques such as OOK and PPM are affected by non-linear signal distortion and inter-symbol interference. Therefore, researchers focus more on MCM techniques than SCM techniques. In addition, MCM provides more bandwidth efficient, however, MCM requires more energy than SCM [11]. OFDM is one variation of MCM in which data streams are transmitted simultaneously by using orthogonal sub-carriers [82]. The implementation of OFDM with intensity modulation (IM) in VLC wireless networks has been demonstrated in [83] and [84], the results from these studies are promising. Nevertheless, some modifications should be done to the conventional OFDM techniques in order to exploit intensity modulation with direct detection (IM/DD) in VLC wireless networks.

There are several variations of OFDM in the literature such as; (i) the coherent optical orthogonal frequency division multiplexing (CO-OFDM) suggested in [85], (ii) the fast orthogonal frequency division multiplexing (F-OFDM) investigated in [86], (iii) reshaped orthogonal frequency division multiplexing (R-OFDM) presented in [87], (iv) polarity reversed optical OFDM (PRO-OFDM) discussed in [88, 89], and (iv) DC biased optical OFDM (DCO-OFDM) and asymmetrically clipped optical OFDM (ACO-OFDM) [90]. Nonetheless, OFDM is vulnerable to channel, source, and amplifier non-linearities due to high peak-to-average power ratio (PAPR) [91]. This factor limits the possibility of using OFDM in OWC systems that require high average power. A novel modulation technique named Hadamard coded modulation (HCM) is presented in [92] and [93] as an alternative to OFDM. In HCM signal are modulated by using the fast Walsh-Hadamard transform (FWHT) instead of OFDM. Results from this study demonstrate that: (i) HCM performs better on average power unconstrained OWC systems such as VLC, (ii) when exploited in VLC systems, HCM yields lower bit error rate than OFDM.

2.6.3. VLC specific modulation techniques

VLC transmitters are expected to perform duo functions, i.e., illumination and providing wireless connection. These objectives can be realized by using white LEDs that involve color mixing or blue LEDs with yellow phosphorous coating. Multi-coloured LEDs provide more options for signal modulation in VLC systems than single coloured LEDs. Signals can be encoded into colour intensities that are emitted by multi-coloured LEDs. Accordingly, the colour shift keying (CSK) has been suggested as the potential modulation technique for VLC in [10]. The performance analysis of the CSK presented in [94] suggests that all the colour band combination in CSK yield different values of BER. A novel CSK modulation technique named metameric modulation (MM) is suggested in [95]. Results suggest that, MM is more energy efficiency and offers colour quality control.

In order to increase communication capacity, the authors in [96] suggest the colour intensity modulation (CIM) that can be exploited in orthogonal and non-orthogonal channels. Another variation of CSK modulation is the digital colour shift keying (DCSK) modulation presented in [97]. The DCSK gives better results than conventional CSK in terms of BER. In order to incorporate spatial modulation with CSK, the authors in [98] present a multi-colour LED specified bipolar CSK modulation for VLC wireless networks. This scheme optimizes CSK constellation thereby enhancing BER in VLC systems. Intensity modulation with direct detection (IM/DD) is another VLC specific modulation techniques in which there is no need of phase information, the power or intensity of light from a LED is modulated by the information bits [99].

There are two advantages of CSK modulation over IM/DD techniques: (i) CSK modulation guarantee constant luminous flux thereby eliminating the flicker effect, (ii) the constant luminous flux improves the reliability of the LED. The recent index modulation (IM) technique demonstrated in [100] can be exploited in VLC to give better results. Furthermore, the generalized LED index modulation (GLIM) for VLC wireless networks suggested in [101–103] has demonstrated significant performance improvement in VLC wireless networks. A summary of different modulation techniques is presented in Table 2.1.

2.7. VLC MAC Protocols

In a network where there are multiple nodes, control of medium access is very important for the well-functioning of a network. In the literature, there are three MAC schemes proposed for VLC wireless networks, viz, Carrier Sense Multiple Access (CSMA), Orthogonal Frequency Division Multiple Access (OFDMA), and Code Division Multiple Access (CDMA). The IEEE 802.15.7 standard proposes the use of the CSMA/CA with two options, i.e., beacon enabled and beacon disabled CSMA/CA. In beacon enabled CSMA/CA, the interval between two consecutive beacons is the duration of a superframe. A superframe contains three periods namely beacon duration, contention access period (CAP), and contention free period (CFP). A device locates the beginning of the next CAP before transmitting. Then it begins transmitting if the channel is found idle, otherwise, it waits for a random back-off time before performing the clear channel assessment (CCA) again. Note that, in CFP each node is assigned its timeslot, therefore, there is no collision. In the beacon disabled scheme, nodes use the conventional un-slotted random access with CSMA. Ref. [104] suggests the CSMA/CA-based MAC protocol for VLC that uses OOK modulation. In [105], the authors extended the MAC protocol suggested in [104] by taking into account multiple FOV.

The OFDMA is an extension of OFDM that supports multi-carrier multiple access. Here, users are assigned resource blocks (sub-carriers in a given time) in exclusive manner for transmitting and receiving data. In the literature, there are two variations of OFDMA, i.e., the optical orthogonal frequency division multiple access (O-OFDMA), and the optical orthogonal frequency division multiplexing interleave division multiple access (O-OFDM-IDMA) [70]. A comparison of these techniques has been done in [106] where results demonstrated that decoding complexity and energy efficiency are major limitations of using OFDMA in VLC wireless networks. In order to avoid interference, Ref. [107] suggests a heuristic algorithm for sub-carrier assignment problem.

Conventional CDMA protocol can be modified and used in VLC wireless networks. Optical CDMA (OCDMA) is a variation of conventional CDMA that uses optical orthogonal codes to provide access to multiple users sharing the same channel. Each device is given a sequence of binary numbers known as optical orthogonal codes (OOC), therefore, data are encoded by turning the LED on and off in time domain [108]. A thoroughly investigation of OCDMA can be found in [109] and [110]. Ref. [108] demonstrates that synchronous OCDMA can be used in VLC by OOC, OOK modulation, and conventional LEDs. The drawback of using OCDMA in VLC wireless networks is that it requires long codes to achieve high optimality. This requirement reduces the data rate of VLC wireless networks. In order to address the challenge of using long codes, the authors in [111] propose the use of code cycle modulation (CCM). In CCM an M-array bits of information is transmitted by different cyclic shifts of the

Table 2.1. A summary of VLC modulation techniques

Modulation type	Modulation method	References	Spectral Efficiency	Energy Efficiency	System Complexity	Data Rate	Dimming Control	Flicker Effect
Single carrier modulation	OOK	[87]	✓	✓	✓	✓	✓	✓
	PPM	[87]	✓	✓	✓	✓	χ	χ
	VPPM	[87]	✓	✓	✓	✓	✓	✓
Multi carrier modulation	OFDM	[84, 101]	✓	χ	✓	✓	✓	✓
	CO-OFDM	[84, 101]	✓	✓	✓	✓	✓	✓
	F-OFDM	[84, 101]	✓	✓	✓	✓	✓	✓
	R-OFDM	[87]	✓	χ	✓	✓	✓	✓
	DCO-OFDM	[90]	✓	χ	✓	✓	✓	✓
	ACO-OFDM	[90]	χ	✓	✓	✓	✓	✓
	PRO-OFDM	[89]	✓	χ	✓	✓	✓	✓
VLC specific modulation	CSK	[94, 97, 121]	✓	χ	✓	✓	✓	χ
	CIM	[96]	✓	✓	✓	✓	✓	✓
	GLIM	[101–103]	✓	χ	✓	✓	✓	✓
	HCM	[92, 93]	✓	✓	✓	✓	✓	✓
	IM/DD	[99]	✓	χ	χ	✓	χ	χ

sequence. Although CCM increases spectral efficiency, it cannot provide dimming support, a potential drawback for using it in VLC wireless networks [112]-[113].

It is difficult to generate OOC when the network size is very large. In [114], the authors propose the random optical code that generates random codes. Results from their study show that random codes can be easily generated for the large number of users, nonetheless, the codes generated are not optimal. Ref. [115] presents the performance analysis of random codes by taking into account the spectral efficiency and the limit of random codes. A new variation of CDMA for VLC is a combination of OCDMA and CSK modulation with trichromatic LED transmitter [116]-[117]. Furthermore, in [118] a hybrid protocol that combines CDMA and OFDM is suggested. A polling based protocol for indoor VLC wireless networks is suggested in [119]. Results from this study reveal that the proposed MAC protocol improves VLC wireless networks performance in terms of delay and throughput compared to conventional MAC protocol. A comprehensive review of VLC specific MAC protocols is provided in [120].

2.8. Challenges of VLC Wireless Networks

Although there is significant effort in advancing the VLC technology, researchers put more efforts on the physical layer only. There is little effort to integrate VLC systems into existing internet industry. For instance, existing research publications assume (i) a point to point communication scenario with one transmitter and one receiver, (ii) half-duplex communication, (iii) consider device to device communication instead of application to application communication etc. These assumptions limit the realization of VLC wireless networks because they ignore actual communication aspects such as bidirectional communication and multi-point communication. Below we describe main challenges facing VLC wireless networks.

2.8.1. Uplink augmentation

Existing research publications on VLC wireless network focus on half-duplex communication (downlink channel) where the LED at the ceiling of a building performs duo functions, viz, illumination and data transmission. This assumption is problematic because it does not offer any description about how the uplink channel can be achieved in VLC wireless networks. Although existing mobile devices contains efficient LEDs such as flashlight cameras, these LEDs cannot be used in VLC wireless networks. This is due to the fact that turning on the LED constantly consumes a significant amount of energy and can cause visual disturbances to users [122]. In order to ensure full-duplex communication in VLC wireless networks, the use of radio or infrared frequency for the uplink channel has been proposed in [37, 42, 44, 54, 70]. Accordingly, VLC and RF or VLC and IRC can coexist as a single system of heterogeneous systems that complement each other. The use of RF-based system for uplink transmission is more ideal because existing mobile devices contains WiFi devices. Nevertheless, the coexistence of VLC and other wireless networks prompts other challenges such as network addressing, MAC, and network management. The potential benefits of VLC wireless networks cannot be attained without addressing these challenges.

2.8.2. Network addressing challenge

When VLC wireless network is complemented by other wireless network technology, network addressing can be problematic in particular when the higher layer of the OSI model such as transport layer is considered. This is because the introduction of another medium imposes the need of another physical devices for modulating and demodulating signals. Consider the transmission control protocol (TCP) communication scenario where a connection between a client and a server is established by using the three-way handshaking mechanism. After establishing a connection, a client generates a synchronize (SYN) message and encapsulates it in the internet protocol (IP) header before sending it by using network interface card (NIC). The client listens to the socket that contains TCP port number and IP address used to generate and encapsulate the SYN message. In this context, any reply packets received from the server with different NIC and different socket details are ignored. In the coexistence of VLC and other wireless networks, the uplink channel is provided by different NIC. Therefore, packets from the server will be ignored. Providing a solution to the network addressing problem from the physical device point of view is rudimentary to eradicate this challenge.

2.8.3. Mobility and coverage

As noted earlier, most of the existing research in VLC wireless networks focus on physical layer while paying little attention to the higher layer of the OSI model. In addition, they focus on stationary devices where the LEDs at the ceiling are assumed to be the access point and the user devices are assumed to be stationary devices located at the ground. This assumption is not realistic because user devices are not always fixed. VLC wireless networks can perform better in indoor environment where user mobility occurs frequently. Therefore, it is imperative to ensure high-speed and uninterrupted connectivity in the presence of user mobility within one network cell and between two or more network cells. When mobility is considered in VLC wireless networks, two challenges must be addressed, i.e., (i) transmitter and receiver alignment, and (ii) drastic variation of SNR within a single VLC cell and between VLC cells [123].

2.8.4. Inter-cell interference

In order to achieve high capacity in VLC wireless networks, cells must have small radii. This requirement prompts deployment of large number of access points (LEDs) in order to increase network coverage. Visible light from different LEDs within the same room can interfere to each other resulting to low SINR. Proper arrangement of LEDs, joint transmission, and multiple input multiple output (MIMO) are potential solutions that can mitigate inter-cell interference in VLC wireless networks [70]. Inter-cell interference in VLC wireless networks is open research issue.

2.8.5. Energy efficiency

In VLC wireless networks, PDs or imaging sensor can be used for receiving visible light signals from LEDs. PDs are more suitable for fixed devices where transmitter and receiver alignment cannot be challenging. Image sensors have larger FOV because of wider concentration lens compared to PDs, therefore, they are more ideal for mobile devices. Thus, the use of image sensor can address the problem of FOV misalignment in mobile devices. Nevertheless, image sensors consist of large number of PDs, consume a lot of energy, and are slow to operate. Accordingly, image sensors lead to low achievable data rate in VLC systems. Therefore, it is imperative to design a receiver that; (i) provides high data rate, (ii) addresses the problem of FOV misalignment, and (iii) is energy efficiency. This is an open research issue that must be investigated in future studies. Although efficient LEDs are incorporated in today's mobile devices as camera flashlight or notification indicator, they can not be used directly for communication. This is because constantly turning on the LED not only consumes significant energy for mobile devices but it also causes visual disturbance to users. Moreover, VLC uplink requires that user's mobile device maintains a directional beam towards the receiver. This requirement can results in significant throughput reductions when the mobile device is constantly moving. In order to address these challenges, the use of infrared or radio frequency in the uplink channel has been suggested in several research publications such as [37, 42, 44, 54, 70].

2.8.6. FOV alignment and shadowing

VLC wireless networks can operate in both LOS and NLOS link configurations, however, in NLOS link configuration the performance of VLC systems deteriorates significantly. User devices such as smartphones and laptop are not fixed; movement and orientation of these devices change frequently thereby, affecting the alignment of the receiver's FOV with the transmitter. Hence, the misalignment of receiver's FOV with the transmitter can occur frequently resulting in connection interruption. Transmitter and receiver alignment limitation is an open research issue. Shadowing is another limitation of indoor VLC wireless network. The LOS requirement in this context is hindered by shadowing effects which occur when human or objects block light from an LED. Blocking light in a VLC system reduces the received optical power and data rate at the receiver. Therefore, addressing the shadowing effect is necessary for the realization of VLC systems.

3. DESIGN OF MAC PROTOCOL FOR AGGREGATED VLC-IR WIRELESS NETWORKS

The increasing bandwidth demand problem can be addressed by exploiting OWC technologies such as IRC, VLC, and UVC. The recent development in LEDs production has enabled the implementation of VLC wireless networks for indoor environments. However, VLC wireless networks cannot provide full-duplex communication because of limitations such as energy consumption, interference, and glares produced by light [30]. Therefore, IR can be used to complement VLC wireless networks in order to ensure full-duplex communication in VLC wireless networks. Nevertheless, this approach cannot be realized without addressing the problem of MAC for aggregated VLC-IR wireless networks. Existing MAC protocols cannot be used directly in aggregated VLC-IR wireless networks because of the difference in physical properties between RF-based wireless networks and OWC wireless networks. This is due to the fact that, existing MAC protocols are specific for RF-based wireless networks. In this chapter, we propose the adaptive polling medium access control (APMAC) protocol for aggregated VLC-IR wireless networks. The APMAC protocol aims at minimizing network delay, collision, and increase system fairness and utilization. Moreover, the APMAC protocol takes into account features of the IEEE 802.15.7 standard, physical properties of OWC.

3.1. Aggregated VLC-IR Wireless Networks

VLC wireless networks has attracted more attention because of the huge bandwidth and the availability of cheap and durable LEDs. IR-based link can be used to provide the uplink channel in VLC wireless network, thereby, achieving full-duplex communication. Resolving the uplink channel by using IR is ideal because IR addresses the challenges of using VLC in the uplink, viz., it does not require dimming, therefore no visual disturbance to users, it provides high data rate like VLC, and it is not restricted to LOS link configuration [124]. In the aggregated VLC-IR wireless network system, VLC is used for the downlink channel while the uplink channel uses

IR. The access point is located at the roof of the ceiling performs duo functions, i.e., illumination and data transmission. Nodes are located at the ground, receive data from the access point through light rays coming from the LED at the roof, and transmit data to the access point through IR. There are LEDs and PDs at the nodes and access point for transmission and reception of signals.

In this chapter, we investigate the problem of medium access control for aggregated VLC-IR wireless networks. For simplicity, we consider a star topology where the access point performs duo functions, viz., illumination and data transmission to nodes within a network. Figure 3.1 demonstrates a sample aggregated VLC-IR wireless network topology that we consider in this chapter. In this context, network nodes refer to devices such as mobile devices and fixed devices. Moreover, both network nodes and access point are enabled with LEDs and PDs for transmitting and receiving light signals. In addition, the uplink channel is IR-based and the downlink channel is VLC-based. The problem is assigning channel to multiple nodes that share the same access point subject to network delay, collision, system utilization, and fairness.

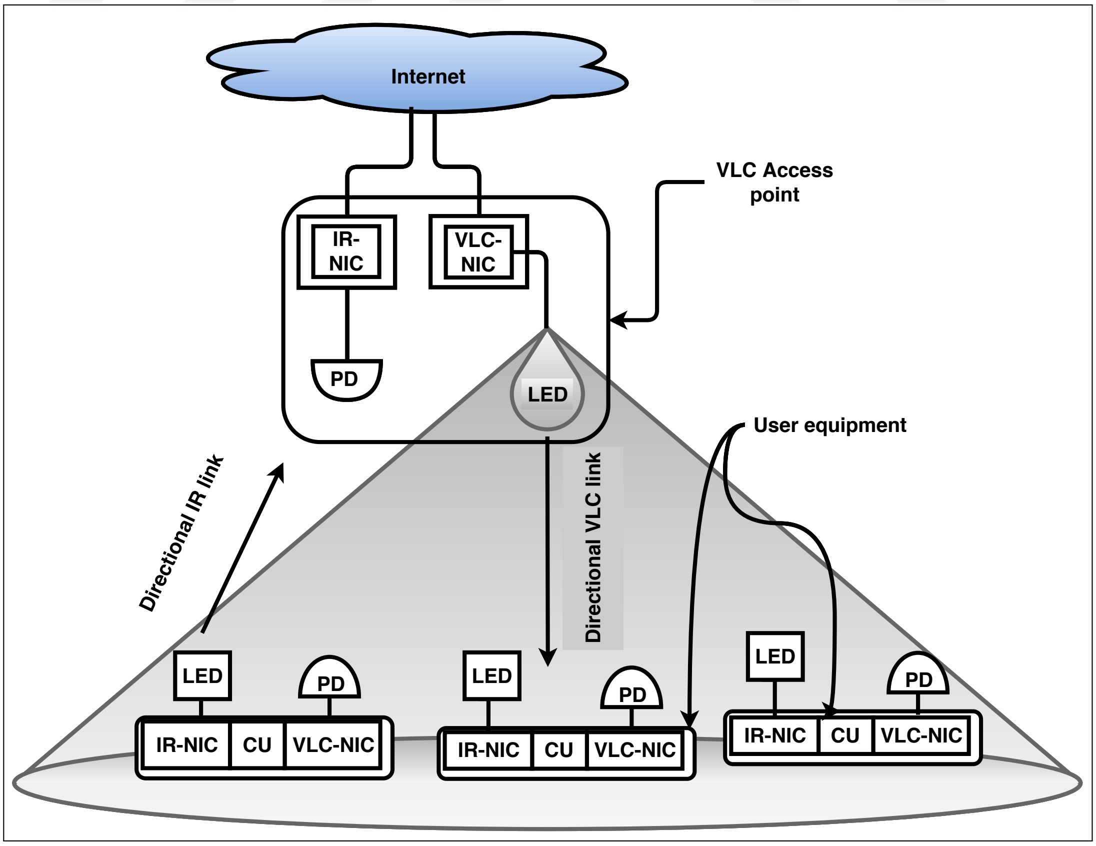

Figure 3.1. Aggregated VLC-IR for indoor wireless networks.

3.2. APMAC Protocol for Aggregated Wireless Networks

In this chapter, we propose the APMAC protocol for aggregated VLC-IR wireless networks. We consider a beacon enabled superframe that includes the beacon (BC), contention access period (CAP), and contention free period (CFP).

3.2.1. APMAC frames structure

In the APMAC protocol there are two types of frames, i.e, control frames, and data frames. Control frames are used for association, error control, and dissociation. Moreover, in order to ensure synchronization between nodes and access point, we use the beacon enabled superframe.

3.2.1.1. Superframe structure

We consider a beacon enabled superframe that is divided into beacon period (BC), CAP, and CFP. This type of superframe is proposed in [10]. The interval between two consecutive beacons is the duration of a superframe. Figure 3.2 depicts the superframe structure used in the APMAC protocol. Association phase takes place in BC and CAS slots whereas data transmission and dissociation phases occur in the CFP.

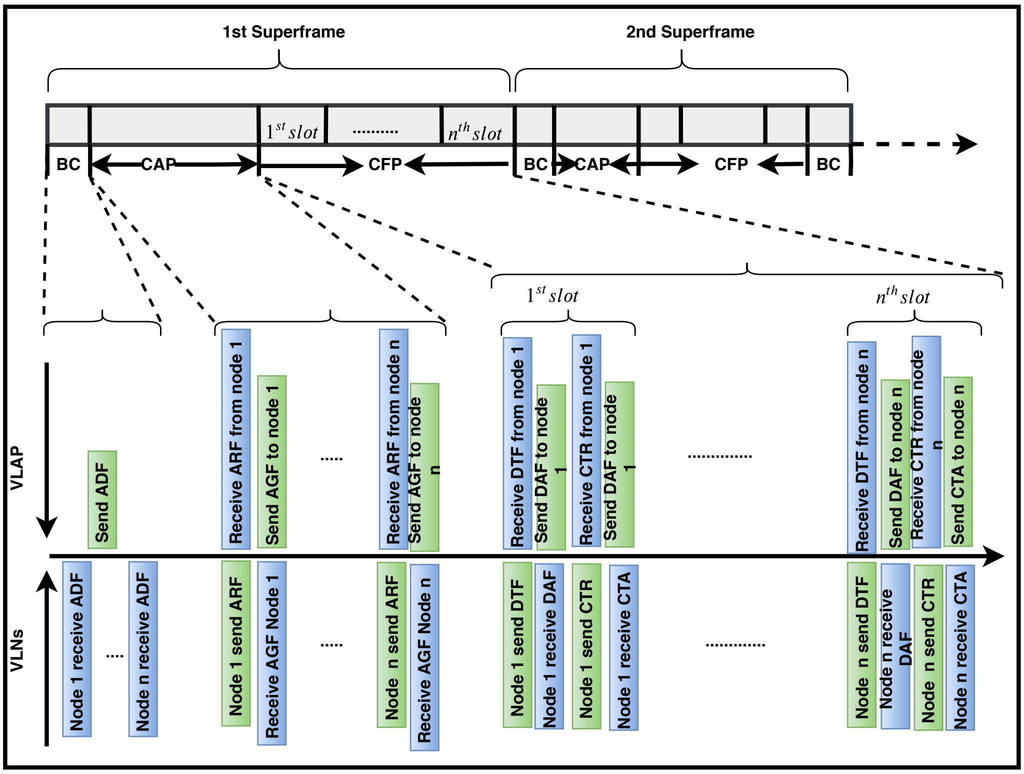

Figure 3.2. The APMAC protocol superframe structure.

3.2.1.2. Frame structure

We categorize the frames used in the APMAC protocol into two groups, i.e., control frames and data frames. For simplicity and without loss of generality, we leverage the IEEE 802.11 MAC frame structure shown in Figure 3.3. Both control frames and data frames use the same structure.

Octets	2	2	6	6	6	2	6	0-2312	4
	FC	Duration	Address 1	Address 2	Address 3	SC	Address 4	Data	FCS

FC = Frame control SC = Sequence control FCS = Frame check sequence

Figure 3.3. The frame structure used in the APMAC protocol.

3.2.2. Network association, channel allocation, and dissociation

In the APMAC protocol there are association, data transmission, and dissociation phases. During the association phase connection establishment takes place. Data transmission phase involves sending packets while connection termination occurs during dissociation phase. Figure 3.4 shows the three states of the APMAC protocol for aggregated VLC-IR wireless networks.

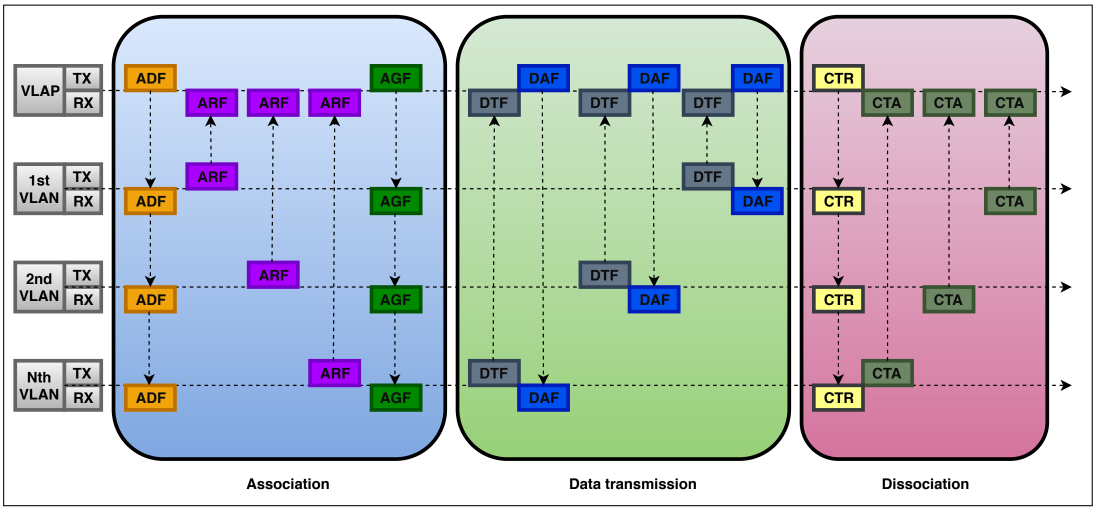

Figure 3.4. The APMAC protocol for aggregated VLC-IR wireless networks.

3.2.2.1. Association phase

The connection between the access point and a node can be initiated by any of the two devices. The access point initiates connection by sending the DTF to the corresponding node, in this case, there is no collision because it is a point to point connection.

However, if a node initiates connection, the odds are that, collisions can occur. The AP broadcasts the ADF to all nodes in the network. The ADF contains the address of the AP, the channel frequency, the beginning and the end of a superframe. Moreover, the access point establishes a polling table (PT) that includes physical addresses of sending and receiving devices, round trip time (RTT), and the available buffer size at the sender. Following ADF reception, nodes send access request, via the ARF, to the access point channel. In this context, the ARF contains the physical address of the node that transmitted the request and the size of data that is available at the requesting node. The process of sending ARFs occurs randomly within the CAP of the superframe, therefore, collision can occur. We address the problem of collision of ARFs during the CAP by using the control frame collision avoidance algorithm (CFCA) proposed in [54]. Suppose the average maximum number of users per AP is denoted by η, and the average round trip time (RTT) between nodes and AP in a network is α_t, then, the maximum contention access slot (CAS) per superfame can be expressed as CAS = $\eta \alpha_t$. Accordingly, the CFCA works as follows:

(i) The AP broadcasts the ADF at the beginning of the CAS slot to all nodes within a network.

(ii) Following receiving the ADF, nodes that need to associate with the AP select a random time $z|\alpha_t < z < \eta \alpha_t|$. If the channel is not active at time z, the node sends ARF to the AP then it waits for the AGF from the AP. The AGF waiting time is $z + 2\alpha_t$. If the channel is not idle at time z, the node waits for $z_i|z + 2\alpha_t|$ before performing another channel assessment.

(iii) If the AGF is not received within $z + 2\alpha_t$, a node checks if $z + 2\alpha_t < \eta \alpha_t - \alpha_t$, then it selects another random time $z_i|z + 2\alpha_t < z_i < \eta \alpha_t - \alpha_t|$. Another ARF is transmitted if the channel is sensed idle at z_i, otherwise, the node checks again if $z + 2\alpha_t < \eta \alpha_t - \alpha_t$ is true and selects another random time z_i. If the condition $z + 2\alpha_t < \eta \alpha_t - \alpha_t$ is not satisfied, the node waits another ADF before starting channel contention process.

(iv) In order to avoid idle waiting and improve system utilization, at $\frac{\eta \alpha_t}{2}$, the AP checks if there is no any ARF that arrived between 0 and $\frac{\eta \alpha_t}{2}$ duration. In case there is no ARF that is received in this duration, the AP resets its timer. The new superframe begins, therefore the AP broadcasts another ADF.

Following ADF broadcasting, the AP records physical address, RTT, and buffer size of each node that sent ARF in the polling table. Initially, the AP calculates the RTT of each node by considering the time between ADF broadcasting time and the arrival time of ARF. After recording details of each request, the AP sends the AGF to each node wherein it specifies the transmission slot, and the maximum transmission unit (MTU). We determine the MTU of each request by using the dynamic future knowledge maximum transmission unit (DFK-MTU) algorithm suggested in [125].

Algorithm 1: DFK-MTU Algorithm adopted from [125].

```
Input: Unassigned Polling Table (PT)
MTU = Average of the current PT.
for each CAP do
    while PT ≠ Empty do
        for each node k : {k = 1,...,n}INPT do
            if node k buffer ≥ current PT MTU then
                The current PT MTU is the MTU for node k.
            end
            if node k buffer < current PT MTU then
                Buffer size of k is the MTU k.
            end
            if node k buffer = current PT MTU then
                The current PT MTU is the MTU for node k.
            end
        end
    end
end
Output: Assigned Polling Table (PT)justification=justified, width=.975
```

The DFK-MTU enables the AP to dynamically adjust the size of the MTU based on the state of the polling table. In DFK-MTU algorithm, the MTU size for each instance of the polling table is the average of buffer size requests. The MTU serves as the upper bound, thus, if the buffer size request from a node is less than the MTU, then, the buffer size request is the MTU for that particular node. The transmission timeslot is obtained by summing the packet propagation and transmission time. Interference is avoided by adding guard time between consecutive packet transmission timeslot.

3.2.2.2. Data transmission phase

The association phase is followed by data transmission phase. In data transmission phase, packets are transmitted between nodes and the AP. Initially, the AP receives DTF from nodes via ARFs requests. Nodes can transmit DTF at its specific time interval as specified in the AGF. The contents of the DTF include payload, remaining buffer size at the node, physical addresses of the AP and the node. If the remaining buffer size is greater than zero, it indicates that there is more data at the node. Accordingly, the AP calculates the following timeslot for the node. Following evaluation of the next timeslot, the VLAP acknowledges the arrival of the DTF by sending DAF to the node. The contents of the DAF include the timeslot and MTU that the node can use in the following timeslot. Eventually, the polling table is updated by modifying the remaining buffer and RTT of the node or by deleting the node from the polling table if there is no more data remaining at the node.

3.2.2.3. Dissociation phase

The process of connection termination occurs in the dissociation phase. Following data transfer, node and AP must decide either to terminate connection or to maintain it. In this context, the device that initiated connection sends the CTR. The CTR frame contains the address of the device that initiates connection termination, CTR sending time, and connection termination time.

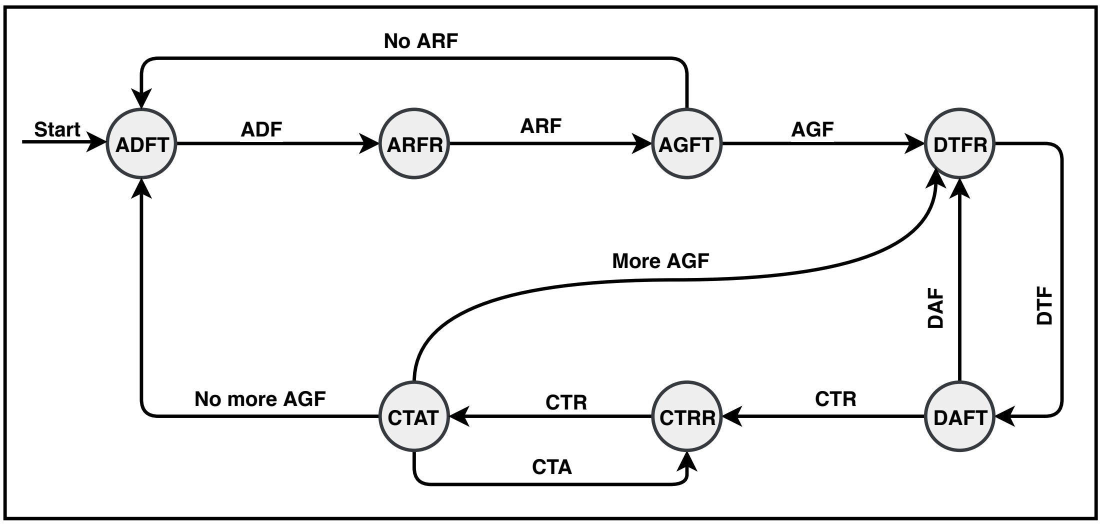

Figure 3.5. The VLAP deterministic finite state machine in the APMAC protocol.

Premature connection termination is avoided by waiting the acknowledgement of CTR. The CTR sending device waits for the CTA, if the CTA arrives within the RTT, then, the connection is terminated, otherwise, it defers for half of the RTT and terminate the connection. Finally, the AP removes the details of the node from the polling table. Figure 3.5 presents the deterministic finite state machine of the VLAP. In addition, Figure 3.6 shows the node deterministic finite state machine.

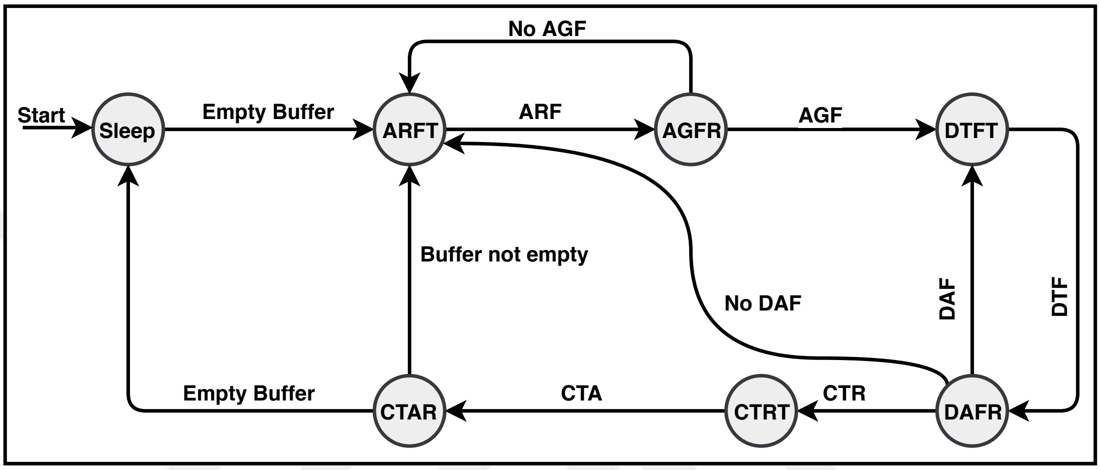

Figure 3.6. The node deterministic finite state machine in the APMAC protocol.

3.3. Experimental Setup and Numerical Results

In order to evaluate the advantage of our protocol over the existing MAC protocols, we conducted simulations by taking into account the following performance metrics: delay, collision, utilization, and fairness. The waiting time in this context is the interval between time at which the node sends the ARF and the time at which it begins sending DTF. In other words, it is the duration the node spends in the association phase. Collision refers to unsuccessful packet transmission and utilization denotes the time at which the system is in data transmission. The fairness index defines how equally resources are distributed to nodes in a network. The fairness index ranges from 0 to 1 where high value implies more fairness. Fairness index can be mathematically written as follows [126]:

$$\text{fairness index} = \frac{\sum(\frac{t_i}{\omega_i})^2}{N(\sum(\frac{t_i}{\omega_i}))^2} \tag{3.1}$$

Here t_i refers to throughput of node i, ω_i is the weight of node i, and N denotes the number of nodes in a network. In conducting simulations, we assumed that all nodes have the same weight and the number of nodes starts from 1 to 10 per access point. We consider a small number of nodes per access point because this is an indoor network and the VLC access points would consume more energy if the network size is very large. The downlink channel uses 120 Mbps, while the uplink channel uses 4 Mbps data rate. In VLC wireless networks, the theoretical maximum propagation distance is 10-15 m, therefore, in our simulations we assume that the maximum propagation distance is 10 m, a sufficient distance to detect light signal reliably. For each node, we randomly generate network traffic as a poison process with the rate λ packets per second. Moreover, we rerun the simulation 50 times for each scenario and the results we demonstrated are average of the results for each scenario with 97% confidence interval. Finally, we show the advantage of our protocol by comparing the results from simulation against existing MAC protocols such as MT-MAC studied presented in [127].

3.3.1. Network delay versus network size and load

Figure 3.7a and Figure 3.7b show the network delay as a function of network size and load. It can be seen in Figure 3.7a that delay increases when the network size also increases. We compare our results against the MT-MAC protocol and the results in Figure 3.7a suggest that APMAC protocol outperforms the MT-MAC protocol significantly in terms of network delay especially when the network size is small. This is because of the use of the DFK-MTU algorithm and non-contention approach in our protocol.

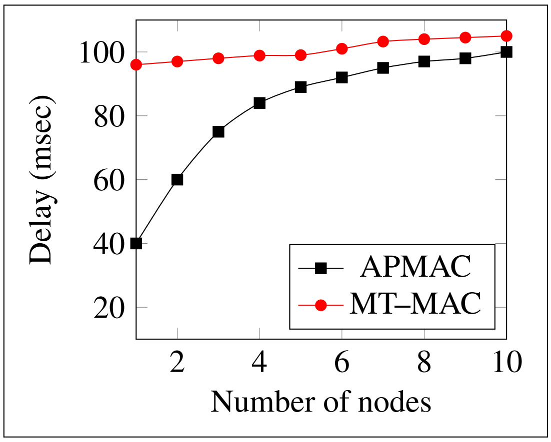

(a)

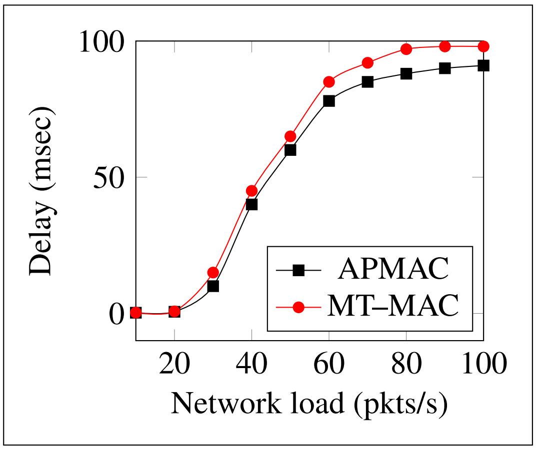

(b)

Figure 3.7. Delay versus network size in (a) and delay versus network load in (b).

There is a considerable increase in network delay when the network load increases for both the APMAC and MT-MAC protocols as shown in Figure 3.7b. When the network load is increased, each node holds resource longer thereby prompting high delay in the network. Nevertheless, our protocol gives better results than the MT-MAC protocol.

3.3.2. Collision versus network size and network load

We evaluate the performance of our protocol by considering packet collision against network size and throughput as shown in Figure 4.9a, and Figure 4.9b. Here, we take into consideration two cases, i.e., 50% and 100% network load. Figure 4.9a shows that collision increases when network increases. This is because when there are many nodes in a network, the odds are that more packets are generated. Accordingly, the rate of collision increases at high network size. Moreover, network load prompts increase in collision as shown in both Figure 4.9a and Figure 4.9b. Furthermore, Figure 4.9b shows that collision affects network throughput, i.e., throughput increases when collision decreases.

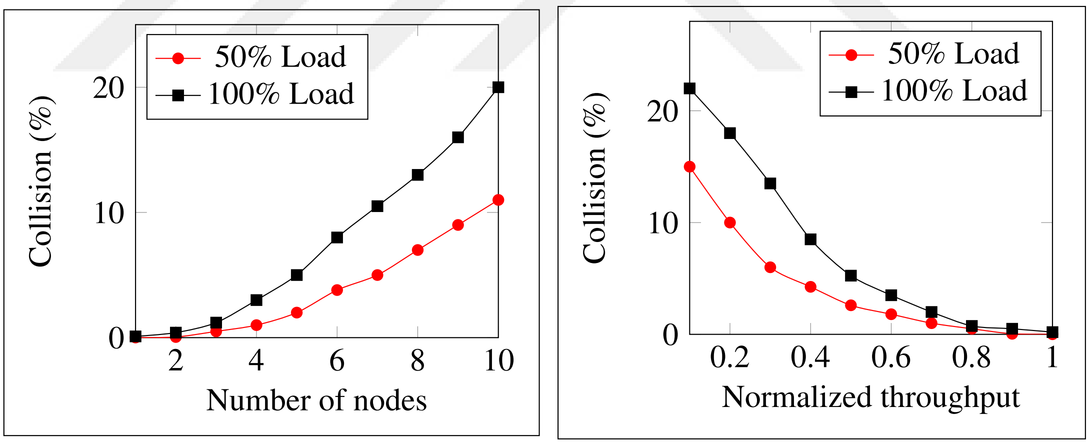

(a) (b)

Figure 3.8. Collision versus network size in (a) and collision versus throughput in (b).

3.3.3. System utilization versus network size and throughput

In Figure 3.9a we demonstrate the system utilization as a function of network size where system utilization decreases when the network size increases. The decrease in utilization is prompted by long time for channel arbitration when the network size is large. Moreover, Figure 3.9b shows numerical results for system utilization against network throughput. Results in this context reveal that system utilization is direct proportional to network throughput. The results in either case are promising, i.e., between 99% and 90%.

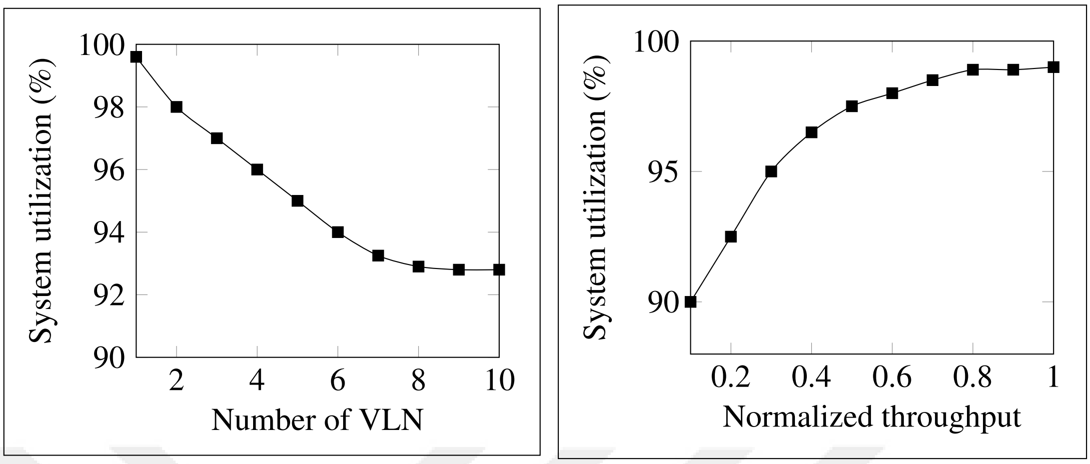

(a) (b)

Figure 3.9. Utilization vs. network size in (a) and utilization vs. network load in (b).

3.3.4. Fairness versus network throughput and load

Furthermore, Figure 3.10a, and Figure 3.10b, show numerical results for the fairness index as a function of network throughput and load respectively. We consider two scenarios, i.e., when the network size is 5 and when the network size is 10. Figure 3.10a shows that the fairness index increases when the network throughput increases. Accordingly, increasing fairness causes increase in throughput.

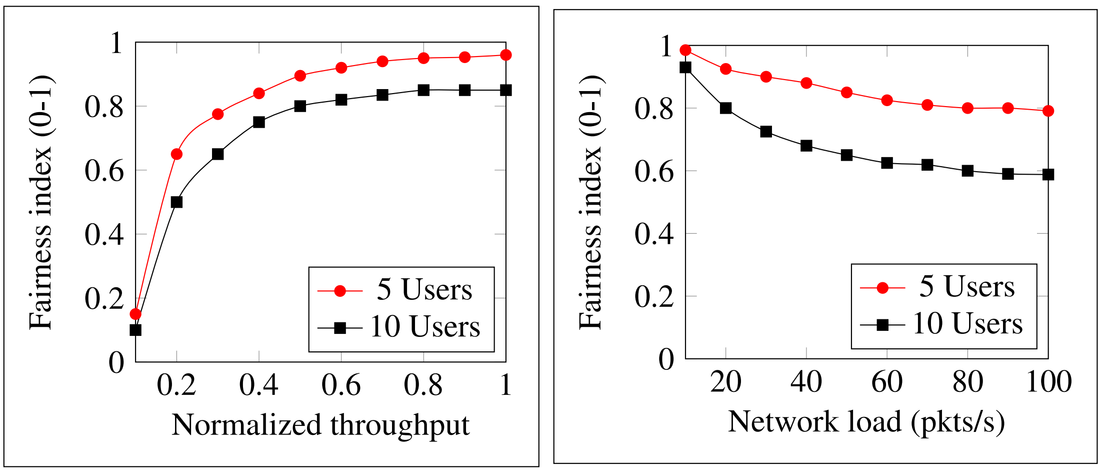

(a) (b)

Figure 3.10. Fairness index vs. throughput in (a) and fairness vs. network load in (b).

In addition, network size affects the system fairness, viz., fairness decreases when network size increases as suggested by the results for five users against ten users in

Figure 3.10b. This is due to the fact that, it is difficult to assign resources fairly when the network size is very large. The results in Figure 3.10b show that the network load affects fairness of the system. Although we consider the dynamic MTU in our protocol, at high network load some nodes still get more resources than other nodes, thereby, affecting system fairness.

3.4. Conclusion

VLC wireless network is promising solution to the ever increasing bandwidth demand. Most of existing research in VLC wireless network focus on downlink channel. The realization of VLC wireless network requires the provision of auxiliary medium for the uplink channel. IR and RF can be used to provide uplink channel in VLC wireless networks. In this chapter, we investigated the problem of medium access control for aggregated VLC-IR wireless networks. We presented the novel non-contention bandwidth assignment protocol named APMAC. The objective is minimizing waiting time and packet collision while increasing system utilization and fairness in aggregated VLC-IR wireless networks. A sample network topology that contains a single access point and several network nodes is presented. Both nodes and the access point are enabled with LEDs and PDs for transmitting and receiving IR and VLC signals. The access point is coordinating communication in the network. We demonstrate the advantage of the APMAC by comparing the results from the simulations against existing protocols such as MT-MAC. Results show that APMAC minimizes delay and collision while increasing system utilization and fairness.

4. DESIGN OF MAC PROTOCOL FOR AGGREGATED VLC-RF WIRELESS NETWORKS

VLC is an emerging technology that uses light rays in the range of 380-740 nm for signal propagation at high data rate compared to radio frequency (RF). Nevertheless, it is not realistic to achieve full-duplex communication in VLC wireless networks because of challenges such as glare, line-of-sight (LOS) transmission requirement, interference, and energy constraint. Infrared or RF can complement VLC wireless networks in order to achieve full-duplex communication. However, aggregated VLC-RF networks cannot be realized without addressing challenges such as MAC techniques.

In this chapter, we present the self-adaptive medium access control (SA-MAC) protocol for aggregated VLC-RF wireless networks. The objective of our study is minimizing non transmission time, energy consumption, and collision while increasing throughput. By leveraging the CSMA/CA and sub-carrier orthogonality we model the SA-MAC protocol for aggregated VLC-RF wireless networks and we demonstrate the Markov chain model that shows the states of a node in SA-MAC protocol. Finally, we simulate our protocol in NS3 discrete events network simulator, then, we compare simulation results with Markov chain model results and other existing protocols in the literature such as the carrier sense multiple access with collision detection hidden node avoidance (CSMA/CD-HA) and dynamic contention window-based successive transmission (DCW-ST). Numerical results from simulation and Markov chain model converge especially when the network size increases. Furthermore, the results from our study show that the proposed protocol increases network performance significantly.

4.1. Introduction

The profound reliance on the internet is a challenge facing the internet industry. Currently, the majority of internet traffic relies on RF. Accordingly, the RF is almost exhausted and cannot accommodate new subscribers. The visible light spectrum is a potential solution to the ever-increasing bandwidth demand. The motivating factors of using VLC include; visible light spectrum is unlicensed, immune to electromagnetic interference, not harmful to human being, and security. The IEEE has introduced the IEEE 802.15.7 standard in order to standardize short range optical wireless communications such as VLC. The IEEE 802.15.7 standard specifies several issues such as collision avoidance, addressing mechanism, network topologies, visibility support, dimming support, and acknowledgement [10]. In terms of network topologies, the IEEE 802.15.7 standard proposes star, broadcast, and peer-to-peer topologies. In addition, the IEEE 802.15.7 standard specifies the physical layer and the medium access control (MAC) techniques. Despite the benefits of visible light spectrum, VLC standalone systems cannot provide full-duplex communication considering constraints such as interference, glare, and power consumption.

Accordingly, the use of infrared or RF to complement VLC in order to achieve full-duplex communication has been demonstrated in [11, 128]. The realization of aggregated wireless networks such as VLC-RF and VLC-IR requires addressing challenges such as network addressing techniques, MAC techniques etc. In this chapter, we present the self-adaptive medium access control (SA-MAC) protocol for aggregated VLC-RF wireless networks wherein the objectives are maximizing network throughput while minimizing energy consumption, non-transmission time, and collision.

Furthermore, the Markov chain model is also presented in order to show the validity of our protocol. The simulation of the proposed protocol is performed by using the NS3 discrete events network simulator. Numerical results for both simulation and the Markov chain model converge especially when network size increases. The rest of this chapter is organized as follows: The literature review is presented in Section 4.1.1, in Section 4.2 we provide details of the problem we address, detailed description of the SA-MAC protocol is presented in Section 4.3, Markov chain model numerical analysis is derived in Section 4.4. Experimental setup and numerical results are demonstrated in Section 4.5. Finally, the conclusion is presented in Section 4.7.

4.1.1. Related studies

An indoor aggregated WiFi-VLC wireless network is proposed in [44]. The authors in this study suggest the use of asymmetric RF-VLC system that utilizes RF for the uplink and VLC for the downlink channel. The proposed system achieves full-duplex communication and increases throughput. Moreover, the authors in [44] provide sufficient details about the networking addressing problem for hybrid RF-VLC wireless networks. However, they did not describe the problem of medium access control (MAC). In order to improve energy efficiency in wireless networks, a hybrid RF-VLC system is proposed in [129]. The problem is modeled as NP-complete and the results from the simulation are promising. Moreover, the problem of network resource optimization for heterogeneous VLC-WiFi networks is investigated in [130]. The authors modelled the problem of resource optimization in VLC-RF wireless networks as a Lyapunov optimization and the numerical results show the trade-off between delay and throughput.

While targeting throughput and transmission probability, a parallel transmission MAC (PT-MAC) protocol for indoor hybrid RF-VLC wireless networks is suggested in [131]. The PT-MAC takes into consideration the CSMA/CA in its design and increases network throughput and transmission probability. The delay analysis for unsaturated full-duplex RF-VLC wireless networks is suggested in [132]. The authors consider aggregated and non-aggregated scenarios in evaluating the delay of coexisting RF-VLC wireless networks. Numerical results from their study show that aggregated scenario provides lower delay than the non-aggregated scenario.

The authors in [133] designed and analyzed the hybrid RF-VLC system wherein numerical results show that per node outage probability decreases in the hybrid RF-VLC networks. Moreover, the design and analysis of heterogeneous RF-VLC indoor wireless networks presented in [134] show that the aggregated RF-VLC wireless networks improves network performance especially in crowded wireless environment. In addition the authors provide a detailed mechanism about network addressing in RF-VLC aggregated networks. A hybrid RF-VLC system with bandwidth aggregation is designed and implemented in [135]. Network throughput of the aggregated system is measured and compared against a standalone WiFi system. Numerical results from this study reveal that the aggregated system outperforms the standalone WiFi system in terms of network throughput, utilization, and delay.

There are several research publications that address the quest for VLC MAC protocols such as [49, 57, 59–62, 66, 136, 137]. However, they are restricted to half-duplex and hybrid RF-VLC wireless networks. Wang *et al.* in [63] present a full-duplex MAC protocol for VLC wireless networks that allows concurrent sending and receiving data. They consider a star network topology in which visible light of different wavelength can be used for bidirectional transmissions. Existing research publications suggest different MAC protocols for hybrid RF-VLC wireless networks. The adaptive polling MAC protocol for aggregated infrared-VLC wireless networks is presented in [54] wherein the focus is minimizing network delay and increasing throughput. Unlike in [54], this study suggests the MAC protocol for aggregated VLC-RF wireless networks taking into consideration full-duplex communication aspect. Following is the outline of the main contributions of this chapter:

(i) Although there are many publications that model MAC protocols for hybrid RF-VLC, they consider the coexistence of RF-VLC systems as standalone networks that complement each other under varying conditions. This assumption attracts many practical challenges such as the requirement for new addressing mechanism, handover, medium access control and load balancing [138]. Moreover, existing studies such as [134, 135] show that aggregated RF-VLC systems outperform hybrid RF-VLC networks significantly. In our study, we consider the aggregated RF-VLC system as the best solution to achieve full-duplex communication. We present the SA-MAC protocol for aggregated RF-VLC wireless networks that combines CSMA/CA and sub-carrier orthogonal techniques to improve network throughput, fairness, energy efficiency, and transmission probability.

(ii) We propose the dynamic superframe size that depends on the number of nodes in a network.

(iii) The 2D Markov chain model-based analysis is conducted to validate the credibility numerical results of our protocol. For each performance metric we compare the simulation results and the Markov chain model results.

(iv) We extend the NS3 discrete events network simulator to model and simulate our protocol.

4.2. Aggregated VLC-RF Wireless Networks and Problem Statement

For simplicity, we consider an aggregated VLC-RF wireless network that contains one access point and several nodes. The access point is located at the ceiling of the building while nodes are located at the ground of the building. The access point consists of a MAC control-unit (CU), LED for both illumination and transmitting signals, and network interface cards (NICs) for VLC and RF. Nodes consist of a PD for receiving signals from LED, CU, RF-NIC, and VLC-NIC. Transmission from nodes to the access point (uplink channel) uses RF while transmission from the access point to nodes (downlink channel) uses VLC. Figure 4.1 illustrates a simple indoor aggregated RF-VLC wireless network that we conisder in this chapter. Note that the addition of extra NIC in both access point and nodes introduces the network addressing and multiple access control problems. Thus, the primary challenges in implementing aggregated VLC-RF wireless networks are network addressing and medium access control.

In Transmission Control Protocol (TCP), the connection is established by the client initiating a three-way handshaking with the server. When the connection is established, the client generates a synchronize (SYN) message and encapsulates it in the internet protocol (IP) header prior to sending it by using the NIC. Following this, the client listens to the socket that contains TCP port number and IP address used to generate and encapsulate the SYN message. In this case, any reply packets received from the server with different NIC and different socket details are ignored. Network addressing in hybrid RF-VLC has been extensively studied in [134, 135]. For simplicity and without loss of generality, in our study, we leverage the network addressing techniques suggested in [134]. Furthermore, in the RF domain the carrier sense multiple access with collision avoidance (CSMA/CA) protocol is used to control access to a shared medium. There are two strategies of controlling access to a shared medium in VLC wireless networks

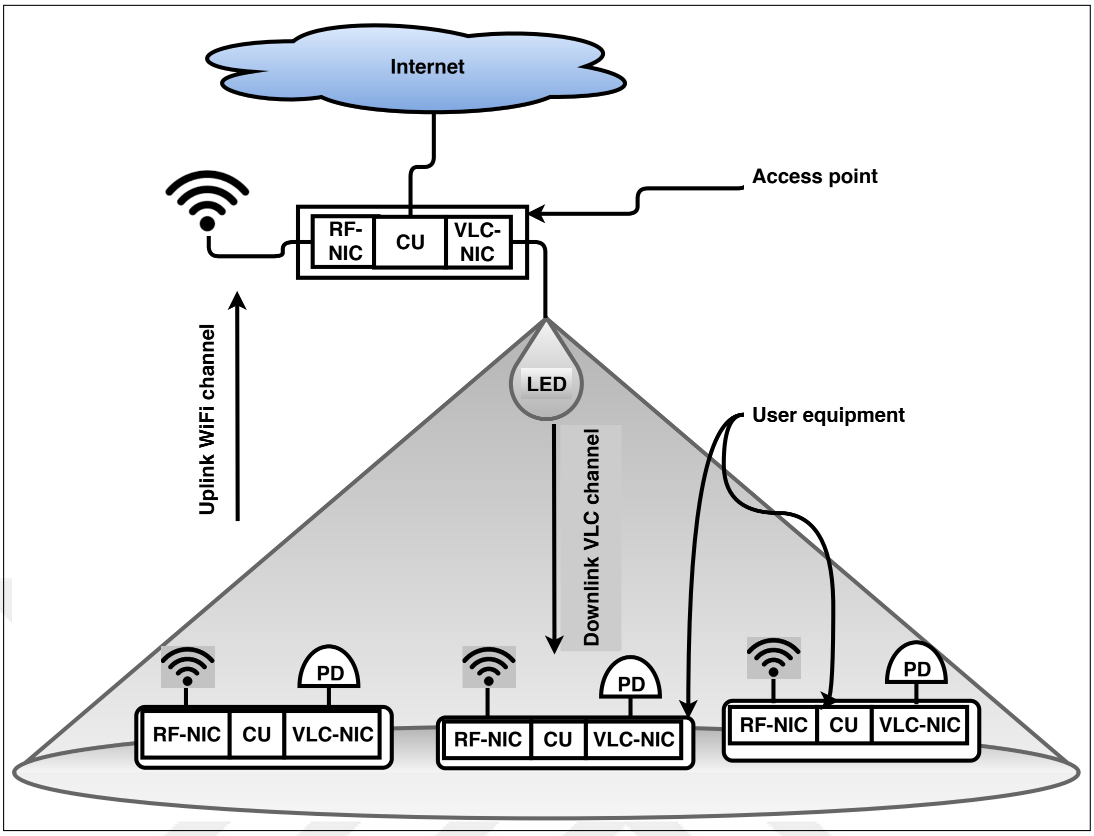

Figure 4.1. Aggregated RF-VLC indoor wireless network.

such as orthogonal frequency division multiple access (OFDMA), and non-orthogonal multiple access (NOMA) [139]. Therefore, there is the need for designing the MAC protocol that takes into consideration the physical properties of the RF and VLC in aggregated VLC-RF wireless networks. We consider a polling based protocol wherein nodes request access to a shared medium in the uplink domain by using CSMA/CA. The downlink channel is shared by using sub-carrier orthogonality. Multiple nodes in a network can receive signals from the access point based on sub-carrier orthogonality. The challenge of using OFDMA in VLC wireless networks is that, sub-carrier with low frequency provides high signal-to-noise ratio (SNR). Therefore, we provide a fairness scheduling algorithm that ensures that all nodes are treated fairly.

4.3. Self-Adaptive Medium Access Control Protocol

The Self-Adaptive Medium Access Control (SA-MAC) protocol for aggregated VLC-RF wireless networks involves three duration, viz., the beacon (BC) duration, the contention access period (CAP), and the contention free period (CFP). In each duration, access point and nodes perform several activities. Below we narrate the superframe structure, activities of nodes and access point in the SA-MAC protocol.

4.3.1. SA-MAC superframe structure

In the SA-MAC protocol, we consider a superframe that consists of BC, CAP, and CFP as shown in Figure 4.2. The size of each duration is determined by Algorithm 2.

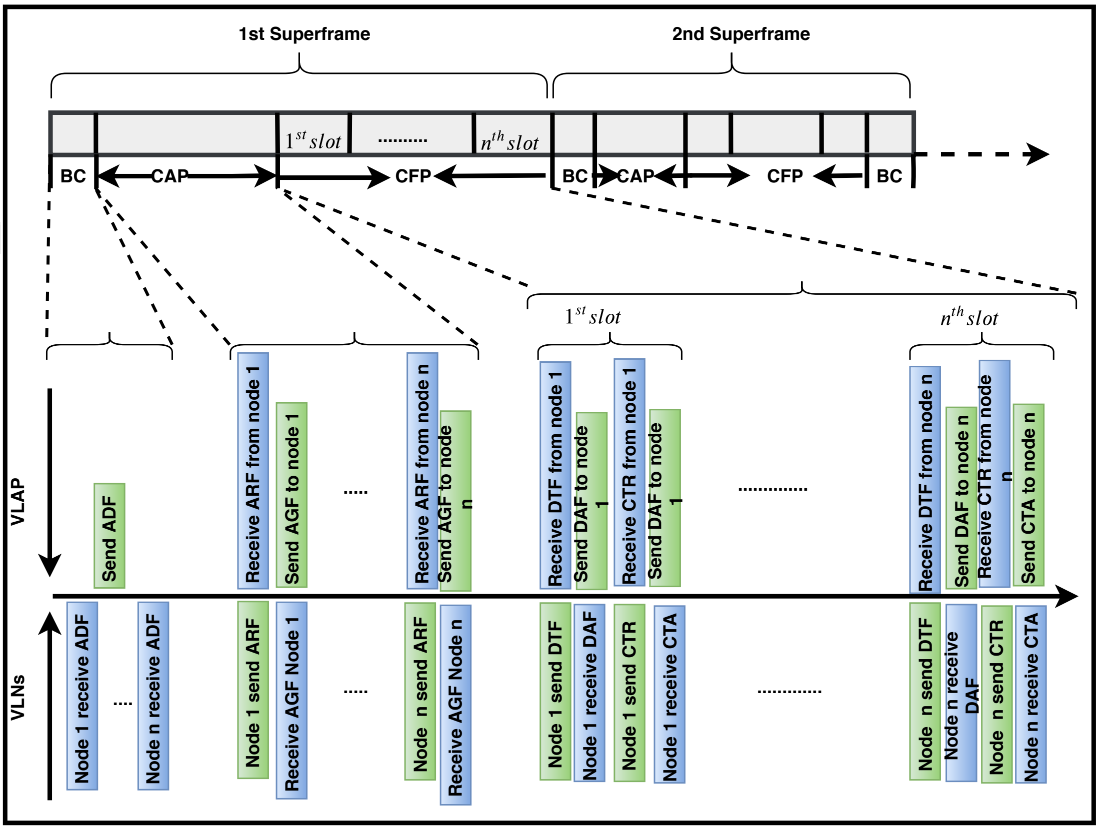

Figure 4.2. The SA-MAC superframe structure.

In the BC duration, the access point broadcasts the beacon frame to all nodes. This is done by using the LED of the access point. The beacon frame helps time synchronization between nodes and access point. During CAP, nodes request time-slot from the access point. The association phase involves sending the request-to-send (RTS) message and receiving the clear-to-send (CTS) message from the access point. The mechanism of contention during CAP is described in Section 4.3. In the CFP there is no contention, each node is assigned a specific time-slot. The size of each node's time-slot is determined by the access point depending on the request from nodes and the size of the CFP.

Furthermore, in order to achieve optimal results, we introduce the dynamic superframe algorithm that approximates optimal superframe size. The dynamic superframe size is achieved by periodically adjusting the CAP and CFP depending on the number of nodes in the polling table (PT). We consider three cases; (i) when the current PT contains no request, (ii) when the current PT contains fewer requests than the PT of the previous superframe, and (iii) when the current PT contains more requests than the PT of the previous superframe.

Algorithm 2: The Algorithm for dynamic superframe size.

Input: t_i, $PT_{t_{i-1}}$ and PT_{t_1}
Initialization:$\beta \leftarrow 2\alpha$
for *each* t_i **do**
    if $PT_{t_i} = \emptyset$ **then**
        $\Phi_{t_{i+1}} \leftarrow (\Phi_{t_{i-1}})/2$,
        $\Psi_{t_{i+1}} \leftarrow (\Psi_{t_{i-1}})/2$,
        $t_{i+1} \leftarrow \beta + \Phi_{t_{i+1}} + \Psi_{t_{i+1}}$
    end
    if $PT_{t_{i-1}} \geq PT_{t_i}$ **then**
        $t_{i+1} \leftarrow t_i - (t_{i-1} - t_i)$,
        $\Phi_{t_{i+1}} \leftarrow \eta_{t_{i+1}} * \alpha$,
        $\Psi_{t_{i+1}} \leftarrow t_{i+1} - (\Phi_{t_{i+1}} + \beta)$
    end
    if $PT_{t_{i-1}} < PT_{t_i}$ **then**
        $t_{i+1} \leftarrow t_i + (t_i - t_{i-1})$,
        $\Phi_{t_{i+1}} \leftarrow \eta_{t_{i+1}} * \alpha$,
        $\Psi_{t_{i+1}} \leftarrow t_{i+1} - (\Phi_{t_{i+1}} + \beta)$
    end
end

In the first case, the next superframe size is half of the previous superframe size. In the second case the next superframe size is obtained by deducting the difference between the previous and current superframe from the current superframe. The last case is addressed by adding the difference between the current and the previous superframe to the current superframe in order to obtain the size of the next superframe. Algorithm 2 describes the mechanism of obtaining dynamic superframe size in SA-MAC protocol. Let η_{t_i} denote the number of nodes in the PT of superframe t_i, α be the maximum round trip time (RTT) between access point and nodes, t_i be the duration of superframe i where $t_i = \{t_1, t_2, ..., \infty\}$, PT_{t_i} be the PT during t_i, β represent the beacon duration, Φt_i be the CAP during ti, and Ψt_i be the CFP during t_i.

4.3.2. Access point flow

Figure 4.3 shows the flowchart of the access point in the SA-MAC protocol for the aggregated VLC-RF wireless networks. Initially, the access point broadcasts the beacon frame to all nodes in the network. The beacon frame contains the physical address of the access point, the superframe duration, and the size of the CAP. After broadcasting the beacon frame, the access point establishes the polling table (PT) in which all requests from the nodes are recorded.

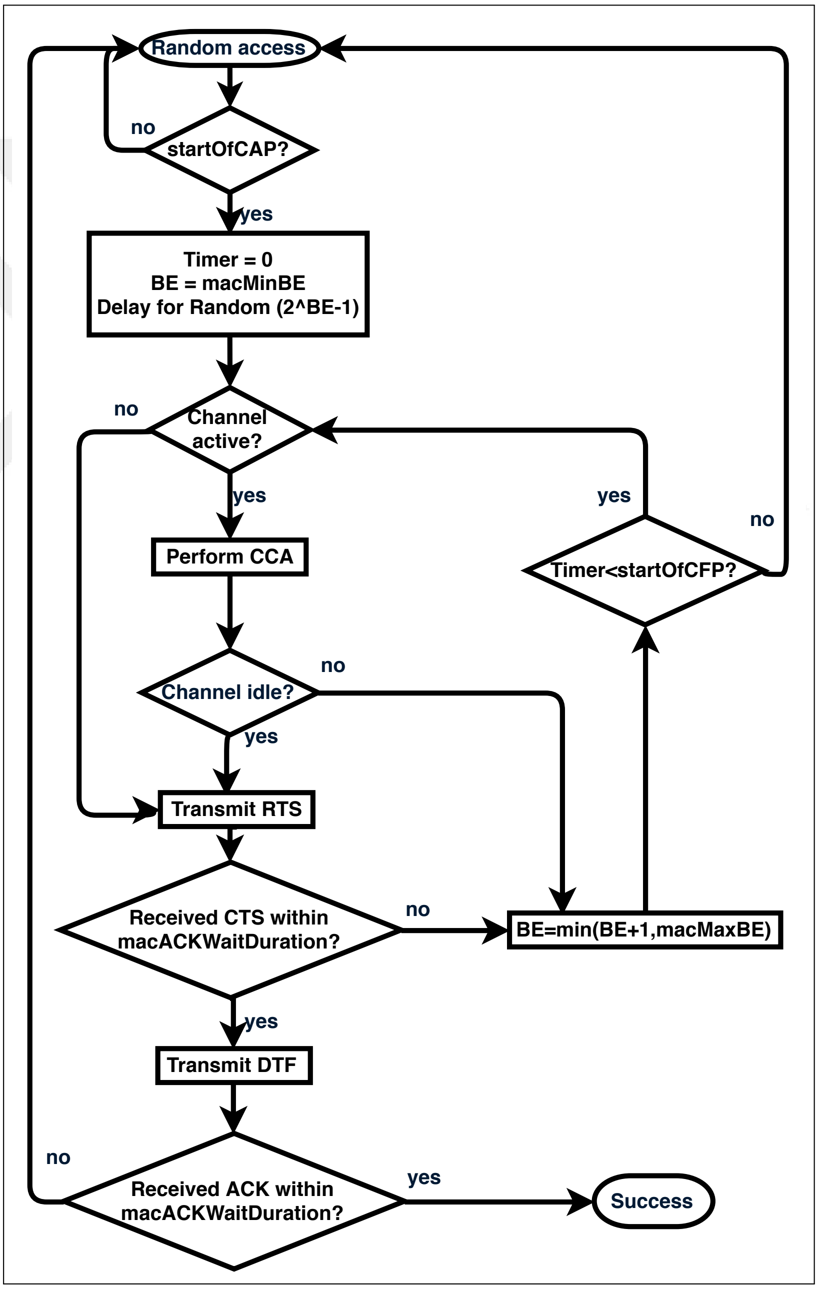

Figure 4.3. SA-MAC protocol access point flowchart.

In addition, the access point sets its timer to zero, then it delays for CAP receiving requests from nodes via RTS messages. At the end of the CAP, the access point checks if there is any request received from nodes, i.e., PT is not empty. If the PT is empty, the access point starts the process again by broadcasting the beacon frame, otherwise, it assigns resources to all requests. Following resource assignment, the access point sends CTS message to all nodes in the PT. The mechanism of resource assignment employed in this study is presented in Algorithm 3.

Algorithm 3: Resource assignment algorithm

for each superframe **do**
    Input: set of sub-carriers = {R,G,B} and PT
    for each CAP **do**
        for *each* k in PT **do**
            for q in $\{R, G, B\}$ **do**
                $H_0^{k,q} \longleftarrow [H_0^q - H_0^k]$
            end
        end
        while $H_0^{k,q+1} \neq$ NULL **do**
            if $H_0^{k,q} \leq H_0^{k,q+1}$ **then**
                $q \longleftarrow k$
            end
            else
                $(q+1) \longleftarrow k$
            end
        end
        for *each* q in $\{R, G, B\}$ **do**
            while request record in q $\neq \emptyset$ **do**
                while CFP in q $\neq 0$ **do**
                    $t_{k,q} \longleftarrow$ MTU
                    $k \longleftarrow t_{k,q}$
                    CFP in q $\longleftarrow$ CFP in q$-t_{k,q}$
                end
            end
        end
    end
    Output: Assignment schedule
end

After sending CTS messages to all nodes the access point receives data from nodes and sends acknowledgement within the CFP. At the end of the CFP, the access point begins a new superframe by sending another beacon frame. The mechanism of assigning resources at the access point is significant in the performance of the network, i.e., it can increase network delay. Therefore, we devise a fair algorithm that assigns resources to requests received from nodes fairly in Algorithm 3. Requests from nodes are recorded in a PT according to the order of arrival. Before resource assignment, requests are classified into three groups depending on the DC channel gain threshold of each request. Here, each group corresponds to one sub-carrier, i.e., red, blue, and green because we consider trichromatic LED. In this context, we calculate the distance between each sub-carrier DC channel gain and the DC channel gain threshold of each request. The request is placed into a sub-carrier with the shortest distance. For each group, the assignment is done based on arrival rate, each request is assigned a timeslot (MTU) in a corresponding sub-carrier. The mechanism of obtaining MTU for each PT is explained in details in [125].

4.3.3. Nodes flow

Initially a node waits for the beacon frame from the access point. Immediately after receiving the beacon frame, a node sets the values of beacon exponents (BE), and timer. Unlike other CSMA-based protocols, in our protocol a node can start the back-off process depending on the probability of successful transmission. Thus, we minimize energy consumption by avoiding unnecessary channel sensing. If the probability of successful transmission is greater than zero a node can start the back-off process, then it performs channel sensing. If the channel is not active the RTS is sent to the access point.

However, if the channel is active, then a node keeps performing the clear channel assessment (CCA) depending on the probability of successful transmission until the channel is detected idle. Note that, in this context, the channel is deemed idle during the beacon and the CAP states. In the CFP state the channel is deemed active. After sending RTS, a node waits for a CTS message from the access point within the maximum acceptable time. Failure to receive the CTS prompts a node to select another BE and checks if the CAP has elapsed. Carrier sense can be performed again if the CAP period has not elapsed, otherwise, a node waits for CAP of the next superframe in order to perform back-off process and channel sensing. If the CTS message arrives within the acceptable time, then, a node sends data to the access point and waits for acknowledgement. Un-acknowledgement of transmitted data implies unsuccessful

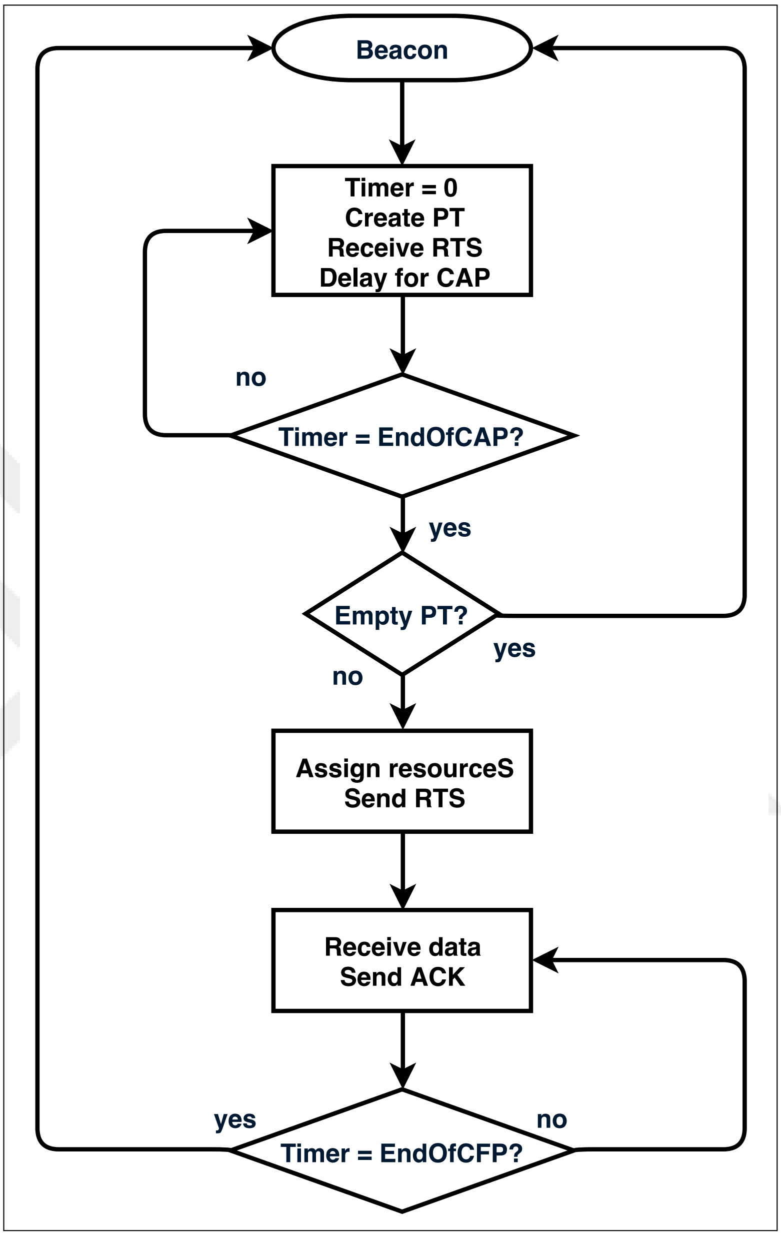

Figure 4.4. SA-MAC protocol node flowchart.

transmission, therefore, a node randomly selects another BE and begins channel sensing again in the CAP of the next superframe. Thus, the process of association is restricted to the CAP, therefore, RTS messages arriving at the access point during CFP are ignored. Figure 4.4 illustrates the node flowchart in the aggregated VLC-RF wireless networks. We provide the sequence diagram of the SA-MAC protocol that shows the association and data transmission in Figure 4.5.

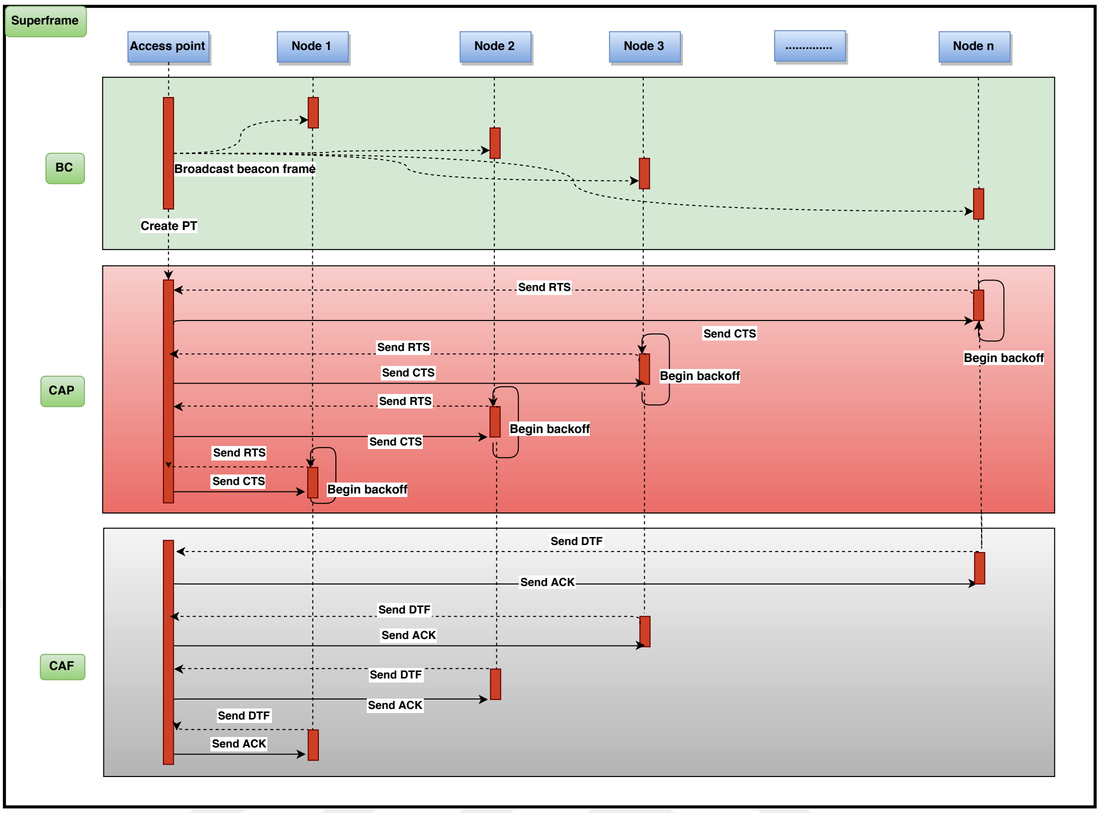

Figure 4.5. SA-MAC protocol sequence diagram.

4.4. Performance Analysis

Markov chain models have been used to study the behaviour of MAC protocols in different studies such as [68, 140, 141]. Therefore, we analyze the performance of our protocol be using the Markov chain model. We present the 2D Markov chain model wherein states of node γ are represented as $(S(\gamma), A(\gamma))$. In this context, $S(\gamma)$ represent the status of node γ, i.e., idle state $S(\gamma) = S$, beacon state $S(\gamma) = 2S$, CAP state $S(\gamma) = 3S$, and CFP state $S(\gamma) = 4S$. Moreover, in each state, $A(\gamma)$ takes different interpretations as follows:

(i) When node γ is in state S, then $A(\gamma)$ is 0 if no packets arrive at node γ and 1 if packets arrive at node γ.

(ii) When node γ is in state 2S, then $A(\gamma)$ is 0 if the beacon frame is not received and 1 if the beacon frame is received.

(iii) When node γ is in state 3S, then $A(\gamma)$ is 0 if back-off process is not initiated, $1, \ldots, M$ if back-off is initiated, $M+1$ if RTS is transmitted, $M+2$ if CTS is

(iv) When node γ is in state 4S, then $A(\gamma)$ is defined as nL if all packets are transmitted and acknowledged successfully, otherwise it is $(n-r)L$. If no packets are transmitted then, A(γ) is 0. Where L is the length of a packet.

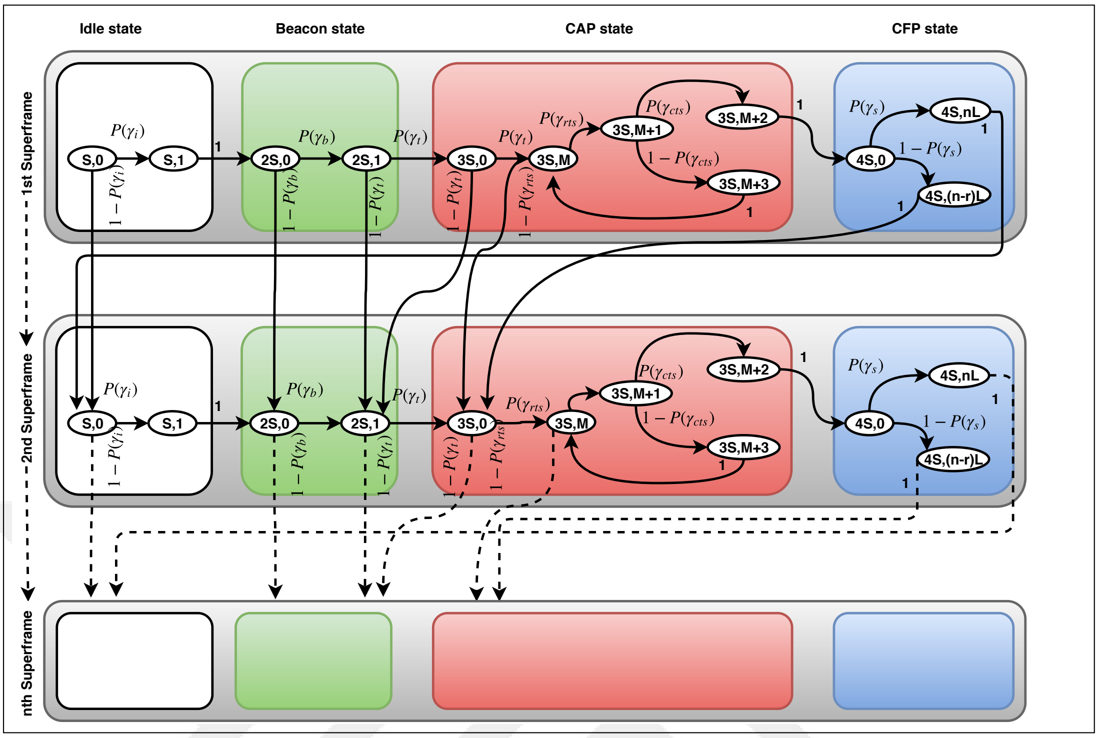

Figure 4.6. The Markov chain model for SA-MAC protocol.

In Table 4.1 we present a summary of the Markov chain model for our protocol. Moreover, Figure 4.6 shows the Markov chain model of the SA-MAC protocol for aggregated VLC-RF wireless networks.

4.4.1. Defining transition probabilities

The process of packet arrival is generally modeled as Poisson distribution, therefore, we assume that same distribution can be adopted for the probability of the node to generate packets in idle state. Thus, the probability of node γ to generate packets in idle state is defined as:

$$p(\gamma_i) = \frac{(\lambda i_t)^k e^{-\lambda i_t}}{k!} \tag{4.1}$$

where k is the number of packets generated, i_t is the duration of idle state and λ is the packet arrival rate. Moreover, when the AP broadcasts the beacon frame, node γ receives the beacon frame with some probabilities $p(\gamma_b)$. Note that $p(\gamma_b)$ depends on the position of the node (node must be within the angle of irradiance of the access point).

Table 4.1. 2D Markov chain model states definition.

State name	S(γ)	A(γ)	**Explanation**
Idle	S	0	No packets arrive at node γ
		1	Packets arrive at node γ
Beacon	2S	0	Beacon frame not received at node γ
		1	Beacon frame received at node γ
CAP	3S	0	Back-off is not initiated at node γ
		1	Back-off is initiated at node γ
		2	Back-off is in progress at node γ
		...	....
		M	End of back-off process
		M+1	RTS is transmitted from node γ
		M+2	CTS received at node γ
		M+3	CTS is not received at node γ
CFP	4S	(n−r)L	If some packets are not successfully transmitted
		nL	If all packets are transmitted successfully

Otherwise, it will not detect any signal from the access point. We therefore, define $p(\gamma_b)$ as follows:

$$p(\gamma_b) = p(x_1 < x < x_2) = \int_{x_1}^{x_2} f(x)dx \tag{4.2}$$

Where x_1 and x_2 are ground coordinates of the network and x is the ground coordinate of the node. In this case, we assume f(x) follows the Gaussian distribution because light intensity decreases when moving away from center of the light source. Moreover, $p(\gamma_{rts})$ is the probability of sending RTS and $p(\gamma_{cts})$ is the probability of receiving CTS, i.e. a node is in the state $(3S, M+2)$. The probability of sending RTS and receiving CTS $p(\gamma_c)$ can be expressed as:

$$p(\gamma_c) = p(\gamma_{cts} | \gamma_{rts}) \tag{4.3}$$

The probability of sending RTS and receiving CTS depends on the probability of receiving a beacon frame, and the probability of successful transmission of RTS. The probability of successful transmission of RTS is given by the probability that exactly one station transmits on the channel, conditioned on the fact that at least one station transmits [142].

$$p(\gamma_{rts}) = \frac{n\tau(1-\tau)^{n-1}}{1-(1-\tau)^n} \tag{4.4}$$

where n is the number of contending nodes in a network, τ is the stationary probability that a node transmits a packet at a random time. For a constant back-off size, and window size W, τ is defined as follows:

$$\tau = \frac{2}{W+1} \tag{4.5}$$

Note that $p(\gamma_t)$ in Figure 4.6 is equal to $p(\gamma_{rts})$ and the downlink channel uses VLC, thus $p(\gamma_{cts})$ can be determined like $p(\gamma_b)$. Therefore:

$$p(\gamma_{cts}) = p(\gamma_b) \tag{4.6}$$

$$p(\gamma_c) = \frac{p(\gamma_{cts} \cap \gamma_{rts})}{p(\gamma_{rts})} \tag{4.7}$$

In CFP, the probability of success is P_{CFP} and $1-P_{CFP}$ is the probability of failure. If node γ generates k packets, the probability of transmitting successfully r out of k packets is given as:

$$p(\gamma_s) = \binom{k}{r} \cdot P^{r}_{CFP}(1-P_{CFP})^{k-r} \tag{4.8}$$

4.4.2. Throughput analysis

For simplicity, we assume that a node generates n packets of equal length L. A node can successfully send packets it reaches the final state, i.e., $\pi_{(4S,nL)} > 0$. Thus, we can establish the throughput of a node if we determine the probability of being in the final state. Let $\pi_e | e = \{0, ..., 11\}$ be the steady state probability of node γ being in state e, i.e.,

$$\pi_e = P(\gamma_e), \tag{4.9}$$

where $\{\pi_0 = (S,0), \pi_1 = (S,1), \pi_2 = (2S,0), \pi_3 = (2S,1), \pi_4 = (3S,0), \pi_5 = (3S,M), \pi_6 = (3S,M+1), \pi_7 = (3S,M+2), \pi_8 = (3S,M+2), \pi_9 = (4S,0), \pi_{10} = (4S,(n-r)L)), \pi_{11} = (4S,nL)\}$. We define the equations for steady state distribution and obtain the steady state probabilities as follows:

$$\pi_0 p(\gamma_i) = \pi_0(1 - p(\gamma_i)) + \pi_{11} \tag{4.10}$$

$$\pi_1 = \pi_0 p(\gamma_i) \tag{4.11}$$

$$\pi_2 p(\gamma_b) + \pi_2(1 - p(\gamma_b)) = \pi_1 \tag{4.12}$$

$$\pi_3 p(\gamma_t) + \pi_3(1 - p(\gamma_t) = \pi_2 p(\gamma_b) \tag{4.13}$$

$$\pi_4 p(\gamma_t) + \pi_4 (1 - p(\gamma_t)) = \pi_3 p(\gamma_t) \tag{4.14}$$

$$\pi_5 p(\gamma_{rts}) + \pi_5(1 - p(\gamma_{rts})) = \pi_4 p(\gamma_t) + \pi_7 \tag{4.15}$$

$$\pi_6 p(\gamma_{cts}) + \pi_6(1 - p(\gamma_{cts})) = \pi_5 p(\gamma_{rts}) \tag{4.16}$$

$$\pi_7 = \pi_6(1 - p(\gamma_{cts}) \tag{4.17}$$

$$\pi_8 = \pi_6 p(\gamma_{cts}) \tag{4.18}$$

$$\pi_9 p(\gamma_s) + \pi_9(1 - p(\gamma_s)) = \pi_8 \tag{4.19}$$

$$\pi_{10} = \pi_9(1 - p(\gamma_s)) \tag{4.20}$$

$$\pi_{11} = \pi_9 p(\gamma_s) \tag{4.21}$$

Note that in steady state the probability distribution for all states must sum to 1, i.e.,

$$\sum_{e=(S,0)}^{4S,nL} \pi_e = 1 \tag{4.22}$$

We can write the transmission probabilities in matrix form as follows:

$$\begin{pmatrix}
1 & 0 & 0 & 0 & 0 & 0 & 0 & 0 & 0 & 0 & 0 & 1 \\
p(\gamma_i) & 1 & 0 & 0 & 0 & 0 & 0 & 0 & 0 & 0 & 0 & 0 \\
0 & 1 & 1 & 0 & 0 & 0 & 0 & 0 & & 0 & 0 & 0 \\
0 & 0 & 0 & p(\gamma_t) & 1 & 0 & 0 & 0 & & 0 & 0 & 0 \\
0 & 0 & 0 & 0 & p(\gamma_t) & 1 & 0 & 1 & 0 & 0 & 0 & 0 \\
0 & 0 & 0 & 0 & 0 & p(\gamma_{rts}) & 1 & 0 & 1 & 0 & 0 & 0 \\
0 & 0 & 0 & 0 & 0 & 0 & p(\gamma cts) & 0 & 1 & 0 & 0 & 0 \\
0 & 0 & 0 & 0 & 0 & 0 & 1-p(\gamma_{cts}) & 1 & 0 & 0 & 0 & 0 \\
0 & 0 & 0 & 0 & 0 & 0 & p(\gamma_{cts}) & 0 & 1 & 0 & 0 & 0 \\
0 & 0 & 0 & 0 & 0 & 0 & 0 & 0 & 1 & 1 & 0 & 0 \\
0 & 0 & 0 & 0 & 0 & 0 & 0 & 0 & 0 & 1-p(\gamma_s) & 1 & 0 \\
0 & 0 & 0 & 0 & 0 & 0 & 0 & 0 & 0 & p(\gamma_s) & 0 & 1
\end{pmatrix}
\begin{pmatrix} \pi_0 \\ \pi_1 \\ \pi_2 \\ \pi_3 \\ \pi_4 \\ \pi_5 \\ \pi_6 \\ \pi_7 \\ \pi_8 \\ \pi_9 \\ \pi_{10} \\ \pi_{11} \end{pmatrix}
=
\begin{pmatrix} 0 \\ 0 \\ 0 \\ 0 \\ 0 \\ 0 \\ 0 \\ 0 \\ 0 \\ 0 \\ 0 \\ 0 \end{pmatrix}$$

After solving these linear equations, we get the following values of steady state probabilities:

$$\pi_0 = \left[p(\gamma_i) - (1 - p(\gamma_i))\right]^{-1} \tag{4.23}$$

$$\pi_1 = \frac{p(\gamma_i)}{p(\gamma_i) - (1 - p(\gamma_i))} \tag{4.24}$$

$$\pi_2 = \left[p(\gamma_b) + (1 - p(\gamma_i))\right]^{-1} \tag{4.25}$$

$$\pi_3 = \frac{p(\gamma_b)}{\left[p(\gamma_t) + (1 - p(\gamma_t)\right]\left[p(\gamma_b) + (1 - p(\gamma_i))\right]} \tag{4.26}$$

$$\pi_4 = \left[\frac{p(\gamma_b)}{\left[p(\gamma_t) + (1 - p(\gamma_t)\right]\left[p(\gamma_b) + (1 - p(\gamma_i))\right]}\right]\left[\frac{p(\gamma_t)}{\left[p(\gamma_t) + (1 - p(\gamma_t))\right]}\right] \tag{4.27}$$

$$\pi_5 = \left[\frac{p(\gamma_b)}{\left[p(\gamma_t)+(1-p(\gamma_t)\right]\left[p(\gamma_b)+(1-p(\gamma_i))\right]}\right]\left[\frac{p(\gamma_t)}{\left[p(\gamma_t)+(1-p(\gamma_t))\right]}\right]$$

$$\left[\frac{(p(\gamma_t))}{\left[p(\gamma_{rts})+(1-p(\gamma_{rts}))\right]}\right] \tag{4.28}$$

$$\pi_6 = \left[\frac{p(\gamma_b)}{\left[p(\gamma_t)+(1-p(\gamma_t)\right]\left[p(\gamma_b)+(1-p(\gamma_i))\right]}\right]\left[\frac{p(\gamma_t)}{\left[p(\gamma_t)+(1-p(\gamma_t))\right]}\right]$$

$$\left[\frac{(p(\gamma_t))}{\left[p(\gamma_{rts})+(1-p(\gamma_{rts}))\right]}\right]\left[\frac{p(\gamma_{rts})}{\left[p(\gamma_{cts})+(1-p(\gamma_{cts}))\right]}\right] \tag{4.29}$$

$$\pi_7 = \left[(1-p(\gamma_{cts})\right]\left[\frac{p(\gamma_{rts})}{p(\gamma_{cts})+(1-p(\gamma_{cts}))}\right]\left[\frac{p(\gamma_b)}{\left[p(\gamma_t)+(1-p(\gamma_t)\right]\left[p(\gamma_b)+(1-p(\gamma_i))\right]}\right]$$

$$\left[\frac{p(\gamma_t)}{\left[p(\gamma_t)+(1-p(\gamma_t))\right]}\right]\left[\frac{(p(\gamma_t))}{\left[p(\gamma_{rts})+(1-p(\gamma_{rts}))\right]}\right] \tag{4.30}$$

$$\pi_8 = \left[p(\gamma_{cts})\right]\left[\frac{p(\gamma_{rts})}{\left[p(\gamma_{cts})+(1-p(\gamma_{cts}))\right]}\right]\left[\frac{p(\gamma_b)}{\left[p(\gamma_t)+(1-p(\gamma_t)\right]\left[p(\gamma_b)+(1-p(\gamma_i))\right]}\right]$$

$$\left[\frac{p(\gamma_t)}{\left[p(\gamma_t)+(1-p(\gamma_t))\right]}\right]\left[\frac{(p(\gamma_t))}{\left[p(\gamma_{rts})+(1-p(\gamma_{rts}))\right]}\right] \tag{4.31}$$

$$\pi_9 = \left[p(\gamma_{cts})\right]\left[\frac{p(\gamma_{rts})}{\left[p(\gamma_{cts})+(1-p(\gamma_{cts}))\right]}\right]\left[\frac{p(\gamma_b)}{\left[p(\gamma_t)+(1-p(\gamma_t)\right]\left[p(\gamma_b)+(1-p(\gamma_i))\right]}\right]$$

$$\left[\frac{p(\gamma_t)}{\left[p(\gamma_t)+(1-p(\gamma_t))\right]}\right]\left[\frac{(p(\gamma_t))}{\left[p(\gamma_{rts})+(1-p(\gamma_{rts}))\right]}\right]\left[p(\gamma_s)+(1-p(\gamma_s))\right]^{-1} \tag{4.32}$$

$$\pi_{10} = \left[(1-p(\gamma_s))\right]\left[p(\gamma_s)+(1-p(\gamma_s))\right]^{-1}\left[\frac{p(\gamma_{cts})p(\gamma_{rts})}{\left[p(\gamma_{cts})+(1-p(\gamma_{cts}))\right]}\right]\left[\frac{p(\gamma_t)}{\left[p(\gamma_t)+(1-p(\gamma_t))\right]}\right]$$

$$\left[\frac{p(\gamma_b)}{\left[p(\gamma_t)+(1-p(\gamma_t)\right]\left[p(\gamma_b)+(1-p(\gamma_i))\right]}\right]\left[\frac{(p(\gamma_t))}{\left[p(\gamma_{rts})+(1-p(\gamma_{rts}))\right]}\right] \tag{4.33}$$

$$\pi_{11} = \left[p(\gamma_s)p(\gamma_{cts})\right]\left[\frac{p(\gamma_{rts})}{\left[p(\gamma_{cts})+(1-p(\gamma_{cts}))\right]}\right]\left[\frac{p(\gamma_b)}{\left[p(\gamma_t)+(1-p(\gamma_t)\right]\left[p(\gamma_b)+(1-p(\gamma_i))\right]}\right]$$

$$\left[\frac{p(\gamma_t)}{\left[p(\gamma_t)+(1-p(\gamma_t))\right]}\right]\left[\frac{(p(\gamma_t))}{\left[p(\gamma_{rts})+(1-p(\gamma_{rts}))\right]}\right]\left[p(\gamma_s)+(1-p(\gamma_s))\right]^{-1} \quad (4.34)$$

From this condition, the probability distribution for each state can be calculated. We calculate the throughput of a node as the probability of being in the final state i.e., $P(\gamma_e) = (4S, nL)$, therefore, per node throughput is calculated as follows:

$$\pi_{11} = \left[p(\gamma_s)p(\gamma_{cts})\right]\left[\frac{p(\gamma_{rts})}{\left[p(\gamma_{cts})+(1-p(\gamma_{cts}))\right]}\right]\left[\frac{p(\gamma_b)}{\left[p(\gamma_t)+(1-p(\gamma_t)\right]\left[p(\gamma_b)+(1-p(\gamma_i))\right]}\right]$$

$$\left[\frac{p(\gamma_t)}{\left[p(\gamma_t)+(1-p(\gamma_t))\right]}\right]\left[\frac{(p(\gamma_t))}{\left[p(\gamma_{rts})+(1-p(\gamma_{rts}))\right]}\right]\left[p(\gamma_s)+(1-p(\gamma_s))\right]^{-1} \quad (4.35)$$

4.4.3. Network delay

Let δ_k be the delay of node k and N_D be the network delay. From the Markov chain model, the delay of a node is the probability of moving from the initial state to the CFP. Mathematically, we represent this as follows:

$$\delta_k = \bigcup_{e=(S,0)}^{(3S,M+2)} p(\gamma_{e+1}|\gamma_e) \quad (4.36)$$

Similarly the expression above gives delay of a single node. The network delay can be written as,

$$N_D = \left(\sum_{k=1}^{N} \bigcup_{e=(S,0)}^{(3S,M+2)} p(\gamma_{e+1}|\gamma_e)\right) N^{-1}. \quad (4.37)$$

4.4.4. Power consumption

Let $E(\gamma)$ denote the normalized power consumed by node γ in state e and N_E be the normalized network energy consumption. The energy used by a node in each state depends on whether a node is idle, receiving, or transmitting. We minimize energy consumption in CAP by allowing the node to begin the back-off process depending on the successful data transfer probability. This is contrary to the CSMA protocol in which a node randomly initiates back-off process thereby, causing unnecessary energy consumption. For each transmission, the normalized energy consumed by node k is denoted by ε_k and is mathematically written as follows:

$$\varepsilon_\gamma = \bigcup_{e=(S,0)}^{(4S,nL)} p\left(\gamma_{e+1}|\gamma_e\right) E\left(\gamma_{e+1}\right) \tag{4.38}$$

Extending the expression above yields the following network delay equation,

$$N_E = \left(\sum_{\gamma=1}^{N} \bigcup_{e=(S,0)}^{(4S,nL)} p\left(\gamma_{e+1}|\gamma_e\right) E\left(\gamma_{e+1}\right)\right) N^{-1}. \tag{4.39}$$

4.4.5. Collision

Collision can occur in the uplink channel because of simultaneous transmission during CAP. Thus, a node encounters collision if it is in CAP and at least one of the remaining $n-1$ nodes transmit simultaneously. Let p_{co} denote the probability of collision that is defined as follows [142].

$$p(\gamma_{co}) = 1-(1-\tau)^{n-1} \tag{4.40}$$

Therefore the normalized collision of node γ denoted as C_γ can be expressed as a function of probability of being in CAP state and p_{co}.

$$C_\gamma = \left(\bigcup_{e=(S,0)}^{(3S,M+1)} p\left(\gamma_{e+1}|\gamma_e\right)\right) \left(1-(1-\tau)^{n-1}\right) \tag{4.41}$$

We extend this expression to achieve the normalized network collision for N number of nodes as follows:

$$N_C = \left(\sum_{\gamma=1}^{N} \left(\bigcup_{e=(S,0)}^{(3S,M+1)} p\left(\gamma_{e+1}|\gamma_e\right)\right) \left(1-(1-\tau)^{n-1}\right)\right) N^{-1} \tag{4.42}$$

4.5. Experimental Setup and Numerical results

We evaluate the performance of our protocol by taking into consideration transmission time, non transmission time, throughput, collision, and energy consumption. We consider different sizes of a network size for each performance metric. In order to evaluate the performance of our protocol, we simulate our protocol in the NS3 discrete event network simulator as shown in Figure 4.7, where packets are transmitted by nodes and received by the access point. For each performance metric, we compare simulation results with Markov chain model. We also compare our results with existing MAC protocols such as carrier sense multiple access with collision detection hidden node avoidance (CSMA/CD-HA) presented in [143], and the dynamic contention window-based successive transmission (DCW-ST) suggested in [60]. For each performance metric we run the simulation 50 times and the results presented are average. In addition, our results are obtained based on the parameters listed in Table 4.2. The results we present are normalized by using the feature scaling that is also known as Min-Max scaling i.e., subtract the minimum value and divide by the range of each column. Each column has 0 as its minimum value and 1 as its maximum value. One possible formula to achieve this is by using the following relation:

$$X_{new} = \frac{X - X_{min}}{X_{max} - X_{min}} \tag{4.43}$$

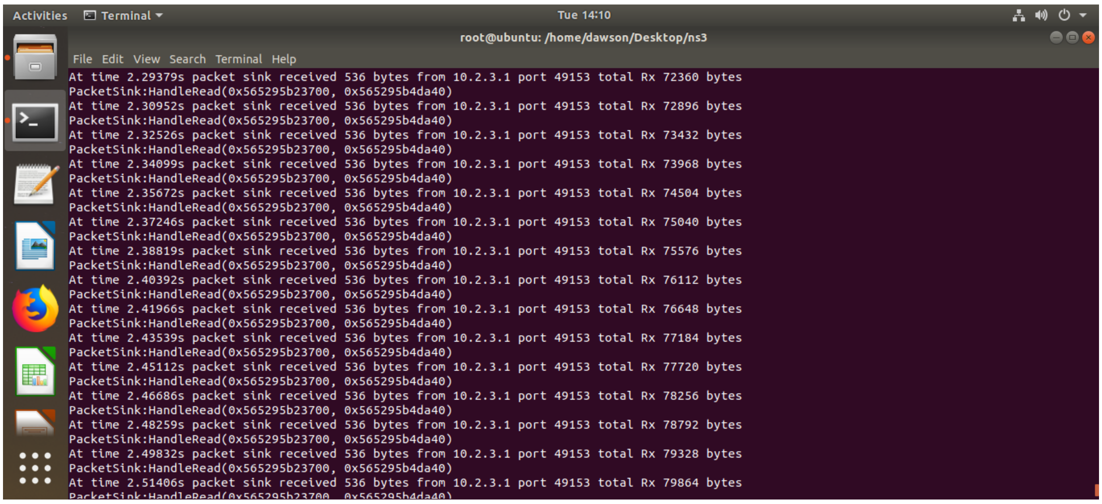

Figure 4.7. A screen-shot of the SA-MAC simulation in NS3.

Table 4.2. Simulation parameters

Description	Setting
Room size (Width x Length x Height)	4m x 4m x 2.5m
Vertical separation	2.5m
FOV of the receiver	60°
Angle of the transmitter	30°
Optical concentrator refractive index	1.5
Photodetector area	1 [cm2]
PD responsivity	0.6 A/W
VLC Data rate	80 Mbps
RF Data rate	54 Mbps
Packet size (L)	1024 Bytes
Window size (W)	32
Mean packet arrival rate (λ)	5
RTS size	44 bytes
CTS size	38 bytes

4.5.1. Throughput

Network throughput is one of the performance metrics that we take into consideration in evaluating the benefits of our study. Throughput in this context refers to the average number of packets successfully transmitted per superframe. Figure 4.8 presents the results considering networks size against normalized throughput. We compare results from SA-MAC simulation, Markov chain model, and the CSMA/CD-HA protocol. Results in Figure 4.8 suggest that throughput decreases when the network size increases. This is prompted by increase in collision in the CAP state when the network size increases. There is a slight difference between simulation and Markov chain model results at low network size, however, the results converge when network size increases. Our simulation and Markov chain model results outperform the CSMA/CD-HA protocol in terms of throughput.

4.5.2. Non transmission time

We evaluate the performance of the SA-MAC protocol for aggregated VLC-RF wireless networks by considering non transmission time (NTT) for both Markov chain model and simulation. Numerical results in Figure 4.9a suggest that simulation results show more NTT compared to Markov chain model results especially when the network size is small. However, the difference in this case is not significant. Moreover, NTT is an

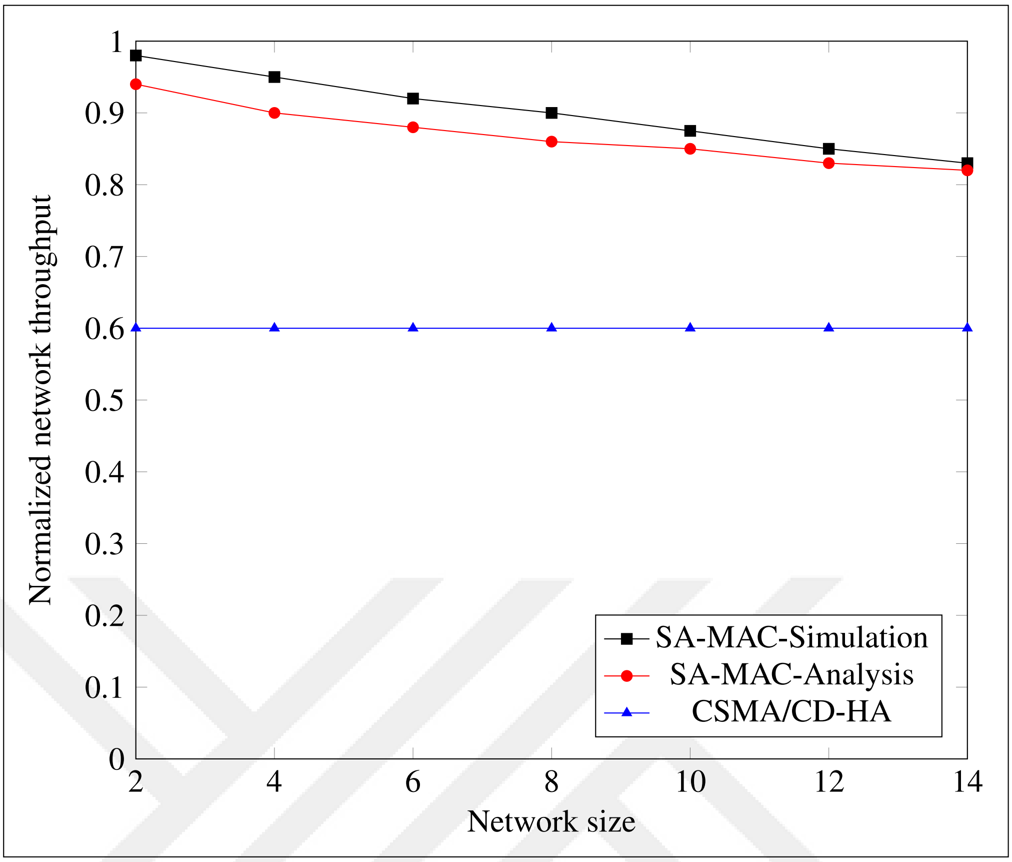

Figure 4.8. Network size versus throughput.

increasing function of network size for both simulation and the Markov chain model. This is because when the number of nodes is large, there is more competition for limited resources available at the access point, viz., p(γ_{rts}) decreases as suggested in Equation 4.4. Furthermore, we demonstrate the impact of RF and VLC channels in NTT in Figure 4.9b. Results from simulations show that RF-channels contribute more NTT than the VLC-channel. This is due to the fact that RF-channel is used in CAP where there is contention. Moreover, the propagation speed of RF is lower than that of VLC. Note that, in Markov chain model the behaviour of a system can be analyzed based on transition and states probability. Therefore, it is not ideal to obtain delay contributed by individual links, i.e., VLC and RF links. Accordingly, in Figure 4.9b, we show results from the simulation only. Figure 4.9a also presents a comparison of our results against the results obtained in the DCW-ST protocol. In this case the SA-MAC protocol outperforms the DCW-ST in terms of networks NTT especially when the network size increases.

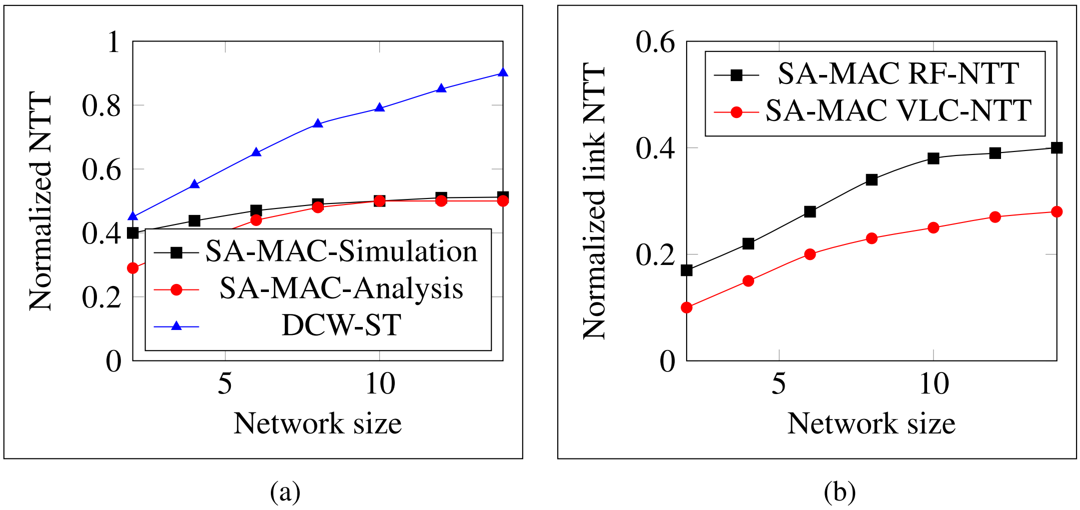

Figure 4.9. Network size versus NTT in (a) and Network size versus link NTT in (b).

4.5.3. Collision

We describe the performance of our protocol by comparing probability of collision in the SA-MAC simulation and Markov chain model and the results are presented in Figure 4.10. In this context, collision probability refers to unsuccessful packet transmission.

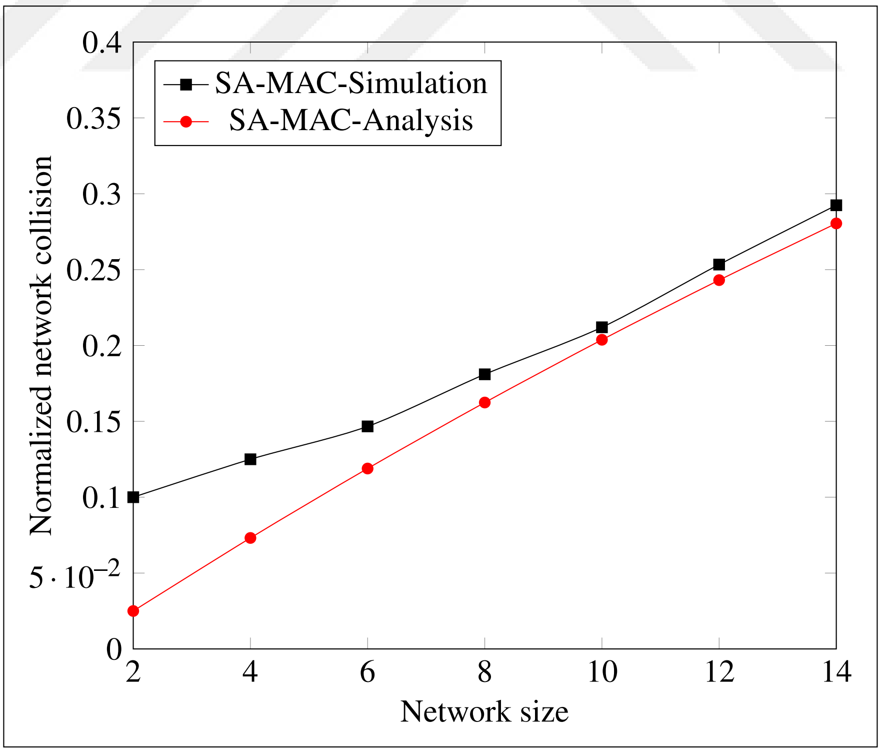

Figure 4.10. Network size versus collision.

The results in this case suggest that collision increases when the network size increases for both simulation and Markov chain model. For example, network collision increases from 0.1 when network size is 2 to 0.29 when network size is 14 for SA-MAC and from 0.025 when network size is 2 to 0.28 when network size is 14 for the Markov chain model results. Simulation results yield more collision than the Markov chain model results especially at when the network size is small. However, difference between simulation results and Markov chain model is negligible especially when the network size increases.

4.5.4. Energy consumption

In Figure 4.11, we present our results considering the rate of energy consumption. Similarly, we compare results from SA-MAC simulation with results from the Markov chain model. For simplicity, we assume that the distribution of energy consumption for the Markov chain model is 0.1, 0.4, and 0.5 in beacon, CAP, and CFP states respectively. In this case, normalized energy consumption increases when network size increases for both the SA-MAC simulation and Markov chain model results, and it converges when the network size is high, i.e. > 8.

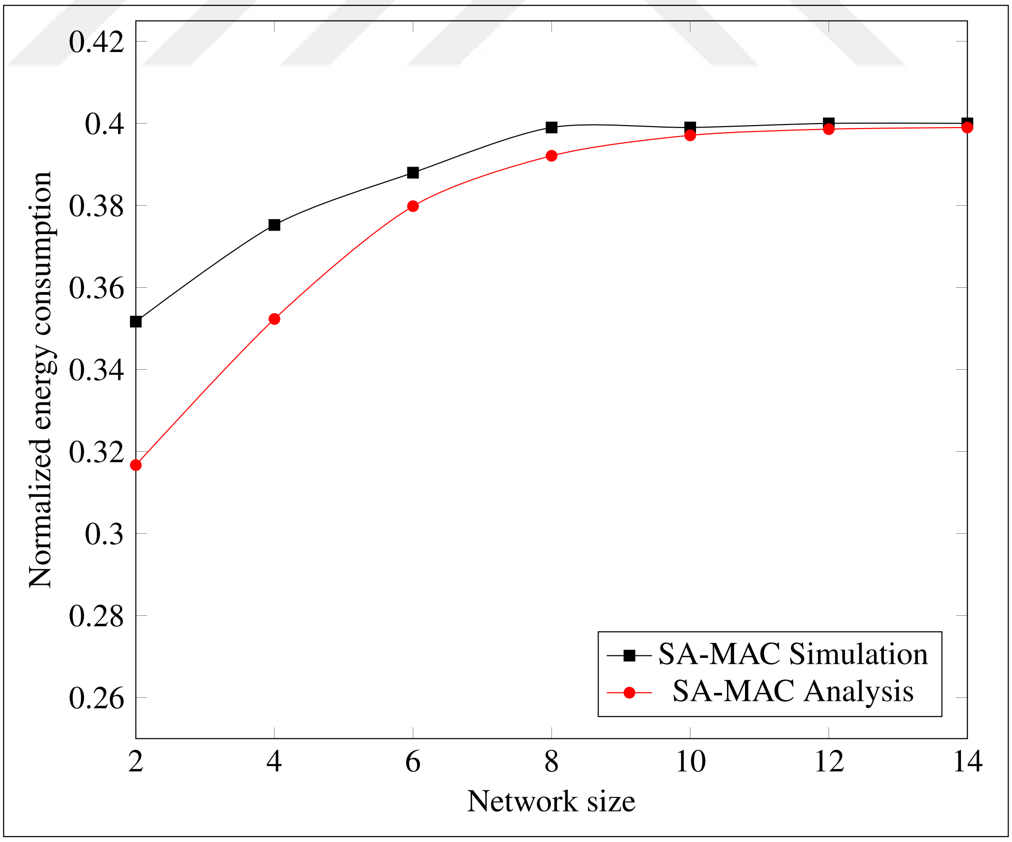

Figure 4.11. Network size versus energy consumption.

At low network size normalized energy consumption is low because the probability of collision is low, hence, small amount of energy is used during the association phase. Collision increases when the network size increases as suggested by Equation 9. However, at steady state, the rate of collision remains constant.

4.5.5. Transmission time

Furthermore, we study the impact of the superframe size to our protocol by applying fixed, random and dynamic superframe sizes. More specific, we compare the transmission time for fixed, random, and dynamic superframe sizes and the results are shown in Figure 4.12. Here, the sizes of superframe ranges from 10 to 40 msec for dynamic superframe. Note that, in the dynamic superframe sizes case, the access point determines the size of the superframe depending on the size of the PT while in fixed superframe size case we use the fixed size, i.e., 40 msec. For the random superframe size case, the access point selects a random superframe size.

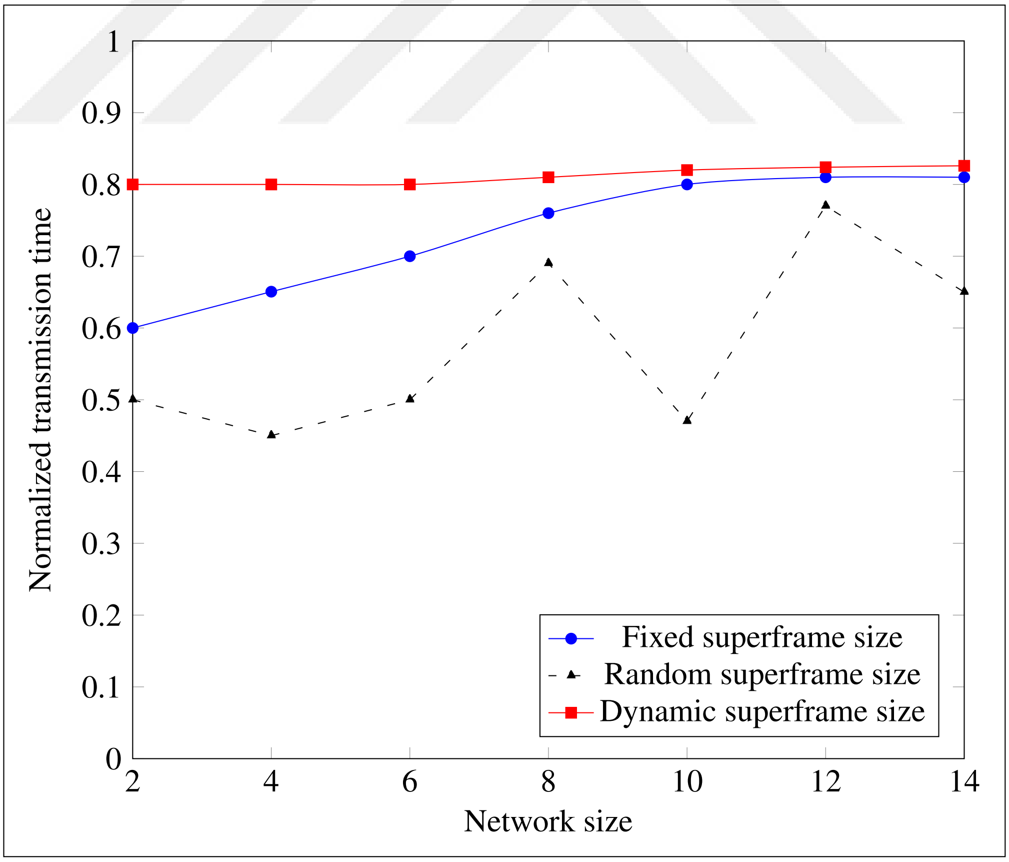

Figure 4.12. Network size versus transmission time.

The results in Figure 4.12 suggest that the dynamic superframe size case yield better results in terms of transmission time compared to the other scheme. In the fixed superframe size scheme, the transmission time is high when the network size increases. Finally, the random superframe scheme provides less promising results because the transmission time is not optimal and deterministic in any case. This is because of selecting a random superframe size without considering the size of the PT.

4.6. A comparison of APMAC and SA-MAC Protocols

In the following we compare the performance of APMAC and SA-MAC protocols in terms of throughput and transmission time. The results in Figure 4.13 show the normalized throughput as a function of network size. Here we compare the results from the APMAC protocol against the SA-MAC protocol simulation and the Markov chain model results.

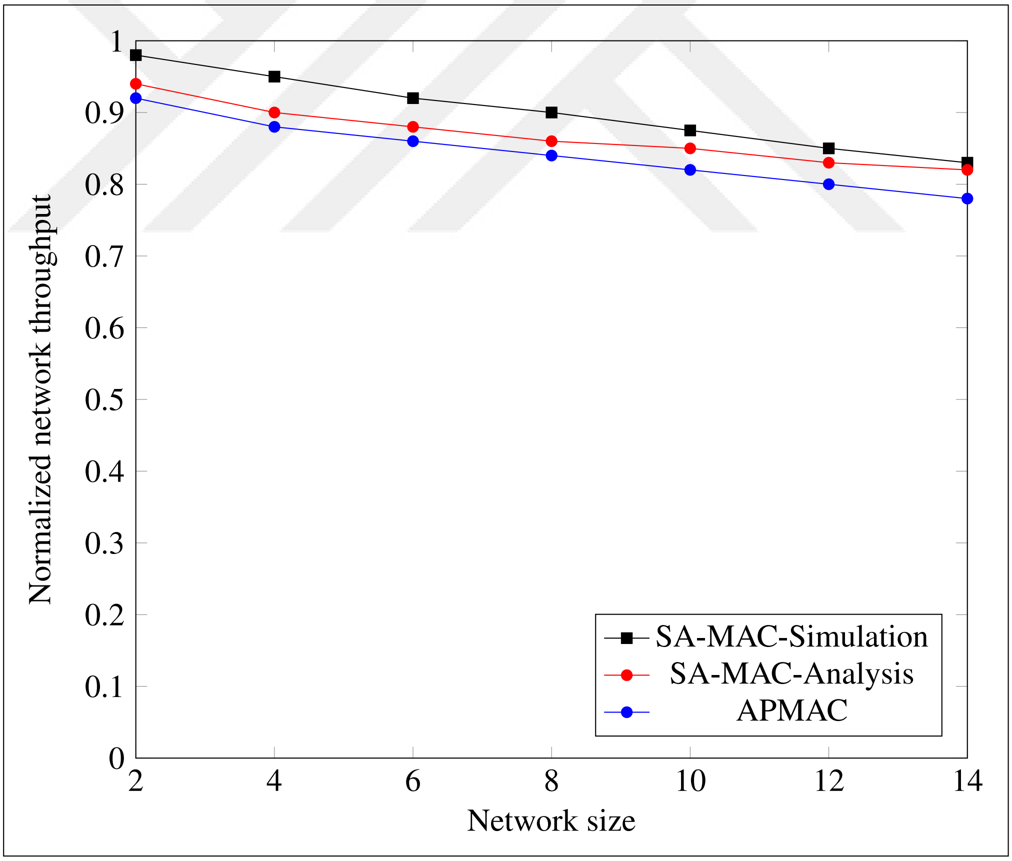

Figure 4.13. Network size versus throughput.

The SA-MAC protocol outperforms the APMAC protocol in both simulation and analysis cases. The results for both protocols show that throughput decreases when the network density increases. In addition, the results for both protocols range between 0.8

and 1, a significant improvement compared to previous works. Although the simulation and analysis results for the SA-MAC protocol differ when the network size is small, the difference is not significant.

In Figure 4.14 we compare the transmission time of the APMAC and SA-MAC protocols. The APMAC protocol uses fixed superframe size while the SA-MAC protocol uses dynamic superframe size. In the APMAC protocol, transmission time decrease when the network size increases. This is prompted by (i) the use of fixed superframe size, and (ii) the contention in CAP, i.e., more time is used for channel arbitration when there are more nodes in a network. The transmission time of the system increases when the number of nodes increases in the SA-MAC protocol. This is due to the fact the SA-MAC protocol uses dynamic superframe size. Nonetheless, in either case the transmission time ranges between 0.8 and 0.98.

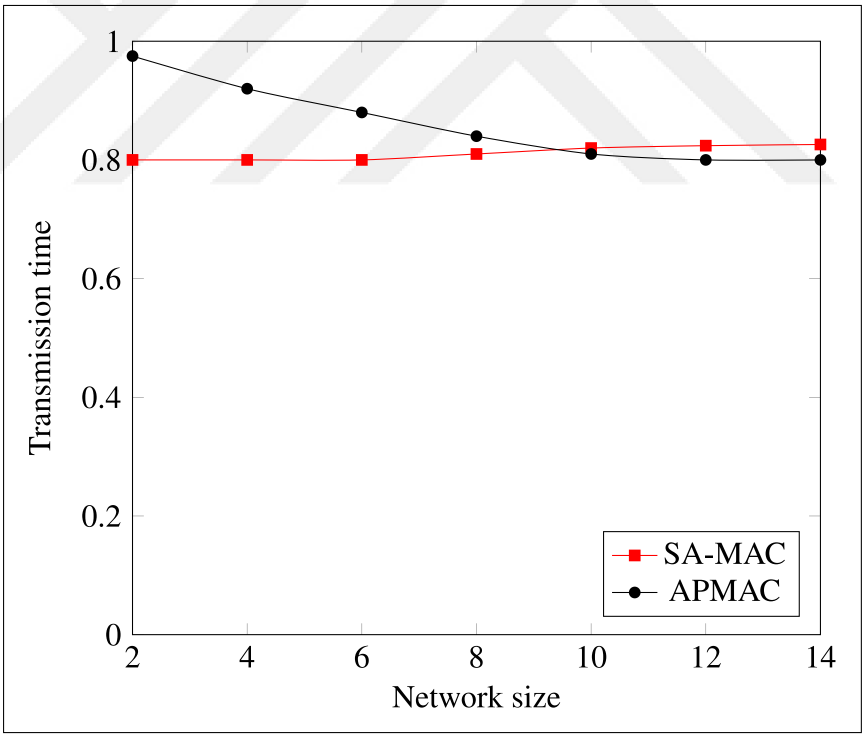

Figure 4.14. Network size versus transmission time.

4.7. Conclusion

The existing internet demand is overwhelming to the RF-based wireless networks. VLC can address the ever-increasing internet demand considering the huge bandwidth available in the visible light spectrum. Nevertheless, VLC standalone system cannot provide full-duplex communication because of several limitations such as network addressing, medium access control, interference, and energy consumption of LEDs. The coexistence of RF and VLC systems can be used to achieve full-duplex communication in indoor wireless networks. In this study, we proposed the aggregate VLC-RF wireless network MAC protocol named SA-MAC protocol. We demonstrated the Markov chain model that shows the behavior of a node in SA-MAC protocol. The simulation of our protocol is done in the NS3 discrete event network simulator. In order to validate our study, results from simulations and Markov chain model are compared for each performance metric. Furthermore, we showed the potential benefits of our study, by comparing our results against existing MAC protocols such as DCW-ST and CSMA/CD-HA. Numerical results from our study suggest that SA-MAC protocol outperforms existing MAC protocols for aggregated VLC-RF wireless networks.

5. CONCLUSION

This thesis investigated the problem of medium access control for aggregated VLC-RF wireless networks. We suggested efficient MAC protocols that properly address the problem of medium access in aggregated VLC-IR and VLC-RF wireless networks. The focus is minimizing delay and collision while increasing throughput, fairness, and system utilization. The novelty of this thesis is to solve the problem of medium access control in aggregated VLC and other wireless networks such as IR and RF. We extended this main idea into two main problems as follows:

Initially we considered the aggregated VLC-IR wireless network in which VLC is used for the downlink channel while the uplink channel uses IR. We designed the MAC protocol for such aggregated wireless networks named the Adaptive Polling MAC (APMAC) protocol for aggregated VLC-IR wireless networks. The focus of APMAC protocol is minimizing delay and collision while increasing throughput, fairness, and utilization.

In the second case we considered aggregated VLC-RF wireless networks wherein the downlink channel uses VLC while the uplink channel uses RF. In this case we designed the Self-Adaptive MAC protocol for aggregated VLC-RF wireless networks. Similarly to APMAC protocol, the SA-MAC protocol minimizes delay, collision, and energy consumption while increasing throughput. In addition, the Markov chain model that analyzes the nodes in the SA-MAC protocol under varying conditions is presented.

Besides considering these two dimensions of the problem of MAC protocol for aggregated VLC and other wireless networks, we conducted simulations of both protocols by using the NS3 network discrete event simulator and presented numerical results that revealed the potential advantage of this thesis.

This thesis focuses on MAC protocols for aggregated VLC and other wireless networks such as RF and IR. However, there exist other challenges that can occur in aggregated VLC-RF and VLC-IR wireless networks such as network addressing. In general, existing studies in VLC wireless networks consider the physical and link layers only. Furthermore, the current literature in VLC focuses on point-to-point communication, and downlink channel only. It is imperative to consider upper layer of the OSI model and extend point-to-point to full mesh network when designing VLC wireless networks. These problems and other future problems can be build on our work.

In this thesis, we introduced a new and important problem for the community, and we explored the problem in detail and investigated several dimensions of the problem. We hope these works can be valuable to the community.

REFERENCES

[1] Cisco, “Cisco VNI Mobile Forecast Highlights, 2016-2021. [online]. Available: https://www.cisco.com/assets/sol/sp/vni/forecast$_{h}$ighlights$_{m}$obile/”, (Date accessed: 12 February 2019).

[2] Khan L. U., Visible Light Communication: Applications, Architecture, Standardization and Research Challenges, *Digital Communications and Networks*, 2017**, 3**(2), 78–88.

[3] Msongaleli D. L., Kucuk K., Reliability and Cost-Aware Network Upgrade for the Next Generation Mobile Networks, in: *International Conference on Computer Science and Engineering (UBMK)*, Antalya, Turkey, 5- 08 October 2017.

[4] Elgala H., Mesleh R., Haas H., Indoor optical wireless communication: potential and state-of-the-art, *IEEE Communications Magazine*, 2011**, 49**(9), 56–62.

[5] PureLiFi, “LiFi Technology. [online]. Available: https://purelifi.com/”, (Date accessed: 12 February 2019).

[6] Visible Light Communications Consortium (VLCC). [online]. Available: http://www.vlcc.net/, (Date accessed: 12 February 2019).

[7] Japan Electronics, Information Technology Industries Association (JEITA). [online]. Available: http://www.jeita.or.jp/, (Date accessed: 12 February 2019).

[8] Visible Light Communications Association (VLCA). [online]. Available: http://vlca.net/, (Date accessed: 12 February 2019).

[9] Infrared Data Association (IrDA). [online]. Available: http://www.irda.org, (Date accessed: 12 February 2019).

[10] IEEE Standard for Local and Metropolitan Area Networks–Part 15.7: Short-Range Wireless Optical Communication Using Visible Light, *IEEE Std 802.15.7-2011*, September 2011(), 1–309.

[11] Haas H., Yin L., Wang Y., Chen C., What is LiFi?, *Journal of Lightwave Technology*, 2016**, 34**(6), 1533–1544.

[12] Rehman S., Ullah S., Chong P. H. J., Yongchareon S., Komosny D., Visible Light Communication: A System Perspective—Overview and Challenges, *Sensors*, 2019**, 19**(5).

[13] Uysal M., Nouri H., Optical Wireless Communications — An Emerging Technology, in: *International Conference on Transparent Optical Networks (ICTON)*, Graz, Austria, 6-10 July 2014.

[14] Chowdhury M. Z., Hossan M. T., Islam A., Jang Y. M., A Comparative Survey of Optical Wireless Technologies: Architectures and Applications, *IEEE Access*, 2018**, 6**(), 9819–9840.

[15] Miller D. A. B., Rationale and Challenges for Optical Interconnects to Electronic Chips, *Proceedings of the IEEE*, 2000**, 88**(6), 728–749.

[16] Kachris C., Tomkos I., A Survey on Optical Interconnects for Data Centers, *IEEE Communications Surveys Tutorials*, 2012**, 14**(4), 1021–1036.

[17] Sichitiu M. L., Kihl M., Inter-vehicle Communication Systems: A Survey, *IEEE Communications Surveys Tutorials*, 2008**, 10**(2), 88–105.

[18] Khalighi M. A., Uysal M., Survey on Free Space Optical Communication: A Communication Theory Perspective, *IEEE Communications Surveys Tutorials*, 2014**, 16**(4), 2231–2258.

[19] Chan V. W. S., Optical Satellite Networks, *Journal of Lightwave Technology*, 2003**, 21**(11).

[20] Xu Z., Sadler B. M., Ultraviolet Communications: Potential and State-Of-The-Art, *IEEE Communications Magazine*, 2008**, 46**(5), 67–73.

[21] Ashtari R., Mao S., Hamilton M. C., A low-cost NLOS ultra-violet V2I identification system for vehicular theft recovery, in: *International Conference on Connected Vehicles and Expo (ICCVE)*, Las Vegas, NV, USA, 2-06 December 2013.

[22] Chen G., Liao L., Li Z., Drost R. J., Sadler B. M., Experimental and simulated evaluation of long distance NLOS UV communication, in: *International Symposium on Communication Systems, Networks Digital Sign (CSNDSP)*, Manchester, UK, 23-25 July 2014.

[23] Wang L., Li Y., Xu Z., Sadler B. M., Wireless ultraviolet network models and performance in noncoplanar geometry, in: *IEEE Globecom Workshops*, Miami, FL, USA, 6-10 December 2010.

[24] Jiao Y., Bai L., Ultraviolet pulse broadening in non-line-of-sight communication system, in: *Proceedings of 2014 3rd Asia-Pacific Conference on Antennas and Propagation*, Harbin, China, 26-29 July 2014.

[25] Zou D., Xu Z., Gong C., Performance of non-line-of-sight ultraviolet scattering communication under different altitudes, in: *IEEE/CIC International Conference on Communications in China (ICCC)*, Chengdu, China, 27-29 July 2016.

[26] Ardakani M. H., Heidarpour A. R., Uysal M., Non-line-of-sight ultraviolet communications over atmospheric turbulence channels, in: *International Workshop on Optical Wireless Communications (IWOW)*, Istanbul, Turkey, 7-08 September 2015.

[27] Noshad M., Brandt-Pearce M., NLOS UV communication systems using spectral amplitude coding, in: *IEEE GLOBECOM Workshops (GC Wkshps)*, Houston, TX, USA, 5-09 December 2011.

[28] Li C., Zhang M., Chen X., Li Q., Luo P., Liu Y., Experimental performance evaluation of mobile sensor and communication system based on ultraviolet, in: *Chinese Control and Decision Conference (CCDC)*, Taiyuan, China, 23-25 May 2012.

[29] Williams S., IrDA: past, present and future, *IEEE Personal Communications*, 2000**, 7**(1), 11–19.

[30] Alresheedi M. T., Hussein A. T., Elmirghani J. M. H., Uplink design in VLC systems with IR sources and beam steering, *IET Communications*, 2017**, 11**(3), 311–317.

[31] Chen L., Zhang Y., Design and Implementation of infrared Wireless Data Transmission System, in: *IEEE International Conference on Information and Automation*, Harbin, China, 20-23 June 2010.

[32] Li Y., Ma C., Design and realization of intelligent infrared data communication system, in: *IEEE International Conference on Mechatronics and Automation*, Tianjin, China, 3-06 August 2014.

[33] Al-Ahmadi S., Maraqa O., Uysal M., Sait S. M., Multi-User Visible Light Communications: State-of-the-Art and Future Directions, *IEEE Access*, 2018**, 6**(), 70555–70571.

[34] Vitsas V., Boucouvalas A. C., Performance Analysis of the Advanced Infrared (AIr) CSMA/CA MAC Protocol for Wireless LANs, *Wireless Networks*, 2003**, 9**(), 495–507.

[35] Tanaka Y., Haruyama S., Nakagawa M., Wireless Optical Transmissions with White Colored LED for Wireless Home Links, in: *IEEE International Symposium on Personal Indoor and Mobile Radio Communications. PIMRC 2000. Proceedings (Cat. No.00TH8525)*, London, UK, United Kingdom, 18-21 September 2000.

[36] Karunatilaka D., Zafar F., Kalavally V., Parthiban R., LED Based Indoor Visible Light Communications: State of the Art, *IEEE Communications Surveys Tutorials*, 2015**, 17**(3), 1649–1678.

[37] Sevincer A., Bhattarai A., Bilgi M., Yuksel M., Pala N., LIGHTNETs: Smart LIGHTing and Mobile Optical Wireless NETworks — A Survey, *IEEE Communications Surveys Tutorials*, 2013**, 15**(4), 1620–1641.

[38] Sunstein D. E., A Scatter Communications Link at Ultraviolet Frequencies, MA thesis, Massachusetts Institute of Technology, 1968.

[39] Bai X., Mcintosh D., Liu H., Campbell J. C., Ultraviolet Single Photon Detection With Geiger-Mode 4H-SiC Avalanche Photodiodes, *IEEE Photonics Technology Letters*, 2007**, 19**(22), 1822–1824.

[40] Shen S., Zhang Y., Yoo D., Limb J., Ryou J., Yoder P. D., Dupuis R. D., Performance of Deep Ultraviolet GaN Avalanche Photodiodes Grown by MOCVD, *IEEE Photonics Technology Letters*, 2007**, 19**(21), 1744–1746.

[41] Ayyash M., Elgala H., Khreishah A., Jungnickel V., Little T., Shao S., Rahaim M., Schulz D., Hilt J., Freund R., Coexistence of WiFi and LiFi toward 5G: concepts, opportunities, and challenges, *IEEE Communications Magazine*, 2016**, 54**(2), 64–71.

[42] Rahaim M. B., Vegni A. M., Little T. D. C., A hybrid Radio Frequency and broadcast Visible Light Communication system, in: *IEEE GLOBECOM Workshops*, Houston, TX, USA, 5-09 December 2011.

[43] Li Z., Shao S., Khreishah A., Ayyash M., Abdalla I., Elgala H., Rahaim M., Little T., Design and Implementation of a Hybrid RF-VLC System with Bandwidth Aggregation, in: *International Wireless Communications Mobile Computing Conference (IWCMC)*, Limassol, Cyprus, 25-29 June 2018.

[44] Shao S., Khreishah A., Rahaim M. B., Elgala H., Ayyash M., Little T. D. C., Wu J., An Indoor Hybrid WiFi-VLC Internet Access System, in: *IEEE International Conference on Mobile Ad-Hoc and Sensor Systems*, Philadelphia, PA, USA, 28-30 October 2014.

[45] Khreishah A., Shao S., Gharaibeh A., Ayyash M., Elgala H., Ansari N., A Hybrid RF-VLC System for Energy Efficient Wireless Access, *IEEE Transactions on Green Communications and Networking*, 2018**, 2**(4), 932–944.

[46] Otomo I., Fujihashi T., Hirota Y., Watanabe T., Cooperative Wi-Fi and Visible Light Communication for Indoor Video Delivery, in: *IEEE International Conference on Communications (ICC)*, Kansas City, MO, USA, 20-24 May 2018.

[47] Basnayaka D. A., Haas H., Design and Analysis of a Hybrid Radio Frequency and Visible Light Communication System, *IEEE Transactions on Communications*, 2017**, 65**(10), 4334–4347.

[48] Gupta A., Garg P., Sharma N., Hybrid LiFi—WiFi indoor broadcasting system, in: *IEEE Annual International Symposium on Personal, Indoor, and Mobile Radio Communications (PIMRC)*, Montreal, QC, Canada, 8-13 October 2017.

[49] Hammouda M., Akin S., Vegni A. M., Haas H., Peissig J., Hybrid RF/VLC Systems under QoS Constraints, *CoRR*, 2018().

[50] Hammouda M., Akın S., Vegni A. M., Haas H., Peissig J., Link Selection in Hybrid RF/VLC Systems Under Statistical Queuing Constraints, *IEEE Transactions on Wireless Communications*, 2018**, 17**(4), 2738–2754.

[51] Little T. D. C., Rahaim M., Network topologies for mixed RF-VLC HetNets, in: *IEEE Summer Topicals Meeting Series (SUM)*, 2015, 163–164.

[52] Huang Z., Ji Y., Design and demonstration of room division multiplexing-based hybrid VLC network, *Chinese Optics Letters*, 2013**, 11**(6), 060–603.

[53] Rao S. P. V. S., Chalam S. V., Rao D. S., A Survey on MAC Protocols for Wireless Multimedia Networks, 2011**, 2**(4), 57–74.

[54] Msongaleli D. L., Kucuk K., Kavak A., Adaptive Polling Medium Access Control Protocol for Optic Wireless Networks, *Applied Sciences*, 2019**, 9**(6).

[55] Mai V. V., Thang T. C., Pham A. T., CSMA/CA-based uplink MAC protocol design and analysis for hybrid VLC/Wifi networks, in: *IEEE International Conference on Communications Workshops (ICC Workshops)*, Paris, France, 21-25 May 2017.

[56] Bao X., Zhu X., Song T., Ou Y., Protocol Design and Capacity Analysis in Hybrid Network of Visible Light Communication and OFDMA Systems, *IEEE Transactions on Vehicular Technology*, 2014**, 63**(4), 1770–1778.

[57] Mao Q., Yue P., Xu M., Ji Y., Cui Z., OCTMAC: A VLC Based MAC Protocol Combining Optical CDMA with TDMA for VANETs, in: *International Conference on Computer, Information and Telecommunication Systems (CITS)*, Dalian, China, 21-23 July 2017.

[58] Le N., Jang Y. M., Broadcasting MAC protocol for IEEE 802.15.7 visible light communication, in: *International Conference on Ubiquitous and Future Networks (ICUFN)*, Da Nang, Vietnam, 2-05 July 2013.

[59] Le N., Choi S., Jang Y. M., Cooperative MAC protocol for LED-ID systems, in: *ICTC 2011*, Seoul, South Korea, 28-30 September 2011.

[60] Liu H., Zhang L., A medium access scheme with dynamic contention window-based successive transmission for visible light communications system, in: *International Conference on Information and Communication Technology Convergence (ICTC)*, Jeju, South Korea, 19-21 October 2016.

[61] Xu B., Zhang M., Sha Y., Design of Media Access Control in Visible Light Communication System and a Simple Way to Avoid Dual Transmit over Dual Access Point, in: *International Conference on Optical Communications and Networks (ICOCN)*, Hangzhou, China, 24-27 September 2016.

[62] Liu H., Zhang L., Jiang M., Energy Efficient Medium Access Scheme for Visible Light Communication System Based on IEEE 802.15.7 with Unsaturated Traffic, *IET Communications*, 2016**, 10**(18), 2534–2542.

[63] Wang Z., Liu Y., Lin Y., Huang S., Full-duplex MAC protocol based on adaptive contention window for visible light communication, *IEEE/OSA Journal of Optical Communications and Networking*, 2015**, 7**(3), 164–171.

[64] Kim B. S., Kim S. W., Fang Y., Wong T. F., Link-Adaptable Polling-based MAC Protocol for Wireless LANs, in: *IEEE Global Telecommunications Conference, GLOBECOM '04.* Dallas, TX, USA, 29 November 2004.

[65] Nishio T., Nishioka R., Morikura M., Yamamoto K., VRMAC: A Novel WLAN Medium Access Control Mechanism Using LEDs and a Camera, in: *IEEE Globecom Workshops*, Atlanta, GA, USA, 9-13 December 2013.

[66] Le N., Jang Y. M., Broadcasting MAC protocol for IEEE 802.15.7 visible light communication, in: *International Conference on Ubiquitous and Future Networks (ICUFN)*, Da Nang, Vietnam, 2-05 July 2013.

[67] Vega M. T., Famaey J., Koonen A. M. J., Liotta A., Resource Allocation in Optical Beam-steered Indoor Networks, in: *IEEE/IFIP Network Operations and Management Symposium*, 25-29 April 2016, 418–426.

[68] Nobar S. K., Mehr K. A., Niya J. M., Comprehensive Performance Analysis of IEEE 802.15.7 CSMA/CA Mechanism for Saturated Traffic, *IEEE/OSA Journal of Optical Communications and Networking*, 2015**, 7**(2), 62–73.

[69] Heting L., Lin Z., Zhiqiang W., A Successive Transmission Medium Access Scheme with Dynamic Contention Window for VLC System with Saturated Traffic, *Photonic Network Communication*, August 2017**, 34**(1), 63–74.

[70] Pathak P. H., Feng X., Hu P., Mohapatra P., Visible Light Communication, Networking, and Sensing: A Survey, Potential and Challenges, *IEEE Communications Surveys Tutorials*, 2015**, 17**(4), 2047–2077.

[71] Umezawa T., Jitsuno K., Dat P. T., Kashima K., Kanno A., Yamamoto N., Kawanishi T., Millimeter-Wave Integrated Photoreceivers for High Data Rate Photonic Wireless Communication, *IEEE Journal of Selected Topics in Quantum Electronics*, 2018**, 24**(2), 1–9.

[72] Ndjiongue A. R., Ferreira H., Ngatched T., Visible Light Communications (VLC) Technology, *Wiley Encyclopedia of Electrical and Electronics Engineering*, 2015(), 1–15.

[73] Young D. P., Brewer J., Chang J., Chou T., Kvam J., Pugh M., Diffuse Mid-UV Communication in the Presence of Obscurants, in: *Conference Record of the Forty Sixth Asilomar Conference on Signals, Systems and Computers (ASILOMAR)*, Pacific Grove, CA, USA, 4-07 November 2012.

[74] Al-Kinani A., Wang C., Zhou L., Zhang W., Optical Wireless Communication Channel Measurements and Models, *IEEE Communications Surveys Tutorials*, 2018**, 20**(3), 1939–1962.

[75] Carruthers J. B., Kahn J. M., Modeling of Non-directed Wireless Infrared Channels, *IEEE Transactions on Communications*, 1997**, 45**(10), 1260–1268.

[76] Kahn J. M., Barry J. R., Wireless Infrared Communications, *Proceedings of the IEEE*, 1997**, 85**(2), 265–298.

[77] Miramirkhani F., Uysal M., Channel Modeling and Characterization for Visible Light Communications, *IEEE Photonics Journal*, 2015**, 7**(6), 1–16.

[78] Miramirkhani F., Uysal M., Visible Light Communication Channel Modeling for Underwater Environments With Blocking and Shadowing, *IEEE Access*, 2018**, 6**(), 1082–1090.

[79] Wu X., Safari M., Haas H., Access Point Selection for Hybrid Li-Fi and Wi-Fi Networks, *IEEE Transactions on Communications*, 2017**, 65**(12), 5375–5385.

[80] Gao J., Yang F., Liu S., Hybrid Multi-and Single-carrier Modulation Approach for Visible Light Communication, in: *IEEE International Conference on Communications (ICC)*, Paris, France, 21-25 May 2017.

[81] Mesleh R., Elgala H., Haas H., Optical Spatial Modulation, *Journal of Optical Communication Networks*, 2011**, 3**(3), 234–244.

[82] Tanaka Y., Komine T., Haruyama S., Nakagawa M., Indoor Visible Communication Utilizing Plural White LEDs as Lighting, in: *IEEE International Symposium on Personal, Indoor and Mobile Radio Communications. PIMRC 2001. Proceedings (Cat. No.01TH8598)*, San Diego, CA, USA, 3October 2001.

[83] Afgani M. Z., Haas H., Elgala H., Knipp D., Visible Light Communication Using OFDM, in: *International Conference on Testbeds and Research Infrastructures for the Development of Networks and Communities, TRIDENTCOM 2006.* Barcelona, Spain, 1-03 March 2006.

[84] Komine T., Haruyama S., Nakagawa M., Performance Evaluation of Narrowband OFDM on Integrated System of Power Line Communication and Visible Light Wireless Communication, in: *International Symposium on Wireless Pervasive Computing*, Phuket, Thailand, 16-18 January 2006.

[85] Tong Z., Hu Y., Wang Y., Zhang W., A PAPR Reduction Rechnique Using FHT with Repeated Companding and Filtering in CO-OFDM Systems, in: *International Conference on Optical Communications and Networks (ICOCN)*, Wuzhen, China, 7-10 August 2017.

[86] Zhao J., Intensity-Modulation Full-field Detection Optical Fast OFDM, *IEEE/OSA Journal of Optical Communications and Networking*, 2013**, 5**(5), 465–474.

[87] Kong L., Xu W., Zhang H., Zhao C., You X., R-OFDM for RGBA-LED-Based Visible Light Communication With Illumination Constraints, *Journal of Lightwave Technology*, 2016**, 34**(23), 5412–5422.

[88] Mirvakili A., Koomson V. J., Rahaim M., Elgala H., Little T. D. C., Wireless Access Test-bed Through Visible Light and Dimming Compatible OFDM, in: *IEEE Wireless Communications and Networking Conference (WCNC)*, New Orleans, LA, USA, 9-12 March 2015.

[89] Shoreh M. H., Fallahpour A., Salehi J. A., Design Concepts and Performance Analysis of Multi-carrier CDMA for Indoor Visible Light Communications, *IEEE/OSA Journal of Optical Communications and Networking*, 2015**, 7**(6), 554–562.

[90] Barrami F., Le Guennec Y., Novakov E., Busson P., An Optical Power Efficient Asymmetrically Companded DCO-OFDM for IM/DD Systems, in: *Wireless and Optical Communication Conference (WOCC)*, Newark, NJ, USA, 9-10 May 2014.

[91] Xiao J., Yu J., Li X., Tang Q., Chen H., Li F., Cao Z., Chen L., Hadamard Transform Combined with Companding Transform Technique for PAPR Reduction in an Optical Direct-Detection OFDM System, *IEEE/OSA Journal of Optical Communications and Networking*, 2012**, 4**(10), 709–714.

[92] Noshad M., Brandt-Pearce M., Hadamard coded modulation: An Alternative to OFDM for Wireless Optical Communications, in: *IEEE Global Communications Conference*, Austin, TX, USA, 8-12 December 2014.

[93] Noshad M., Brandt-Pearce M., Hadamard-Coded Modulation for Visible Light Communications, *IEEE Transactions on Communications*, 2016**, 64**(3), 1167–1175.

[94] Singh R., O'Farrell T., David J. P. R., Performance Evaluation of IEEE 802.15.7 CSK Physical Layer, in: *IEEE Globecom Workshops (GC Wkshps)*, Atlanta, GA, USA, 9-13 December 2013.

[95] Butala P. M., Chau J. C., Little T. D. C., Metameric Modulation for Diffuse Visible Light Communications with Constant Ambient Lighting, in: *International Workshop on Optical Wireless Communications (IWOW)*, Pisa, ltaly, 22 October 2012.

[96] Ahn K., Kwon J. K., Color Intensity Modulation for Multicolored Visible Light Communications, *IEEE Photonics Technology Letters*, December 2012**, 24**(24), 2254–2257.

[97] Murata N., Kozawa Y., Umeda Y., Digital Color Shift Keying With Multicolor LED Array, *IEEE Photonics Journal*, August 2016**, 8**(4), 01–13.

[98] Xu W., Wang J., Shen H.and Zhang H., Multi-colour LED Specified Bipolar Colour Shift Keying Scheme for Visible Light Communications, *Electronics Letters*, 2016**, 52**(2), 133–135.

[99] Mardoyan H., Mestre M. A., Estarán J. M., Jorge F., Blache F., Angelini P., Konczykowska A., Riet M., Nodjiadjim V., Dupuy J., Bigo S., 84-, 100-, and 107-GBd PAM-4 Intensity-Modulation Direct-Detection Transceiver for Datacenter Interconnects, *Journal of Lightwave Technology*, March 2017**, 35**(6), 1253–1259.

[100] Basar E., Wen M., Mesleh R., Di Renzo M., Xiao Y., Haas H., Index Modulation Techniques for Next-Generation Wireless Networks, *IEEE Access*, 2017**, 5**(), 16693–16746.

[101] Yesilkaya A., Basar E., Miramirkhani F., Panayirci E., Uysal M., Haas H., Optical MIMO-OFDM With Generalized LED Index Modulation, *IEEE Transactions on Communications*, 2017**, 65**(8), 3429–3441.

[102] Başar E., Panayirci E., Uysal M., Haas H., Generalized LED Index Modulation Optical OFDM for MIMO Visible Light Communications Systems, in: *IEEE International Conference on Communications (ICC)*, Kuala Lumpur, Malaysia, 22-27 May 2016.

[103] Le Tran M., Kim S., Ketseoglou T., Ayanoglu E., LED Selection and MAP Detection for Generalized LED Index Modulation, *IEEE Photonics Technology Letters*, 2018**, 30**(19), 1695–1698.

[104] Schmid S., Corbellini G., Mangold S., Gross T. R., LED-to-LED Visible Light Communication Networks, in: *Proceedings of the Fourteenth ACM International Symposium on Mobile Ad Hoc Networking and Computing*, MobiHoc '13, Bangalore, India: ACM, 29 July 2013.

[105] Wang Q., Giustiniano D., Communication Networks of Visible Light Emitting Diodes with Intra-Frame Bidirectional Transmission, in: *ACM International on Conference on Emerging Networking Experiments and Technologies*, CoNEXT '14, Sydney, Australia: ACM, 2- 05 December 2014.

[106] Dang J., Zhang Z., Comparison of Optical OFDM-IDMA and Optical OFDMA for Uplink Visible Light Communications, in: *International Conference on Wireless Communications and Signal Processing (WCSP)*, Huangshan, China, 25-27 October 2012.

[107] Bykhovsky D., Arnon S., Multiple Access Resource Allocation in Visible Light Communication Systems, *Journal of Lightwave Technology*, 2014**, 32**(8), 1594–1600.

[108] Guerra-Medina M. F., Gonzalez O., Rojas-Guillama B., Martin-Gonzalez J. A., Delgado F., Rabadan J., Ethernet-OCDMA System for Multi-user Visible Light Communications, *Electronics Letters*, 2012**, 48**(4), 227–228.

[109] Salehi J. A., Code Division Multiple-Access Techniques in Optical Fiber Networks. I. Fundamental Principles, *IEEE Transactions on Communications*, 1989**, 37**(8), 824–833.

[110] Salehi J. A., Brackett C. A., Code Division Multiple-Access Techniques in Optical Fiber Networks. II. Systems Performance Analysis, *IEEE Transactions on Communications*, 1989**, 37**(8), 834–842.

[111] Kumar P. V., Omrani R., Touch J., Willner A. E., Saghari P., CTH01-5: A Novel Optical CDMA Modulation Scheme: Code Cycle Modulation, in: *IEEE Globecom 2006*, San Francisco, CA, USA, 27 November 2006.

[112] Noshad M., Brandt-Pearce M., Application of Expurgated PPM to Indoor Visible Light Communications—Part II: Access Networks, *Journal of Lightwave Technology*, 2014**, 32**(5), 883–890.

[113] Noshad M., Brandt-Pearce M., High-speed Visible Light Indoor Networks Based on Optical Orthogonal Codes and Combinatorial Designs, in: *IEEE Global Communications Conference (GLOBECOM)*, Atlanta, GA, USA, 9-13 December 2013.

[114] Martin-Gonzalez J. A., Poves E., Lopez-Hernandez F. J., Random Optical Codes Used in Optical Networks, *IET Communications*, 2009**, 3**(8), 1392–1401.

[115] Guerra-Medina M. F., Rojas-Guillama B., González O., Martín-González J. A., Poves E., López-Hernández F. J., Experimental Optical Code-division Multiple Access System for Visible Light Communications, in: *Wireless Telecommunications Symposium (WTS)*, New York City, NY, USA, 13-15 April 2011.

[116] Chen S., Chow C., Color-Shift Keying and Code-Division Multiple-Access Transmission for RGB-LED Visible Light Communications Using Mobile Phone Camera, *IEEE Photonics Journal*, 2014**, 6**(6), 1–6.

[117] Luna-Rivera J. M., Perez-Jimenez R., Rabadan-Borjes J. A., Rufo-Torres J. F., Guerra V., Suarez-Rodriguez C., Multiuser Scheme for Indoor Visible Light Communications Using RGB LEDs, in: *IEEE International Work-Conference on Bioinspired Intelligence*, Liberia, Costa Rica, 16-18 July 2014.

[118] Yang C., Wang Y., Wang Y., Huang X., Chi N., Demonstration of High-speed Multi-user Multi-carrier CDMA Visible Light Communication, *Optics Communications*, 2015**, 336**(), 269–272.

[119] Hou J., O'Brien D. C., Polling Scheme for Indoor LOS Optical Wireless LAN, *Electronics Letters*, 2003**, 39**(10), 794–795.

[120] Bawazir S. S., Sofotasios P. C., Muhaidat S., Al-Hammadi Y., Karagiannidis G. K., Multiple Access for Visible Light Communications: Research Challenges and Future Trends, *IEEE Access*, 2018**, 6**(), 26167–26174.

[121] Rajagopal S., Roberts R. D., Lim S., IEEE 802.15.7 Visible Light Communication: Modulation Schemes and Dimming Support, *IEEE Communications Magazine*, 2012**, 50**(3), 72–82.

[122] Rehman S., Ullah S., Chong P. Han J., Yongchareon S., Komosny D., Visible Light Communication: A System Perspective—Overview and Challenges, *Sensors*, 2019**, 19**(5).

[123] Zhang J., Zhang X., Wu G., Dancing with Light: Predictive In-frame Rate Selection for Visible Light Networks, in: *IEEE Conference on Computer Communications (INFOCOM)*, Kowloon, Hong Kong, 26 April 2015.

[124] Alresheedi M. T., Elmirghani J. M. H., Hologram Selection in Realistic Indoor Optical Wireless Systems with Angle Diversity Receivers, *IEEE/OSA Journal of Optical Communications and Networking*, 2015**, 7**(8), 797–813.

[125] Msongaleli D. L., Kucuk K., Dynamic future knowledge maximum transmission unit (DFK-MTU) for optic wireless networks, *IEEE Signal Processing and Communications Applications Conference (SIU)*, 2018().

[126] Guo C., Sheng M., Zhang Y., Wang X., A Jain's Index Perspective on -Fairness Resource Allocation over Slow Fading Channels, *IEEE Communications Letters*, 2013**, 17**(4), 705–708.

[127] Kalfas G., Pleros N., An Agile and Medium-Transparent MAC Protocol for 60 GHz Radio-Over-Fiber Local Access Networks, *Journal of Lightwave Technology*, 2010**, 28**(16), 2315–2326.

[128] Ayyash M., Elgala H., Khreishah A., Jungnickel V., Little T., Shao S., Rahaim M., Schulz D., Hilt J., Freund R., Coexistence of WiFi and LiFi Toward 5G: Concepts, Opportunities, and Challenges, *IEEE Communications Magazine*, 2016**, 54**(2), 64–71.

[129] Khreishah A., Shao S., Gharaibeh A., Ayyash M., Elgala H., Ansari N., A Hybrid RF-VLC System for Energy Efficient Wireless Access, *IEEE Transactions on Green Communications and Networking*, 2018**, 2**(4), 932–944.

[130] Wu W., Zhou F., Yang Q., Adaptive Network Resource Optimization for Heterogeneous VLC/RF Wireless Networks, *IEEE Transactions on Communications*, 2018**, 66**(11), 5568–5581.

[131] Guo W., Li Q., Yu H., Liu J. H., A Parallel Transmission MAC Protocol in Hybrid VLC-RF Network, *Journal of Communications*, 2015**, 10**(), 80–85.

[132] Shao S., Khreishah A., Delay Analysis of Unsaturated Heterogeneous Omnidirectional-Directional Small Cell Wireless Networks: The Case of RF-VLC Coexistence, *IEEE Transactions on Wireless Communications*, 2016**, 15**(12), 8406–8421.

[133] Basnayaka D. A., Haas H., Design and Analysis of a Hybrid Radio Frequency and Visible Light Communication System, *IEEE Transactions on Communications*, 2017**, 65**(10), 4334–4347.

[134] Shao S., Khreishah A., Ayyash M., Rahaim M. B., Elgala H., Jungnickel V., Schulz D., Little T. D. C., Hilt J., Freund R., Design and Analysis of a Visible-Light-Communication Enhanced WiFi System, *Journal of Optical Communication and Networking*, 2015**, 7**(10), 960–973.

[135] Li Z., Shao S., Khreishah A., Ayyash M., Abdalla I., Elgala H., Rahaim M., Little T., Design and Implementation of a Hybrid RF-VLC System with Bandwidth Aggregation, in: International Wireless Communications Mobile Computing Conference (IWCMC), Limassol, Cyprus, 25-29 June 2018.

[136] Kafafy M., Fahmy Y., Abdallah M., Khairy M., Power Efficient Downlink Resource Allocation for Hybrid RF/VLC Wireless Networks, in: *IEEE Wireless Communications and Networking Conference (WCNC)*, San Francisco, CA, USA, 19-22 March 2017.

[137] Hsiao Y. C., Chen C. M., Lin C., Energy Efficiency Maximization in Multi-User Miso Mixed RF/VLC Heterogeneous Cellular Networks, in: *Annual IEEE International Conference on Sensing, Communication, and Networking (SECON)*, Hong Kong, China, 11-13 June 2018.

[138] Li X., Zhang R., Hanzo L., Cooperative Load Balancing in Hybrid Visible Light Communications and WiFi, *IEEE Transactions on Communications*, 2015**, 63**(4), 1319–1329.

[139] Marshoud H., Kapinas V. M., Karagiannidis G. K., Muhaidat S., Non-Orthogonal Multiple Access for Visible Light Communications, *IEEE Photonics Technology Letters*, 2016**, 28**(1), 51–54.

[140] Alshanyour A., Agarwal A., Three-Dimensional Markov Chain Model for Performance Analysis of the IEEE 802.11 Distributed Coordination Function, in: *IEEE Global Telecommunications Conference*, Honolulu, HI, USA, 30 November 2009.

[141] Mehr K. A., Nobar S. K., Niya J. M., IEEE 802.15.7 MAC Under Unsaturated Traffic: Performance Analysis and Queue Modeling, *IEEE/OSA Journal of Optical Communications and Networking*, 2015**, 7**(9), 875–884.

[142] Bianchi G., Performance analysis of the IEEE 802.11 distributed coordination function, *IEEE Journal on Selected Areas in Communications*, 2000**, 18**(3), 535–547.

[143] Wang Q., Giustiniano D., Intra-Frame Bidirectional Transmission in Networks of Visible LEDs, *IEEE/ACM Transactions on Networking*, 2016**, 24**(6), 3607–3619.

PUBLICATIONS AND WORKS

Msongaleli D. L., Kucuk K., Kavak A., Bayilmis C., Akbulut O., Self-Adaptive Medium Access Control Protocol for Aggregated VLC-RF Wireless Networks," *IEEE/OSA Journal of Optical Communication and Networking,* (Under Review).

Msongaleli D. L., Kucuk K., "Optimal Resource Utilization Algorithm for VLC-Based VANETs," *IET Intelligent Transport Systems* (revised and resubmitted).

Kucuk K, Bayilmis C., **Msongaleli D. L.**, "Designing Real-Time IoT System Course: Prototyping with Cloud Platforms, Laboratory Experiments and Term Project," *The International Journal of Electrical Engineering and Education,* July 2019, DOI: 10.1177/0020720919862496.

Msongaleli D. L., Kucuk K., Kavak A. "Adaptive Polling Medium Access Control Protocol for Optic Wireless Networks," *Journal of Applied Sciences* March 2019; 9(6):1071.

Asshad, M., Khan, S. A., Kavak, A., Küçük, K. and **Msongaleli D. L.**, "Cooperative communications using relay nodes for next-generation wireless networks with optimal selection techniques: A review," *IEEJ Transaction on Electrical and Electronic Engineering,* vol. 14, no. 5, 658-669, March 2019.

Msongaleli D. L. and Kucuk K., "Dynamic future knowledge maximum transmission unit (DFK-MTU) for optic wireless networks," *IEEE Signal Processing and Communications Applications Conference (SIU),* Izmir, Turkey, 2-5 May 2018.

Msongaleli D. L. and Kucuk K., "Electronic mail forensic algorithm for crime investigation and dispute settlement," *IEEE International Symposium on Digital Forensic and Security (ISDFS),* Antalya, Turkey, 22-25 March 2018.

Msongaleli D. L. and Kucuk K., "Reliability and cost-aware network upgrade for the next generation mobile networks," *IEEE International Conference on Computer Science and Engineering (UBMK),* Antalya, Turkey, 5-8 October 2017, 496-501.

Msongaleli D. L., Dikbiyik F., Zukerman M., and Mukherjee B., "Disaster-Aware Submarine Fiber-Optic Cable Deployment for Mesh Networks," *IEEE/OSA Journal of Lightwave Technology,* vol. 34, 4293-4303, September 2016.

Msongaleli D. L., Dikbiyik F., Zukerman M., and Mukherjee B., "Disaster-aware submarine fiber-optic cable deployment," *IEEE International Conference on Optical Network Design and Modeling (ONDM),* Pisa, Italy, 11-14 May 2015, 245-250.

CURRICULUM VITAE

Dawson Ladislaus Msongaleli received the BSc. in Computer Science from Ruaha University College (A former Constituent College of St. Augustine University of Tanzania) in 2011. He joined Sakarya University, Turkey, where he received his MSc. in Computer and Information Engineering in 2015. During his MSc. studies he conducted a research on the design of survivable submarine fiber optic networks. His work was under the project titled “Cost effective and survivable wide-area topology of telecommunication cabling”. This project was supported by a grant from the Research Grants Council of the Hong Kong Special Administrative Region, China (Project No. CityU8/CRF/13G). Currently, he is a Ph.D. student at the Department of Computer Engineering, Kocaeli University, Turkey. His Ph.D. thesis is based on designing medium access control protocol for aggregated VLC and other wireless networks such as infrared and radio frequency. He is a student member of IEEE.